AD_____

Award Number: DAMD17-03-01-0077

TITLE: Development and Pre-Clinical Evaluation of a Novel Prostate-Restricted Replication Competent Adenovirus-AD-IU-1

PRINCIPLE INVESTIGATOR: Thomas A. Gardner, M.D.

CONTRACTING ORGANIZATION: Indiana University School of Medicine
                                                Indianapolis, IN 46202-5167

REPORT DATE: May 2006

TYPE OF REPORT: Final

PREPARED FOR: U.S. Army Medical Research and Materiel Command
                        Fort Detrick, Maryland 21702-5012

DISTRIBUTION STATEMENT: Approved for Public Release;
                                        Distribution Unlimited

REPORT DOCUMENTATION PAGE

1. REPORT DATE 01-05-2006	2. REPORT TYPE Final	3. DATES COVERED 1 May 2003 – 30 Apr 2006

4. TITLE AND SUBTITLE

Development and Pre-Clinical Evaluation of a Novel Prostate-Restricted Replication Competent Adenovirus-AD-IU-1

5a. CONTRACT NUMBER

5b. GRANT NUMBER
DAMD17-03-1-0077

5c. PROGRAM ELEMENT NUMBER

6. AUTHOR(S)

Thomas A. Gardner, M.D.

5d. PROJECT NUMBER

5e. TASK NUMBER

5f. WORK UNIT NUMBER

7. PERFORMING ORGANIZATION NAME(S) AND ADDRESS(ES)

Indiana University School of Medicine
Indianapolis, IN 46202-5167

8. PERFORMING ORGANIZATION REPORT NUMBER

9. SPONSORING / MONITORING AGENCY NAME(S) AND ADDRESS(ES)
U.S. Army Medical Research and Materiel Command
Fort Detrick, Maryland 21702-5012

10. SPONSOR/MONITOR'S ACRONYM(S)

11. SPONSOR/MONITOR'S REPORT NUMBER(S)

12. DISTRIBUTION / AVAILABILITY STATEMENT
Approved for Public Release; Distribution Unlimited

13. SUPPLEMENTARY NOTES
Original contains colored plates: ALL DTIC reproductions will be in black and white.

14. ABSTRACT

Recently we generated a prostate specific chimeric promoter, called PSES, by combining the active prostate specific enhancers from PSA and PSMA genes which are prominently expressed in androgen independent prostate cancers. The goal of this research is to develop a novel therapeutic agent, Ad-IU-1, using PSES to control the replication of adenovirus and the expression of a therapeutic gene, herpes simplex thymidine kinase (TK). AD-IU-1 replicate as efficient as a wild type adenovirus in PSA/PSMA positive cells, but not in PSA/PSMA negative cells. Prodrug GCV augmented Ad-IU-1's killing activity against PSA/PSMA positive cells, but not PSA/PSMA negative cells in vitro. Ad-IU-1 was more effective in inhibit the growth of androgen-independent CWR22rv tumors. Due to recent improvement in our adenoviral vector construction which allows us to insert a bigger transgene into the viral genome, we further investigated a fusing suicide gene, FCYttk, by combining two suicide genes, a yeast cytosine deaminase, FCY, and improved TK, ttk. FCYttk had a better killing activity than TK against prostate cancer cells. We are on the process of constructing FCYttk-armed prostate restricted replicative adenovirus for future clinical investigation.

15. SUBJECT TERMS
TRANSCRIPTIONAL REGULATION OF ADENOVIRAL REPLICATION,GENE THERAPY,PSESCHIMERIC PROMOTER, TISSUE RESTRICTED REPLICATION COMPETENT ADENOVIRUS, MICROPET IMAGING

16. SECURITY CLASSIFICATION OF:			17. LIMITATION OF ABSTRACT	18. NUMBER OF PAGES	19a. NAME OF RESPONSIBLE PERSON USAMRMC
a. REPORT U	b. ABSTRACT U	c. THIS PAGE U	UU	82	19b. TELEPHONE NUMBER *(include area code)*

Standard Form 298 (Rev. 8-98)
Prescribed by ANSI Std. Z39.18

TABLE OF CONTENTS

INTRODUCTION

Metastatic human prostate cancer (PC) is commonly treated by hormone, radiation, and/or chemotherapy. Inevitably, these patients will eventually relapse and develop androgen-independent disease with osseous metastasis. Since no effective therapy is presently available for the treatment of PC metastasis, we are developing a novel gene therapy modality for hormonal refractory prostate cancer based on a prostate-specific chemic promoter, PSES, generated in my laboratory. In this study, we proposed to generate a herpes simplex virus thymidine kinase armed prostate restricted replicative adenovirus to treat androgen-independent prostate cancers. Specific Aim 1 intends to simplify and combine the most important enhancer elements from PSA and PSMA enhnacers/promoters to generate a strong and simple prostate-specific chimeric enhancer, sPSES. Specific Aim 2 will test whether sPSES retains prostate specific activity in an adenoviral vector. Specific Aim 3 will test whether sPSES can control adenoviral replication by controlling adenovirus E1a and E1b expression, and investigate how replication competent adenovirus eradicates prostate cancers by micro positron emission tomography (microPET) imaging.

BODY

Task 1. To generate a strong and simple prostate-specific enhancer. (Months 1-6):

　　　　　a.　　Generate deletion consrtuct (Months 1-4). We have successfully deleted

　　　　　　　　L2 and L5 in AREc3 (Figure 1), and replaced the 90 bp proximal region

Figure 1. Sequences of the enhancer core of the PSA gene, AREc3, located the 4.3 kb upstream of PSA promoter. Sequence analysis on AREc3 revealed 6 putative GATA transcriptional factor binding sites besides reported 3 androgen response elements.

Figure 2. Sequences of PSME located in the third intron in the PSMA gene (*FOLH*1). PSME is characterized by the repeat sequence (marked by underline and bold) and an Alu sequence (marked by lower case). Several potential transcription factor binding sites, such as AP-1, AP-3, and SRY/SOX, are indicated.

(marked by italic in Figure 2) of PSME with simple AP-3 binding site. These manipulations reduced the size of PSES from 513 bp to 407 bp. The simplified version of PSES is called m6.

b. Test the tissue-specificity of new deletion constructs (Months 3-6). The tissue specific activity of m6 has been tested in several cell lines. Figure 3 demonstrated that m6 retained a strong prostate specificity, active only in PSA/PSMA positive prostate cancer LNCaP and C4-2 cells.
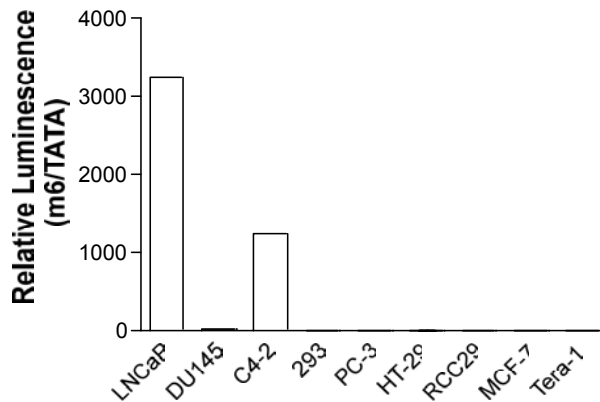
Figure 3. pGL3/m6/TATA (0.5 μg) was transfected into various cell lines (2 x 10^5 cells for each). After 2 days, cells were harvested, lysed with passive lysis buffer (Promega) and analyzed for luciferase activities. This experiment was conducted in the absence of androgen. The luciferase activity was determined by being divided by the basal activity represented by transfection of pGL3/TATA. pGL3/m6/TATA is avtive only in PSA/PSMA postivie LNCaP and C4-2 cells.

Task 2. To test tissue-specificity of the modified PSES chimeric enhancer, m6, in an adenoviral vector (Months 7-24):

a. Construct Ad-m6-Luc (Months 7-12). Ad-m6-Luc has been generated.

b. Test the tissue-specificity of Ad-m6-Luc in tissue culture cells (Months 13-18). Ad-m6-Luc exhibited the same prostate specificity in all cell lines tested. However, this study was not continued due to a technical difficulty in making Ad-IU-1 initially (see discussion below).

c. Test the tissue-specificity of Ad-m6-Luc in vivo (Months 19-22). This study was not continued due to a technical difficulty in making Ad-IU-1 initially (see discussion below).

Task 3.   Investigate the capability of m6 to drive adenovirus replication in a prostate cancer-specific manner (Months 13-36):

a.   Construct Ad-IU-1 (Months 7-16). The first attempt to make Ad-IU-1 according to the original plan has failed due to a size limitation of adenoviral vector. We have changed our construction strategy and made Ad-IU-1 as illustrated below.

ITR   ψ   TK   E1b   F4   E1a   ITR
                PSES   M6
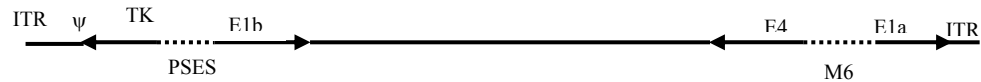
b.   In vitro test tissue-specific expression of TK, E1a and E1b proteins in Ad-IU-1 infected cells (Months 17-20). This study was skipped due to the unexpected difficulty in making AD-IU-1 originally.

c.   In vitro test the tissue specific replication of Ad-IU-1 (Months 19-22). Ad-IU-1 replicated as efficient as AdE4PSESE1a, a PSES controlled replicative adenovirus, in PSA/PSMA positive cells, and its replication efficiency was dramatically attenuated in PSA/PSMA negative cells (see Table 1 in the attached manuscript).

d.   In vitro test the therapeutic efficacy of Ad-IU-1 (Months 20-23). Ad-IU-1 had less toxicity than AdE4PSESE1a in treating PSA/PSMA positive cell in the absence of prodrug GCV; on the other hand, Ad-IU-1 was 10 to 100 fold more potent than AdE4PSESE1a in killing PSA/PSMA positive cell in the absence of the prodrug ganciclovir, GCV. Ad-IU-1 had minimal toxicity toward PSA/PSMA negative cells DU145 in the presence or absence of GCV (see Figure 2 in the attached manuscript)

e.   In vivo test the therapeutic efficacy of Ad-IU-1 (Months 22-36). CWR22rv subcutaneous tumors in the castrated nude mice were used to test the therapeutic efficacy of Ad-IU-1. The therapeutic efficacy of Ad-IU-1 was significantly enhanced by GCV. Without GCV, Ad-IU-1 has a

similar therapeutic effect as AdE4PSESE1a on CWR22rv tumors (see Figure 4 and 5 in the attached manuscript).

f. MicroPet image C4-2 tumors (Months 9-20). It has been finished and published (see Reportable Outcomes section). In general, microPET imaging of tumor is less sensitive than PSA assay. The reviewers of this proposal also pointed out this problem.

g. MicroPET image the therapeutic effect of Ad-IU-1 (Months 21-36). We have made 8-[^{18}F]-fluoropenciclovir for TK microPET imaging study (see Reportable Outcomes section). However, due to the unexpected delay of this project, this study is still ongoing.

Additional results: It has been reported that cytosine deaminase (CD)- thymdine kinase (TK) fusion fusion gene (CD/TK) exert a much better therapeutic effect than CD and TK themselves. CD/TK-based gene therapy has been studied extensively in clinic to treat prostate cancer by Svend O. Freytag (1-6). We constructed a fusion gene, FCYttk, between a yeast cytosine deaminase (FCY) and a modified thymidine kinase (ttk), an N-terminal deleted form of sr39TK. FCYttk demonstrated better killing activity than bacterial CD when supplemented with the prodrug 5-FC, and demonstrated similar killing

Figure 4. FCYttk in vitro cell killing assay. CWR22rv cells were seeded in a 24-well (1×10^5 cells/well) plate and transfected with pAd1020PSESFCYttk. The cells were treated with GCV (5 ug/mL), 5-FC (25 uM) 24 hours after transfection. Medium was changed every 2 days. At 5day, cell number was analyzed using crystal violet staining. GCV at 5 μg/ml and 5-FC at 25 uM concentration are no-toxic to CRW22rv (unpublished data).

activity to sr39TK when supplemented with the prodrug, GCV (unpublished data). We transfected pcDNA3.1-FCYttk expression vector into CWR22rv cells and treated the cells with PBS, GCV, 5-FC or GCV+5-FC. FCYttk/GCV/5-FC treatment exerted much stronger killing activity than FCYttk/GCV or FCYttk/5-FC treatment alone (Figure 4).

We are on the process of constructing a FCYttk-armed prostate-restricted replicative adenovirus.

h.   **KEY RESEARCH ACCOMPLISHMENTS**

1.   Successfully shorten PSES as planned and demonstrate the prostate specific activity of the shortened form of PSES, m6.

2.   Successfully construct Ad-m6-Luc and Ad-IU-1.

3.   Have tested [^{11}C]-choline and [^{18}F]-FDG microPET imaging in prostate cancer nude mice model.

4.   Successfully synthesize 9-(4-[18F]fluoro-3-hydroxymethylbutyl)guanine ([18F]FHBG) for microPET imaging Ad-IU-1 activity.

5.   Ad-IU-1 demonstrated a prostate specific replication and killing activity.

6.   The tumor killing activity of Ad-IU-1 is significantly enhanced by GCV as hypothesized originally.

REPORTABLE OUTCOMES

Some of the results of this study have been published.

1. Q-H. Zheng, **T.A. Gardner,** S.P. Raikwar, C. Kao, K.L. Stone, T.D. Martinez, B.H. Mock, X. Fei, J-Q. Wang, G.D. Hutchins: [11C]Choline as a PET biomarker for assessment of prostate cancer tumor models. *Bioorg. Med. Chem.* **2004**, *12*, 2887-2893.

2. J-Q. Wang, Q-H. Zheng, X. Fei, X. Liu, **T.A. Gardner,** C. Kao, S.P. Raikwar, B.E. Glick-Wilson, M.L. Sullivan, B.H. Mock, G.D. Hutchins: An improved total synthesis of PET HSV-tk gene expression imaging agent 9-[(3-[18F]fluoro-1-hydroxy-2-propoxy)methyl]guanine ([18F]FHPG). *Syn. Commun.* **2004**, *34(5)*, 917-932.

3. Q-H. Zheng, J-Q. Wang, X. Liu, X. Fei, B.H. Mock, B.E. Glick-Wilson, M.L. Sullivan, S.P. Raikwar, **T.A. Gardner,** C. Kao, G.D. Hutchins: An improved total synthesis of PET HSV-tk gene reporter probe 9-(4-[18F]fluoro-3-hydroxymethylbutyl)guanine ([18F]FHBG). *Syn. Commun.*, **2004**, *34(4)*, 689-704.

CONCLUSIONS

We have successfully shortened PSES as planned and demonstrated the prostate specific activity of the shortened form of PSES, m6. We made a prostate restricted replicative adenovirus-armed with TK, Ad-IU-1, as proposed. Ad-IU-1 replicated efficiently in PSA/PSMA positive prostate cancer cells. Its replication efficiency was significantly attenuated in PSA/PSMA negative cells. Both in vitro and in vivo tumor-killing activities of Ad-IU-1 are significantly enhanced by the prodrug GCV as our original hypothesis. We are on the process of conducting a toxicology

studies to prepare Ad-IU-1 for clinical investigation. At the same time, we are improving Ad-IU-1 by replacing it TK gene with a more powerful suicide gene, FCYttk.

REFERENCES

1.   Rogulski, K. R., Kim, J. H., Kim, S. H., and Freytag, S. O. Glioma cells transduced with an Escherichia coli CD/SHV-1 TK fusion gene exhibit enhanced metabolic sucide and radiosensitivity. Human Gene Therapy, *8:* 73-85, 1997.
2.   Freytag, S. O., Rogulski, K. R., Paielli, D. L., Gilbert, J. D., and Kim, J. H. A novel three-pronged approach to kill cancer cells selectively: concomitant viral, double suicide gene, and radiotherapy [see comments]. Hum Gene Ther, *9:* 1323-1333, 1998.
3.   Rogulski, K. R., Wing, M. S., Paielli, D. L., Gilbert, J. D., Kim, J. H., and Freytag, S. O. Double suicide gene therapy augments the antitumor activity of a replication-competent lytic adenovirus through enhanced cytotoxicity and radiosensitization. Hum Gene Ther, *11:* 67-76., 2000.
4.   Barton, K. N., Paielli, D., Zhang, Y., Koul, S., Brown, S. L., Lu, M., Seely, J., Kim, J. H., and Freytag, S. O. Second-generation replication-competent oncolytic adenovirus armed with improved suicide genes and ADP gene demonstrates greater efficacy without increased toxicity. Mol Ther, *13:* 347-356, 2006.
5.   Freytag, S. O., Stricker, H., Pegg, J., Paielli, D., Pradhan, D. G., Peabody, J., DePeralta-Venturina, M., Xia, X., Brown, S., Lu, M., and Kim, J. H. Phase I study of replication-competent adenovirus-mediated double-suicide gene therapy in combination with conventional-dose three-dimensional conformal radiation therapy for the treatment of newly diagnosed, intermediate- to high-risk prostate cancer. Cancer Res, *63:* 7497-7506, 2003.
6.   Freytag, S. O., Khil, M., Stricker, H., Peabody, J., Menon, M., DePeralta-Venturina, M., Nafziger, D., Pegg, J., Paielli, D., Brown, S., Barton, K., Lu, M., Aguilar-Cordova, E., and Kim, J. H. Phase I study of replication-competent adenovirus-mediated double suicide gene therapy for the treatment of locally recurrent prostate cancer. Cancer Res, *62:* 4968-4976, 2002.

ELSEVIER

Synthesis of 2-amino-6-(4-[11C]methoxyphenylthio)-9-[2-(phosphonomethoxy)ethyl]purine bis(2,2,2-trifluoroethyl) ester as a novel potential PET gene reporter probe for HBV and HSV-tk in cancers

Ji-Quan Wang,[a] Xiangshu Fei,[a] Thomas A. Gardner,[b] Gary D. Hutchins[a] and Qi-Huang Zheng[a],*

[a]Department of Radiology, Indiana University School of Medicine, Indianapolis, IN 46202, USA
[b]Department of Urology, Indiana University School of Medicine, Indianapolis, IN 46202, USA

Abstract—Acyclic nucleoside 2-amino-6-(4-methoxyphenylthio)-9-[2-(phosphonomethoxy)ethyl]purine bis(2,2,2-trifluoroethyl) ester (ABE, **1**) is a new hepatitis B virus (HBV) specific antiviral reagent and shows high anti-HBV activity. Carbon-11 labeled ABE may serve as a novel reporter probe for positron emission tomography (PET) to image HBV and herpes simplex virus thymidine kinase (HSV-tk) in cancers. The radiolabeling precursors 2-amino-6-(4-hydroxyphenylthio)-9-[2-(phosphonomethoxy)ethyl]purine bis(2,2,2-trifluoroethyl) ester (**10**) and 2-N-Boc protected analogue 2-N-bis(Boc)amino-6-(4-hydroxyphenylthio)-9-[2-(phosphonomethoxy)ethyl]purine bis(2,2,2-trifluoroethyl) ester (**12**), and the reference standard ABE were synthesized from bis(trifluoroethyl) (2-iodoethoxy)methylphosphonate (**5**), guanine (**6**), and 2-amino-6-chloropurine (**8**). The target radiotracer 2-amino-6-(4-[11C]methoxyphenylthio)-9-[2-(phosphonomethoxy)ethyl]purine bis(2,2,2-trifluoroethyl) ester ([11C]ABE, [11C]1) was prepared by O-[11C]methylation of the unprotected HO-precursor **10**, or 2-N-Boc protected HO-precursor **12** with [11C]methyl triflate followed by a quick deprotection reaction, and isolated by solid-phase extraction (SPE) purification in 40–55% radiochemical yields.
© 2004 Elsevier Ltd. All rights reserved.

1. Introduction

Hepatitis B virus (HBV) infection is responsible for both acute and chronic hepatitis. Chronic HBV infection dramatically increases risks for development of liver cancer and cirrhosis.[1–3] The World Health Organization (WHO) estimates about 400 million chronic carriers worldwide, with roughly 4 million deaths annually from the resulting cirrhosis and hepatocellular carcinoma. Treatment of HBV infection constitutes one of the therapeutic challenges in virology, and only a few drugs are currently available for the clinical treatment of HBV such as interferon α and lamivudine.[4] Several nucleoside analogues like 9-[2-(phosphonomethoxy)ethyl]adenine (PMEA) and its analogues,[5–8] ganciclovir (GCV), penciclovir (PCV), and 5-substituted analogue of thymidine

1-(2'-deoxy-2'-fluoro-β-D-arabinofuranosyl)-5-iodouracil (FIAU) have also been investigated as potent chemotherapeutic agents against viruses, for example, HBV and human immunodeficiency virus (HIV), and certain forms of cancer.[1–3] Radiolabeled fluorinated (fluorine-18) or iodinated (iodine-124, 125, and 131) prodrugs such as fluorinated GCV and PCV analogues 8-[18F]-fluoroganciclovir ([18F]FGCV), 9-[(3-[18F]fluoro-1-hydroxy-2-propoxy)methyl]guanine ([18F]FHPG), 8-[18F]-fluoropenciclovir ([18F]FPCV), 9-(4-[18F]fluoro-3-hydroxymethylbutyl)guanine ([18F]FHBG); and fluorinated and iodinated FIAU analogues [18F]FIAU, [124I]FIAU, and [125/131I]FIAU have been synthesized as gene reporter probes for biomedical imaging techniques positron emission tomography (PET) or single photon emission computed tomography (SPECT) to image herpes simplex virus thymidine kinase (HSV-tk) gene expression,[9–22] and we have also developed new carbon-11 labeled GCV and PCV analogues 8-[11C]methoxyganciclovir ([11C]MeOGCV) and

* Corresponding author. Tel.: +1 317 278 4671; fax: +1 317 278 9711; e-mail: qzheng@iupui.edu

8-[¹¹C]methoxypenciclovir ([¹¹C]MeOPCV) as novel HSV-tk gene reporter probes (Fig. 1).[23,24] 2-Amino-6-(4-methoxyphenylthio)-9-[2-(phosphonomethoxy)ethyl]-purine bis(2,2,2-trifluoroethyl) ester (ABE, 1) is a novel HBV-specific antiviral reagent and shows high anti-HBV activity in vitro, and its active metabolite was highly detected in the liver.[4] Compound ABE might be suitable for hepatitis B chemotherapy. Carbon-11 labeled antiviral nucleoside analogue 2-amino-6-(4-[¹¹C]methoxyphenylthio)-9-[2-(phosphonomethoxy)-ethyl]purine bis(2,2,2-trifluoroethyl) ester ([¹¹C]ABE, [¹¹C]1) may serve as a novel reporter probe for PET to image HBV and HSV-tk in cancers. In this study, we report the synthesis of [¹¹C]ABE, for the first time.
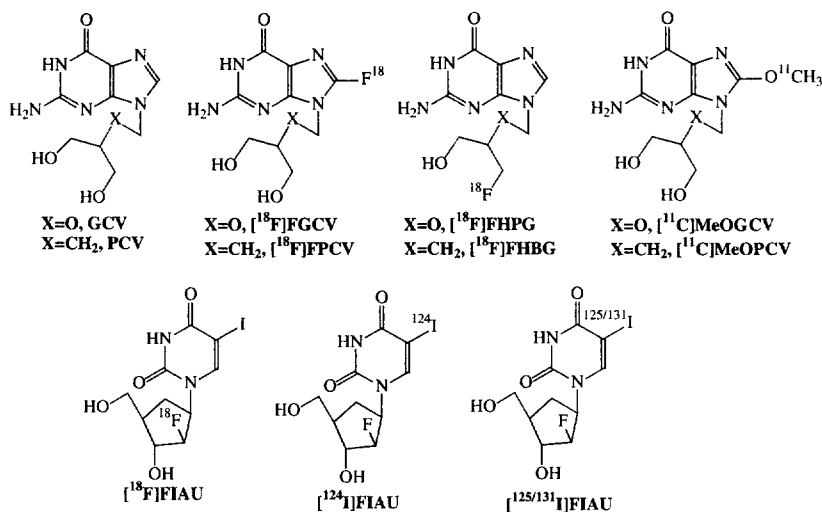
2. Results and discussion

2.1. Chemistry

The synthesis of the unprotected HO-precursor 2-amino-6-(4-hydroxyphenylthio)-9-[2-(phosphonomethoxy)-ethyl]purine bis(2,2,2-trifluoroethyl) ester (10) and reference standard ABE, 1 as indicated in Scheme 1 was performed with the modifications according to procedures reported in the literature.[4] 2-Chloroethyl chloromethyl ether (2) was treated with tris(2,2,2-trifluoroethyl)phosphite (3) to quantitatively give bis(trifluoroethyl) (2-chloroethoxy)methylphosphonate (4). Compound 4 was converted to bis(trifluoroethyl) (2-iodoethoxy)methylphosphonate (5) with sodium iodide through halogen exchange reaction in 80% yield. Following the procedures reported in the literature,[25] guanine (6) was treated first with trifluoroacetic anhydride and then with 4-methoxybenzenethiol and eventually with ethanolic methylamine to afford 2-amino-6-[(4-methoxyphenyl)sulfanyl]purine (7) in 66% yield. Compound 7 was treated first with 1,8-diazabicyclo-[5,4,0]undec-7-ene (DBU) and then with compound 5

to yield the reference standard 1 in 42% yield. 2-Amino-6-chloropurine (8) was treated first with DBU and then with compound 5 to provide desired 9-isomer N⁹-substituted product 2-amino-6-chloro-9-[2-(phosphono-methoxy)ethyl]purine bis(2,2,2-trifluoroethyl) ester (9) as the major product in 33% yield, and undesired 7-isomer N⁷-substituted product as the minor byproduct.[18–20] Compound 9 was then reacted with 4-hydroxythiophenol to give the unprotected precursor 10 in 55% yield.

The synthesis of compound 1 has been reported in the reference,[4] in which it was synthesized from compound 9 with 4-methoxybenzenethiol. In this paper, an improved synthetic approach[25] through the reaction of compound 7 with compound 5 was used for the synthesis of compound 1. The purpose of this modification is to increase the yield of compound 1 through the avoidance of the formation and separation of undesired N⁷-substituted product, the 7-isomer of compound 9. However, the improved method[25] did not work well for the synthesis of compound 10, since the hydroxyl group in 4-hydroxythiophenol will be also reacted with compound 5, therefore, the reported method[4] through compound 9 appears to be the only approach to prepare compound 10.

The 2-amino group in purine ring may affect the O-[¹¹C]methylation of the unprotected HO-precursor 10, therefore, we also designed and synthesized a 2-N-Boc protected HO-precursor 2-N-bis(Boc)amino-6-(4-hydroxyphenylthio)-9-[2-(phosphonomethoxy)ethyl]-purine bis(2,2,2-trifluoroethyl) ester (12).[26,27] The synthesis of the 2-N-Boc protected precursor 12 as outlined in Scheme 2 was performed with the modifications according to procedures indicated in the Scheme 1. Compound 9 was reacted with t-butoxycarbonyl anhydride (Boc₂O) to afford 2-N-bis(Boc)amino-6-chloro-9-[2-(phosphonomethoxy)ethyl]purine bis(2,2,2-trifluoroethyl) ester (11) in 77% yield. Compound 11

Figure 1. Chemical structures of GCV, PCV; [¹⁸F]FGCV, [¹⁸F]FPCV; [¹⁸F]FHPG, [¹⁸F]FHBG; [¹¹C]MeOGCV, [¹¹C]MeOPCV; [¹⁸F]FIAU, [¹²⁴I]FIAU, and [¹²⁵/¹³¹I]FIAU.
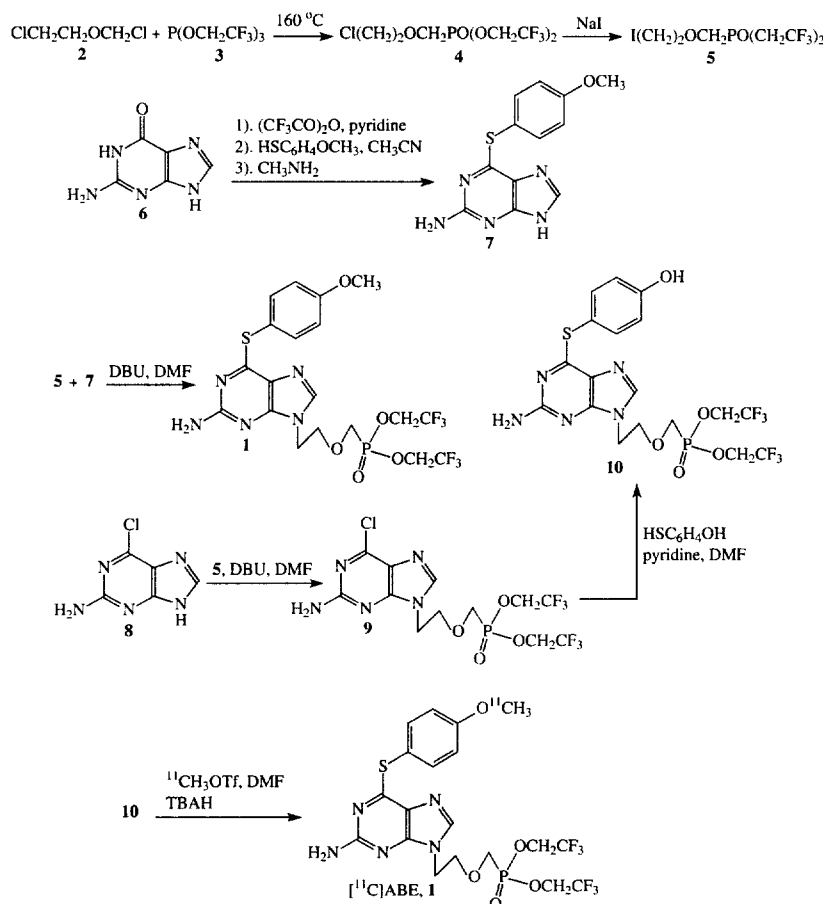
Scheme 1. Synthesis of 2-amino-6-(4-[^{11}C]methoxyphenylthio)-9-[2-(phosphonomethoxy)ethyl]purine bis(2,2,2-trifluoroethyl) ester ([^{11}C]ABE, [^{11}C]1) using unprotected HO-precursor 10.

was then reacted with 4-hydroxythiophenol to give the 2-N-Boc protected precursor **12** in 31% yield. The direct methylation of compound **12** with methyl triflate (CH₃OTf) gave the O-methylated product 2-N-bis(Boc)-amino-6-(4-methoxyphenylthio)-9-[2-(phosphonomethoxy)ethyl]purine bis(2,2,2-trifluoroethyl) ester (**13**) in very low yield, in which compound **13** will serve as a reference intermediate for the radiolabeling of 2-N-Boc protected precursor **12**. Thus, the small-scale synthesis of compound **13** was carried out, in which the reference standard **1** was directly reacted with Boc₂O to provide compound **13** in 45% yield. The deprotection of compound **13** with 1 N HCl in acetonitrile gave the reference standard **1**. The methylation of 2-N-Boc protected precursor **12** with CH₃OTf under basic conditions using tetrabutylammonium hydroxide (TBAH) followed by a quick deprotection with 1 N HCl to remove the 2-N-Boc groups also gave the reference standard **1**.

2-Amino-6-(3-methoxyphenylthio)-9-[2-(phosphonomethoxy)ethyl]purine bis(2,2,2-trifluoroethyl) ester (*meta*-ABE, IC₅₀ 0.04 μM) and 2-amino-6-(2-methoxyphenylthio)-9-[2-(phosphonomethoxy)ethyl]purine bis(2,2,2-trifluoroethyl) ester (*ortho*-ABE, IC₅₀ 0.08 μM) have similar in vitro anti-HBV activity to the target

compound **1** (*para*-ABE, IC₅₀ 0.03 μM).[4] The potentiation effect order of 6-arylthio analogues is *para* > *meta* > *ortho*, which is consistent with the potentiation effect order of O⁶-benzylguanine (O⁶-BG) analogues,[28–31] most likely because the steric effect at the *ortho*-position plays a more important role than the electronic effect. Therefore, *para*-ABE was designed as the target compound for radiolabeling.

2.2. Radiochemistry

The synthesis of the target tracer [^{11}C]ABE, [^{11}C]1 using both unprotected precursor **10** and protected precursor **12** are outlined in Schemes 1 and 2. The unprotected HO-precursor **10** was labeled by [^{11}C]methyl triflate (^{11}CH₃OTf)[32,33] through O-[^{11}C]methylation of hydroxyphenyl position under basic conditions using TBAH.[34–38] The tracer was isolated by solid-phase extraction (SPE) purification[34,39,40] to produce pure target compound radiolabeled [^{11}C]1 with 50–55% radiochemical yields, based on ^{11}CO₂, decay corrected to end of bombardment (EOB). The large polarity difference between the HO-precursor and the labeled methylated product permitted the use of SPE technique for purification of labeled product from radiolabeling
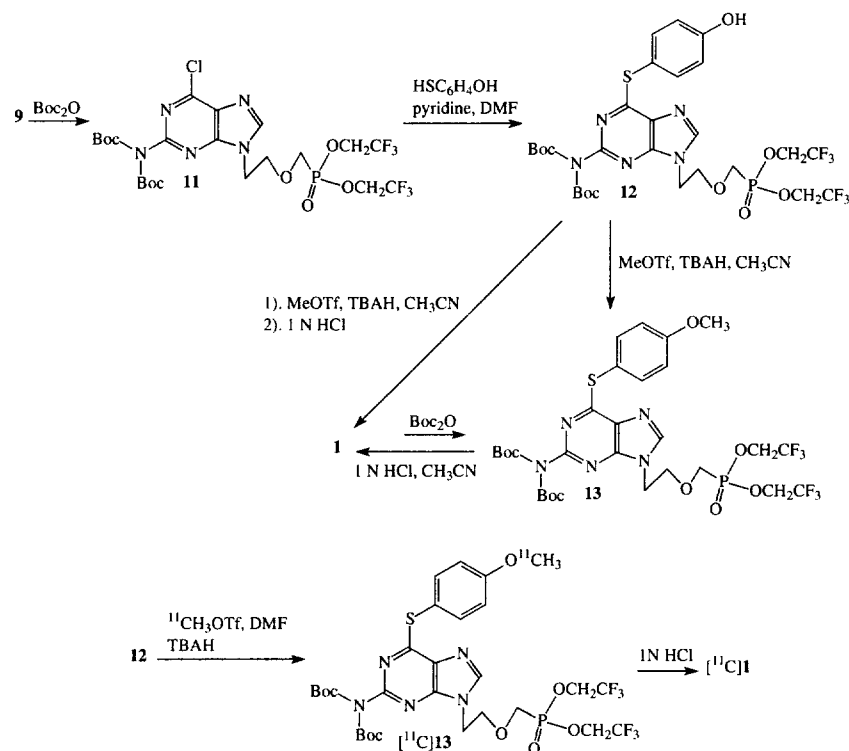
Scheme 2. Synthesis of 2-amino-6-(4-[^{11}C]methoxyphenylthio)-9-[2-(phosphonomethoxy)ethyl]purine bis(2,2,2-trifluoroethyl) ester ([^{11}C]ABE, [^{11}C]1) using 2-N-Boc protected HO-precursor 12.

reaction mixture. The reaction mixture was diluted with NaHCO$_3$ and loaded onto C-18 cartridge by gas pressure. The cartridge column was washed with water to remove unreacted ^{11}CH$_3$OTf and precursor and reaction solvent, and then final labeled product was eluted with ethanol. Similarly, 2-N-Boc protected HO-precursor 12 was labeled with ^{11}CH$_3$OTf followed by a quick deprotection reaction with 1N HCl and isolated by SPE purification technique to produce [^{11}C]1 in 40–55% radiochemical yields. Comparing the radiochemistry of unprotected precursor 10 and protected precursor 12, no distinct difference was found. It is likely the concern that 2-amino group in purine ring may affect the O-[^{11}C]methylation reaction of HO-precursor is unnecessary. The N-[^{11}C]methylation at 2-amino group in the purine ring is a potential competing reaction in comparison with the O-[^{11}C]methylation at 4-hydroxyl group in the 6-(4-hydroxyphenylthio) ring. However, we do not have any evidence for labeling of the 2-amino group in the purine ring, it is consistent with our previous works on the synthesis of the radiolabeled O^6-BG analogues.[28,29,31] It is also consistent with the theoretical explanation that the deprotonization at the 4-hydroxyl group is easier than at the 2-amino group since the acidity of HO– is greater than the acidity of H$_2$N–, and the [^{11}C]methylation with [^{11}C]methyl triflate will prefer to occur at the oxygen position rather than at the nitrogen position.[38] The identity of the labeled product was determined by analytical high pressure liquid chromatography (HPLC) method, and the evidence provided by the exact same HPLC reten-

tion time data of the labeled product [^{11}C]1 and reference standard 1 shows [^{11}C]methyl triflate does not label the 2-amino group and confirms the theoretical explanation. Chemical purity, radiochemical purity and specific radioactivity were determined by analytical HPLC method. The chemical purity of precursors 10, 12, and reference standard 1 was >97%. The radiochemical purity of target tracer [^{11}C]1 was >95%, and the chemical purity of target tracer [^{11}C]1 was >93%. The average (n = 3–5) specific radioactivity of target tracer [^{11}C]1 was 0.6–0.8 Ci/μmol at the end-of-synthesis (EOS).

3. Conclusion

An efficient and convenient chemical and radiochemical synthesis of the unprotected precursor and 2-N-Boc protected precursor, reference intermediate and standard, and target tracer of ABE has been developed. Radiosynthesis produced [^{11}C]ABE in amounts and purity suitable for the preclinical application of [^{11}C]ABE in animal studies by PET imaging techniques. Labeled product suitable for injection, with the specific radioactivities in a range of 0.6–0.8 Ci/μmol at EOS, can be obtained in 20–25 min from EOB, including SPE purification and formulation. These chemistry results provide the foundation for further biological evaluation of [^{11}C]ABE as a novel potential PET cancer imaging agent for hepatitis B virus and herpes simplex virus thymidine kinase in vivo.

4. Experimental

4.1. General

All commercial reagents and solvents were used without further purification unless otherwise specified. Melting points were determined on a MEL-TEMP II capillary tube apparatus and were uncorrected. ^{1}H NMR spectra were recorded on a Bruker QE 400 NMR spectrometer using tetramethylsilane (TMS) as an internal standard. Chemical shift data for the proton resonances were reported in parts per million (δ) relative to internal standard TMS (δ 0.0). The low resolution mass spectra (LRMS) were obtained using a Bruker Biflex III MALDI-Tof mass spectrometer, and the high resolution mass spectra (HRMS) measurements were obtained using a Kratos MS80 mass spectrometer, in the Department of Chemistry at Indiana University. Chromatographic solvent proportions are expressed on a volume: volume basis. Thin layer chromatography was run using Analtech silica gel GF uniplates ($5 \times 10 \, \text{cm}^2$). Plates were visualized by UV light. Normal phase flash chromatography was carried out on EM Science silica gel 60 (230–400 mesh) with a forced flow of the indicated solvent system in the proportions described below. All moisture-sensitive reactions were performed under a positive pressure of nitrogen maintained by a direct line from a nitrogen source.

Analytical HPLC was performed using a Prodigy (Phenomenex) 5 μm C-18 column, $4.6 \times 250 \, \text{mm}$; 3:1:3 CH_3CN–MeOH–20 mM, pH 6.7 $KHPO_4^-$ mobile phase, 1.5 mL/min flow rate, UV (240 nm) and γ-ray (NaI) flow detectors. Semi-prep C-18 guard cartridge column $1 \times 1 \, \text{cm}$ was obtained from E. S. Industries, Berlin, NJ, and part number 300121-C18-BD 10 μm. Sterile vented Millex-GS 0.22 μm vented filter unit was obtained from Millipore Corporation, Bedford, MA.

4.2. Bis(trifluoroethyl) (2-chloroethoxy)methylphosphonate (4)

Compound 4 was prepared by the reaction[4] of 2-chloroethyl chloromethyl ether (2) with tris(2,2,2-trifluoroethyl)phosphite (3) as a colorless liquid in a quantitative yield, $R_f = 0.58$ (1:1 hexane/EtOAc).

4.3. Bis(trifluoroethyl) (2-iodoethoxy)methylphosphonate (5)

Compound 5 was prepared by the reaction[4] of compound 4 with sodium iodide as a light brown liquid in 80% yield, $R_f = 0.31$ (CH_2Cl_2). ^{1}H NMR (CDCl$_3$, ppm): δ 4.40–4.55 (m, 4H, CH_2CF_3), 4.01 (d, 2H, $J = 8.08 \, \text{Hz}$, OCH$_2$P), 3.86 (t, 2H, $J = 6.61 \, \text{Hz}$, ICH$_2$-CH_2O), 3.27 (t, 2H, $J = 6.62 \, \text{Hz}$, ICH_2CH$_2$O). LRMS (FAB, m/z): 453 [(M+Na)$^+$, 100%]. HRMS (FAB, m/z): calcd for $C_7H_{10}F_6INaO_4P$ 452.9163. Found: 452.9163.

4.4. 2-Amino-6-[(4-methoxyphenyl)sulfanyl]purine (7)

To a 250 mL two-necked flask containing guanine (6, 5.00 g, 31.1 mmol) and dry pyridine (50 mL) was added

trifluoroacetic anhydride (17.0 mL, 120 mmol) dropwise over a period of 10 min at 0 °C. After 30 min, a solution of 4-methoxybenzenethiol (10 mL, 81.3 mmol) in dry acetonitrile (10 mL) was added dropwise over a period of 15 min. The reaction was allowed to warm up to rt and was stirred at rt overnight. Then ethanolic methylamine (16 mL) was added and the solution was stirred at rt for 2 h. After concentration under reduced pressure, the residue obtained was triturated with petroleum ether (bp 40–60 °C) and was then collected by filtration. The solid was suspended in water (100 mL), stirred, and filtered. Crystallization of the resultant solid from ethanol give a colorless crystalline solid 7 (5.58 g, 66%), mp 259–260 °C. ^{1}H NMR (DMSO-d_6, ppm): δ 12.54 (s, 1H, 9-NH), 7.93 (s, 1H, 8-CH), 7.49 (d, 2H, $J = 8.82 \, \text{Hz}$, Ph), 7.00 (d, 2H, $J = 8.82 \, \text{Hz}$, Ph), 6.13 (s, 2H, 2-NH$_2$), 3.79 (s, 3H, OCH$_3$). LRMS (FAB, m/z): 154 (100%), 296 [(M+Na)$^+$, 9.6%]. HRMS (FAB, m/z): calcd for $C_{12}H_{11}N_5NaOS$ 296.0582. Found 296.0582.

4.5. 2-Amino-6-(4-methoxyphenylthio)-9-[2-(phosphonomethoxy)ethyl]purine bis(2,2,2-trifluoroethyl) ester (ABE, 1)

To a 100 mL two-necked flask were charged with compound 7 (1.00 g, 3.66 mmol), dry DMF (20 mL) and DBU (0.6 mL, 4.01 mmol). The solution was heated at 80 °C for 1 h. Then compound 5 (1.74 g, 4.04 mmol) was added to the reaction mixture and the mixture was heated at 100 °C overnight. Solvent was removed by rotatory evaporation, and the residue was dissolved in CH_2Cl_2 and transferred to the top of a silica gel column. The column was eluted with 50:1 CH_2Cl_2/MeOH to afford a white solid 1 (0.88 g, 42%), mp 84–85 °C, $R_f = 0.36$ (20:1 CH_2Cl_2/MeOH). The chemical purity (CP) of compound 1 was determined by analytical HPLC method, $t_R1 = 6.95 \, \text{min}$, CP1 = 99.4%. The analysis of the chemical purity of compound 1 was also confirmed by the ^{1}H NMR method. ^{1}H NMR (CDCl$_3$, ppm): δ 7.70 (s, 1H, 8-CH), 7.52 (d, 2H, $J = 8.09 \, \text{Hz}$, Ph), 6.93 (d, 2H, $J = 8.83 \, \text{Hz}$, Ph), 4.90 (s, 2H, NH$_2$, D$_2$O exchangeable), 4.30–4.50 (m, 4H, OCH$_2$CF$_3$), 4.10–4.30 (m, 2H, NCH_2CH$_2$O), 3.85–4.01 (m, 4H, OCH$_2$P and NCH$_2$$CH_2$O), 3.82 (s, 3H, OCH$_3$).

4.6. 2-Amino-6-chloro-9-[2-(phosphonomethoxy)ethyl]-purine bis(2,2,2-trifluoroethyl) ester (9)

Compound 9 was prepared by the reaction[4] of 2-amino-6-chloropurine (8) with compound 5 in dry DMF and DBU as a white solid in 33% yield, mp 103–104 °C, $R_f = 0.26$ (25:1 CH_2Cl_2/MeOH). ^{1}H NMR (CDCl$_3$, ppm): δ 7.83 (s, 1H, 8-CH), 5.08 (s, 2H, 2-NH$_2$), 4.25–4.45 (m, 6H, NCH_2CH$_2$O and CH$_2$CF$_3$), 3.88–3.98 (m, 4H, OCH$_2$P and NCH$_2$$CH_2$O). LRMS (EI, m/z): 212 (100%), 471 (M$^+$, 42%). HRMS (EI, m/z): calcd for $C_{12}H_{13}ClF_6N_5O_4P$ 471.0298. Found 471.0289.

4.7. 2-Amino-6-(4-hydroxyphenylthio)-9-[2-(phosphonomethoxy)ethyl]purine bis(2,2,2-trifluoroethyl) ester (10)

Compound 10 was prepared by the reaction[4] of compound 9 with 4-hydroxythiophenol in dry pyridine

and dry DMF as a white solid in 55% yield, mp 55 °C (dec.), R_f = 0.20 (25:1 CH$_2$Cl$_2$/MeOH). The chemical purity (CP) of compound **10** was determined by analytical HPLC method, t_R**10** = 4.10 min, CP10 = 98.7%. The analysis of the chemical purity of compound **10** was also confirmed by the ^{1}H NMR method. ^{1}H NMR (DMSO-d_6, ppm): δ 9.85 (s, 1H, OH, D$_2$O exchangeable), 7.88 (s, 1H, 8-CH), 7.36 (d, 2H, J = 8.09 Hz, Ph), 6.83 (d, 2H, J = 8.83 Hz, Ph), 6.26 (s, 2H, 2-NH$_2$, D$_2$O exchangeable), 4.55–4.73 (m, 4H, CH$_2$CF$_3$), 4.20 (t, 2H, J = 5.14 Hz, NCH$_2$CH$_2$O), 4.13 (d, 2H, J = 8.09 Hz, OCH$_2$P), 3.86 (t, 2H, J = 5.15 Hz, NCH$_2$CH$_2$O). LRMS (EI, m/z): 561 (M$^+$, 100%). HRMS (EI, m/z): calcd for C$_{18}$H$_{18}$F$_6$N$_5$O$_5$PS 561.0670. Found 561.0665.

4.8. 2-N-Bis(Boc)amino-6-chloro-9-[2-(phosphonomethoxy)ethyl]purine bis(2,2,2-trifluoroethyl) ester (11)

To a 25 mL two-necked flask equipped with a stir-bar were charged with compound **9** (0.50 g, 1.06 mmol), 4-dimethylaminopyridine (DMAP, 0.010 g, 0.082 mmol), dry THF (10 mL), and Boc$_2$O (0.7 mL, 3.05 mmol). The reaction mixture was stirred at rt overnight. After removal of solvent, the residue was dissolved in CH$_2$Cl$_2$ and transferred to a silica gel column. The column was eluted with 50:1 CH$_2$Cl$_2$/MeOH to give a viscous solid **11** (0.55 g, 77%), R_f = 0.18 (50:1 CH$_2$Cl$_2$/MeOH). ^{1}H NMR (CDCl$_3$, ppm): δ 8.22 (s, 1H, 8-CH), 4.32–4.52 (m, 6H, NCH$_2$CH$_2$O and CH$_2$CF$_3$), 3.98 (t, 2H, J = 5.15 Hz, NCH$_2$CH$_2$O), 3.94 (d, 2H, J = 7.35 Hz, OCH$_2$P), 1.47 (s, 18H, Boc). LRMS (EI, m/z): 471 (100%), 671 (M$^+$, 2.1%). HRMS (EI, m/z): calcd for C$_{22}$H$_{29}$ClF$_6$N$_5$O$_8$P 671.1346. Found 671.1338.

4.9. 2-N-Bis(Boc)amino-6-(4-hydroxyphenylthio)-9-[2-(phosphonomethoxy)ethyl]purine bis(2,2,2-trifluoroethyl) ester (12)

To a 25 mL two-necked flask fitted with a condenser were charged with compound **11** (0.52 g, 0.77 mmol), 4-hydroxythiophenol (0.12 g, 0.95 mmol), pyridine (0.2 mL), and DMF (5 mL). The mixture was heated at 60 °C for 5 h. After removal of solvent at 45–50 °C, the residue was dissolved in CH$_2$Cl$_2$ and transferred to the top of a silica gel column. The column was eluted with 50:1 CH$_2$Cl$_2$/MeOH to give a white foam solid **12** (0.18 g, 31%), R_f = 0.15 (40:1 CH$_2$Cl$_2$/MeOH). The chemical purity (CP) of compound **12** was determined by analytical HPLC method, t_R**12** = 2.68 min, CP12 = 98.3%. The analysis of the chemical purity of compound **12** was also confirmed by the ^{1}H NMR method. ^{1}H NMR (CDCl$_3$, ppm): δ 8.07 (s, 1H, 8-CH), 7.46 (d, 2H, J = 8.83 Hz, Ph), 6.83 (d, 2H, J = 8.83 Hz, Ph), 5.73 (s, 1H, OH), 4.31–4.48 (m, 6H, NCH$_2$CH$_2$O and CH$_2$CF$_3$), 3.86–4.00 (m, 4H, NCH$_2$CH$_2$O and OCH$_2$P), 1.36 (s, 18H, Boc). LRMS (EI, m/z): 561 (100%), 761 (M$^+$, 4%). HRMS (EI, m/z): calcd for C$_{28}$H$_{34}$F$_6$N$_5$O$_9$PS 761.1719. Found 761.1721.

4.10. 2-N-Bis(Boc)amino-6-(4-methoxyphenylthio)-9-[2-(phosphonomethoxy)ethyl]purine bis(2,2,2-trifluoroethyl) ester (13)

To a 100 mL two-necked flask containing compound **1** (0.10 g, 0.17 mmol), DMAP (0.001 g), and dry THF

(30 mL) was added Boc$_2$O (0.16 mL, 0.70 mmol). The solution was stirred at rt overnight. Solvent was removed at reduced pressure. The residue was dissolved in CH$_2$Cl$_2$, and transferred to the top of a silica gel column. The column was eluted first with CH$_2$Cl$_2$, then 50:1 CH$_2$Cl$_2$/MeOH to afford a viscous solid **13** (0.060 g, 45%), R_f = 0.18 (50:1 CH$_2$Cl$_2$/MeOH). The chemical purity (CP) of compound **13** was determined by analytical HPLC method, t_R**13** = 4.34 min, CP13 = 97.8%. The analysis of the chemical purity of compound **13** was also confirmed by the ^{1}H NMR method. ^{1}H NMR (CDCl$_3$, ppm): δ 8.06 (s, 1H, 8-H), 7.52 (d, 2H, J = 8.82 Hz, Ph), 6.92 (d, 2H, J = 8.82 Hz, Ph), 4.30–4.50 (m, 6H, NCH$_2$CH$_2$O and CH$_2$CF$_3$), 3.87–4.00 (m, 4H, NCH$_2$CH$_2$OCH$_2$P), 3.84 (s, 3H, OCH$_3$), 1.35 (s, 18H, Boc). LRMS (EI, m/z): 121 (100%), 775 (M$^+$, 12.5%). HRMS (EI, m/z): calcd for C$_{29}$H$_{36}$F$_6$N$_5$O$_9$PS 775.1876. Found 775.1879.

4.11. 2-Amino-6-(4-[^{11}C]methoxyphenylthio)-9-[2-(phosphonomethoxy)ethyl]purine bis(2,2,2-trifluoroethyl) ester ([^{11}C]ABE, [^{11}C]1)

4.11.1. Starting from unprotected precursor 10. ^{11}CO$_2$ was produced by the ^{14}N(p,α)^{11}C nuclear reaction in small volume (12.3 cm^3) aluminum gas target (CTI) from 11 MeV proton cyclotron on research purity nitrogen (+3% O$_2$) in a Siemens radionuclide delivery system (RDS-112). The precursor **10** (0.6–1.0 mg) was dissolved in CH$_3$CN (300 μL). To this solution was added TBAH (2–3 μL, 1 M solution in methanol). The mixture was transferred to a small volume, three-neck reaction tube. ^{11}CH$_3$OTf that was produced by the gas-phase production method[32] from ^{11}CO$_2$ through ^{11}CH$_4$ and ^{11}CH$_3$Br was passed into the air-cooled reaction tube at −15 to −20 °C, which was generated by a Venturi cooling device powered with 100 psi compressed air, until radioactivity reached a maximum (~3 min), then the reaction tube was heated at 70–80 °C for 3 min. The contents of the reaction tube were diluted with NaHCO$_3$ (1 mL, 0.1 M). This solution was passed onto a C-18 cartridge by gas pressure. The cartridge was washed with H$_2$O (2 × 3 mL), and the aqueous washing was discarded. The product was eluted from the column with EtOH (2 × 3 mL), and then passed onto a rotatory evaporator. The solvent was removed by evaporation under high vacuum. The labeled product [^{11}C]1 was formulated with NaH$_2$PO$_4$ (50 mM), whose volume was dependent upon the use of the labeled product **1** in tissue biodistribution studies (~6 mL, 3 × 2 mL) or in micro-PET imaging studies (1–3 mL) of tumor-bearing athymic mice[39], sterile-filtered through a sterile vented Millex-GS 0.22 μm cellulose acetate membrane and collected into a sterile vial. Total radioactivity was assayed and total volume was noted. The overall synthesis, purification and formulation time was ~20 min from EOB. The decay corrected yield, from ^{11}CO$_2$, was 50–55%. Retention times in the analytical HPLC system were: t_R10 = 4.10 min, t_R[^{11}C]1 = 6.95 min.

4.11.2. Starting from protected precursor 12. The solution of the precursor **12** (0.6–1.0 mg) in CH$_3$CN (300 μL) and TBAH (2–3 μL, 1 M solution in methanol) was reacted with ^{11}CH$_3$OTf. The radiolabeling mixture

containing [^{11}C]13 in reaction tube was added with 1 N HCl (0.5 mL) and heated at 70–80 °C for another 3 min. The contents of the reaction tube were diluted with NaHCO$_3$ (0.5 mL, 0.1 M). The target tracer [^{11}C]1 was isolated from the radiolabeling mixture by a C-18 cartridge through SPE purification in ~25 min with 40–55% radiochemical yield. Retention times in the analytical HPLC system were t_R12 = 2.68 min, t_R[^{11}C]13 = 4.34 min, t_R[^{11}C]1 = 6.95 min.

References and notes

1. Shaw, T.; Locarnini, S. *Drugs* 2000, *60*, 517.
2. Hong, J. H.; Choi, Y.; Chun, B. K.; Lee, K.; Chu, C. K. *Arch. Pharm. Res.* 1998, *21*, 89.
3. Gumina, G.; Song, G.-Y.; Chu, C. K. *Antiviral Chem. Chemother.* 2001, *12*, 93.
4. Sekiya, K.; Takashima, H.; Ueda, N.; Kamiya, N.; Yuasa, S.; Fujimura, Y.; Ubasawa, M. *J. Med. Chem.* 2002, *45*, 3138.
5. Starrett, J. E.; Tortolani, D. R.; Russell, J.; Hitchcock, M. J.; Whiterock, V.; Martin, J. C.; Mansuri, M. M. *J. Med. Chem.* 1994, *37*, 1857.
6. Holy, A.; Gunter, J.; Dvorakova, H.; Masojidkova, M.; Andrei, G.; Snoeck, R.; Balzarini, J.; De Clercq, E. *J. Med. Chem.* 1999, *32*, 2064.
7. Li, X.; Carmichael, E.; Feng, M.; King, I.; Doyle, T. W.; Chen, S. H. *Bioorg. Med. Chem. Lett.* 1998, *8*, 57.
8. Anastasi, C.; Vlieghe, P.; Hantz, O.; Schorr, O.; Pannecouque, C.; Witvrouw, M.; De Clercq, E.; Clayette, P.; Dereuddre-Bosquet, N.; Dormont, D.; Gondois-Rey, F.; Hirsch, I.; Kraus, J. L. *Bioorg. Med. Chem. Lett.* 2003, *13*, 2459.
9. Iyer, M.; Barrio, J. R.; Namavari, M.; Bauer, E.; Satyamurthy, N.; Nguyen, K.; Toyokuni, T.; Phelps, M. E.; Herschman, H. R.; Gambhir, S. S. *J. Nucl. Med.* 2001, *42*, 96.
10. Gambhir, S. S.; Barrio, J. R.; Herschman, H. R.; Phelps, M. E. *Nucl. Med. Biol.* 1999, *26*, 481.
11. Gambhir, S. S.; Barrio, J. R.; Phelps, M. E.; Iyer, M.; Namavari, M.; Satyamurthy, N.; Wu, L.; Green, L. A.; Bauer, E.; MacLaren, D. C.; Nguyen, K.; Berk, A. J.; Cherry, S. R.; Herschman, H. R. *Proc. Natl. Acad. Sci. U.S.A.* 1999, *96*, 2333.
12. Gambhir, S. S.; Bauer, E.; Black, M. E.; Liang, Q.; Kokoris, M. S.; Barrio, J. R.; Iyer, M.; Namavari, M.; Phelps, M. E.; Herschman, H. R. *Proc. Natl. Acad. Sci. U.S.A.* 2000, *97*, 2785.
13. Alauddin, M. M.; Conti, P. S.; Mazza, S. M.; Hamzeh, F. M.; Lever, J. R. *Nucl. Med. Biol.* 1996, *23*, 787.
14. Alauddin, M. M.; Shahinian, A.; Kundu, R. K.; Gordon, E. M.; Conti, P. S. *Nucl. Med. Biol.* 1999, *26*, 371.
15. Shiue, G. G.; Shiue, C. Y.; Lee, R. L.; MacDonald, D.; Hustinx, R.; Eck, S. L.; Alavi, A. A. *Nucl. Med. Biol.* 2001, *28*, 875.
16. Tjuvajev, J. G.; Doubrovin, M.; Akhurst, T.; Cai, S.; Balatoni, J.; Alauddin, M. M.; Finn, R.; Bornmann, W.; Thaler, H.; Conti, P. S.; Blasberg, R. G. *J. Nucl. Med.* 2002, *43*, 1072.
17. Alauddin, M. M.; Conti, P. S. *Nucl. Med. Biol.* 1998, *25*, 175.
18. Wang, J.-Q.; Zheng, Q.-H.; Fei, X.; Mock, B. H.; Hutchins, G. D. *Bioorg. Med. Chem. Lett.* 2003, *13*, 3933.
19. Wang, J.-Q.; Zheng, Q.-H.; Fei, X.; Liu, X.; Gardner, T. A.; Kao, C.; Raikwar, S. P.; Glick-Wilson, B. E.; Sullivan, M. L.; Mock, B. H.; Hutchins, G. D. *Synth. Commun.* 2004, *34*, 917.
20. Zheng, Q.-H.; Wang, J.-Q.; Liu, X.; Fei, X.; Mock, B. H.; Glick-Wilson, B. E.; Sullivan, M. L.; Raikwar, S. P.; Gardner, T. A.; Kao, C.; Hutchins, G. D. *Synth. Commun.* 2004, *34*, 689.
21. Vaidyanathan, G.; Zalutsky, M. R. *Nucl. Med. Biol.* 1998, *25*, 487.
22. Mangner, T. J.; Klecker, R. W.; Anderson, L.; Shields, A. F. *Nucl. Med. Biol.* 2003, *30*, 215.
23. Wang, J.-Q.; Zheng, Q.-H.; Fei, X.; Hutchins, G. D. *Abstracts of Papers of the American Chemical Society* 2003, *226*, 133-MEDI.
24. Zheng, Q.-H.; Wang, J.-Q.; Fei, X.; Hutchins, G. D. *Synthesis* 2003, *18*, 2785.
25. Brand, B.; Reese, C. B.; Song, Q.; Visintin, C. *Tetrahedron* 1999, *55*, 5239.
26. Yun, M.; Oh, S. J.; Ha, H. J.; Ryu, J. S.; Moon, D. H. *Nucl. Med. Biol.* 2003, *30*, 151.
27. Dey, S.; Garner, P. *J. Org. Chem.* 2000, *65*, 7697.
28. Zheng, Q.-H.; Liu, X.; Fei, X.; Wang, J.-Q.; Ohannesian, D. W.; Erickson, L. C.; Stone, K. L.; Hutchins, G. D. *Nucl. Med. Biol.* 2003, *30*, 405.
29. Liu, X.; Zheng, Q.-H.; Fei, X.; Wang, J.-Q.; Ohannesian, D. W.; Erickson, L. C.; Stone, K. L.; Hutchins, G. D. *Bioorg. Med. Chem. Lett.* 2003, *13*, 641.
30. Liu, X.; Zheng, Q.-H.; Hutchins, G. D.; Fei, X. S.; Erickson, L. C.; Miller, K. D.; Mock, B. H.; Glick-Wilson, B. E.; Winkle, W. L.; Stone, K. L.; Carlson, K. A. *Synth. Commun.* 2003, *33*, 941.
31. Zheng, Q.-H.; Liu, X.; Fei, X. S.; Wang, J.-Q.; Ohannesian, D. W.; Erickson, L. C.; Stone, K. L.; Martinez, T. D.; Miller, K. D.; Hutchins, G. D. *J. Labelled Compd. Radiopharm.* 2002, *45*, 1239.
32. Mock, B. H.; Mulholland, G. K.; Vavrek, M. T. *Nucl. Med. Biol.* 1999, *26*, 467.
33. Jewett, D. M. *Appl. Radiat. Isot.* 1992, *43*, 1383.
34. Zheng, Q.-H.; Mulholland, G. K. *Nucl. Med. Biol.* 1996, *23*, 981.
35. Zheng, Q.-H.; Fei, X.; Liu, X.; Wang, J.-Q.; Sun, H. B.; Mock, B. H.; Stone, K. L.; Martinez, T. D.; Miller, K. D.; Sledge, G. W.; Hutchins, G. D. *Nucl. Med. Biol.* 2002, *29*, 761.
36. Zheng, Q.-H.; Fei, X.; DeGrado, T. R.; Wang, J.-Q.; Stone, K. L.; Martinez, T. D.; Gay, D. J.; Baity, W. L.; Mock, B. H.; Glick-Wilson, B. E.; Sullivan, M. L.; Miller, K. D.; Sledge, G. W.; Hutchins, G. D. *Nucl. Med. Biol.* 2003, *30*, 753.
37. Fei, X.; Zheng, Q.-H.; Liu, X.; Wang, J.-Q.; Sun, H. B.; Mock, B. H.; Stone, K. L.; Miller, K. D.; Sledge, G. W.; Hutchins, G. D. *Bioorg. Med. Chem. Lett.* 2003, *13*, 2217.
38. Fei, X. S.; Zheng, Q.-H.; Hutchins, G. D.; Liu, X.; Stone, K. L.; Carlson, K. A.; Mock, B. H.; Winkle, W. L.;

Glick-Wilson, B. E.; Miller, K. D.; Fife, R. S.; Sledge, G. W.; Sun, H. B.; Carr, R. E. *J. Labelled Compd. Radiopharm.* **2002**, *45*, 449.

39. Zheng, Q.-H.; Stone, K. L.; Mock, B. H.; Miller, K. D.; Fei, X.; Liu, X.; Wang, J.-Q.; Glick-Wilson, B. E.; Sledge, G. W.; Hutchins, G. D. *Nucl. Med. Biol.* **2002**, *29*, 803.

40. Zheng, Q.-H.; Liu, X.; Fei, X.; Wang, J.-Q.; Mock, B. H.; Glick-Wilson, B. E.; Sullivan, M. L.; Hutchins, G. D. *Bioorg. Med. Chem. Lett.* **2003**, *13*, 1787.

[11C]Choline as a PET biomarker for assessment of prostate cancer tumor models

Qi-Huang Zheng,[a,*] Thomas A. Gardner,[b] Sudhanshu Raikwar,[b] Chinghai Kao,[b]
K. Lee Stone,[a] Tanya D. Martinez,[a] Bruce H. Mock,[a] Xiangshu Fei,[a] Ji-Quan Wang[a]
and Gary D. Hutchins[a]

[a]Department of Radiology, Indiana University School of Medicine, 1345 West 16th Street, L-3 Room 202, Indianapolis,
IN 46202-2111, USA
[b]Department of Urology, Indiana University School of Medicine, 975 West Walnut Street, Indianapolis, IN 46202-5121, USA

Abstract—[11C]Choline has been evaluated as a positron emission tomography (PET) biomarker for assessment of established human prostate cancer tumor models. [11C]Choline was prepared by the reaction of [11C]methyl triflate with 2-dimethylamino-ethanol (DMAE) and isolated and purified by solid-phase extraction (SPE) method in 60–85% yield based on [11C]CO$_2$, 15–20 min overall synthesis time from end of bombardment (EOB), 95–99% radiochemical purity and specific activity >0.8 Ci/μmol at end of synthesis (EOS). The biodistribution of [11C]choline was determined at 30 min post iv injection in prostate cancer tumor models C4-2, PC-3, CWR22rv, and LNCaP tumor-bearing athymic mice. The results showed the accumulation of [11C]choline in these tumors was 1.0% dose/g in C4-2 mouse, 0.4% dose/g in PC-3 mice, 3.2% dose/g in CWR22rv mice, and 1.4% dose/g in LNCaP mice; the ratios of tumor/muscle (T/M) and tumor/blood (T/B) were 2.3 (T/M, C4-2), 1.4 (T/M, PC-3), 2.5 (T/M, CWR22rv), 1.2 (T/M, LNCaP) and 2.6 (T/B, C4-2), 2.6 (T/B, PC-3), 7.8 (T/B, CWR22rv), 3.2 (T/B, LNCaP), respectively. The micro-PET imaging of [11C]choline in prostate cancer tumor models was acquired from a C4-2, PC-3, CWR22rv, or LNCaP implanted mouse at 30 min post iv injection of 1 mCi of the tracer using a dedicated high resolution (<3 mm full-width at half-maximum) small FOV (field-of-view) PET imaging system, IndyPET-II scanner, developed in our laboratory, which showed the accumulation of [11C]choline in C4-2, PC-3, CWR22rv, or LNCaP tumor implanted in a nude athymic mouse. The initial dynamic micro-PET imaging data indicated the average T/M ratios were approximately 3.0 (C4-2), 2.1 (PC-3), 3.5 (CWR22rv), and 3.3 (LNCaP), respectively, which showed the tumor accumulation of [11C]choline in all four tumor models is high. These results suggest that there are significant differences in [11C]choline accumulation between these different tumor types, and these differences might offer some useful measure of tumor biological process.
© 2004 Elsevier Ltd. All rights reserved.

1. Introduction

Prostate cancer is the most commonly diagnosed cancer and is the second leading cause of cancer death in men over the age 40 in the United States.[1] According to estimates, about 220,900 American men would be diagnosed with prostate cancer in the year of 2003 and 28,900 men would die from this disease. Detection of prostate cancer by various imaging methods is vital to overall management and treatment of prostate cancer

patients. Biomedical imaging technique positron emission tomography (PET) coupled with appropriate radiopharmaceuticals has become a clinically valuable and accepted diagnostic tool to image prostate cancer.[2] PET has been widely used in the diagnosis and staging of primary tumors, detection of subclinical disease, assessment of therapy response, and detection of recurrence.[3]

The most widely used radiopharmaceutical for studies in oncology is [18F]-2-fluoro-2-deoxyglucose (FDG). FDG is the only PET cancer imaging agent used clinically. FDG has been reported to be an effective imaging agent for the detection of primary and metastatic prostate cancer. FDG-PET has been used successfully in an

* Corresponding author. Tel.: +1-317-278-4671; fax: +1-317-278-9711;
e-mail: qzheng@iupui.edu

increasing number of oncological applications and is considered a valuable adjunct to anatomic imaging methods, providing unique functional information for better characterization of disease.[4] FDG has shown promise in predicting outcomes and detecting prostate tumors based on metabolic activity of the tumor(s); however, the low cellular uptake rate of FDG in prostate cancer limits its usefulness, and several other radiopharmaceuticals have been developed that evaluate prostate tumors based on other physiologic properties. For example, [11C]choline has been used as a PET tracer for human cancer detection and succeeded in visualizing prostate cancer and many other types of cancers in patients.[5–8] [18F]Fluorocholine and F-18 labeled choline analogues also have been developed as new and promising oncologic PET tracers for prostate cancer and breast cancer in human.[9–11] However, the mechanism of the choline accumulation in tumors is not clear. The concept of [11C]choline as an oncologic PET tracer has been reported as follows. An elevated level of phosphatidylcholine has been revealed in tumors, which is the most abundant phospholipid in the cell membranes of all eukaryotic cells and provides a potential target for tumor imaging. This elevation is thought as the result of increased uptake of choline, a precursor of the biosynthesis of phosphatidylcholine.[5] Thus, [11C]choline, [18F]fluorocholine, and F-18 labeled choline analogues can be used as PET biomarkers for imaging choline kinase in cell membranes in cancers, and [11C]choline and [18F]fluorocholine have been found clinically useful in humans for the study of prostate cancer.

PET has been used clinically to measure enzyme reactions, ligand–receptor interactions, cellular metabolism, and cell proliferation. Until recently, however, PET has not been suitable for small animal models because of resolution limitations.[12,13] In an effort to develop novel prostate cancer biomarkers for molecular imaging,[14] a series of PET cancer imaging agents that target either receptors or enzymes have been synthesized in this laboratory.[15–22] In an effort to develop micro-PET instrumentation for small and intermediate sized animals imaging applications, high-resolution, high-sensitivity dedicated research scanners, IndyPET and IndyPET-II, have been designed and characterized by the same laboratory.[23,24] Development of micro-PET instrumentation for small animal imaging and the availability of positron-emitting tracers have made this technology accessible for the noninvasive, quantitative, and repetitive imaging of biological function in living animals. Because small animal PET is immediately extrapolated to the clinic, laboratory advances should rapidly be translated to clinical practice.[12] To the best of our knowledge, the [11C]choline study of the prostate cancer animal models is still not reported in the literature. We have used [11C]choline-PET for imaging of breast cancer animal models,[25] and we extrapolated whether [11C]choline might be able to assess prostate cancer tumor models using micro-PET in vivo. In this paper, we evaluate the behavior of [11C]choline in four established human prostate cancer tumor models C4-2, PC-3, CWR22rv, and LNCaP tumor-bearing athymic mice.

2. Results and discussion

2.1. Synthesis of [11C]choline

[11C]Choline was prepared by the reaction of [11C]methyl triflate[26] with 2-dimethylaminoethanol (DMAE) and isolated and purified by solid-phase extraction (SPE) method[27,28] in 60–85% yield based on [11C]CO$_2$, 15–20 min overall synthesis time from end of bombardment (EOB), 95–99% radiochemical purity, and specific activity >0.8 Ci/μmol at end of synthesis (EOS). [11C]Choline was synthesized before by others using very similar chemistry.[6,8,29,30] The difference in the present paper is that [11C]methyl triflate is used instead of [11C]methyl iodide, in which [11C]methyl triflate is a proven methylation reagent with greater reactivity than [11C]methyl iodide.[31] A simple home-built technique[32] for convenient labeling and isolation of [11C]-methyl]quaternary amines by N-11C-methylation method was employed in the radiosynthesis of [11C]choline. The quality control (QC) process to determine the radiochemical purity of [11C]choline and the quantity of DMAE in the final product was performed using HPLC methods. The UV-detector we used did have the detection threshold for DMAE, and we did establish the retention time of DMAE, however, the chromatogram obtained from the HPLC system that we utilized did not show the peak of DMAE in the final [11C]choline solution. It was therefore impossible to determine accurately the quantity of DMAE in the final product. The published QC data for the concentration of DMAE in the final solution were 9–13 ppm using two separate reverse phase HPLC methods[33] and 6.9 ppm using cation-exchange chromatography,[30] which employed the same SPE technique for the [11C]choline synthesis. The final solution of [11C]choline with low concentration of starting material we prepared is suitable for injection in animals.

2.2. Prostate cancer tumor models

The prostate cancer tumor models we used were the human prostate cancer/athymice mouse xenograft models implanted with several popular human prostate cancer cell lines C4-2, PC-3, CWR22rv, and LNCaP. LNCaP, an androgen-responsive, androgen receptor (AR) positive, prostate-specific antigen (PSA) secreting human prostate cancer cell line, was derived from a cervical lymph node metastasis by Horoszewicz et al.[34] It serves as a parental cell line. C4-2 is a hormone-refractory derivative of the LNCaP epithelial prostate cancer cell line that was derived by passing through castrated mice and remains AR- and PSA-positive.[35,36] PC-3 is an androgen-independent (AI), AR-, and PSA-negative human prostate cancer cell line established by Kaighn et al.[37] from the bone marrow aspirates of a patient with confirmed metastatic disease. CWR22rv is one of the more recently developed transplantable human prostate tumor models.[38,39] This tumor exhibits androgen-dependent growth and PSA secretion in male nude athymic mice and regresses in response to androgen withdrawal. The CWR22rv cell line is a valuable

tool for studying prostate cancer progression to a hormone-refractory state, because it possesses features of clinical advanced disease: AR expression, AI proliferation, and androgen-responsiveness. It serves as a model possessing an intermediate, or transition, phenotype between that of hormone-sensitive, AR-positive cell lines (e.g., LNCaP) and AI-, AR-negative cell lines (e.g., PC-3).[40] These models have proven to be useful and become popular for investigations of human prostate cancer.

2.3. In vivo biodistribution of [^{11}C]choline in tumor models

In vivo biodistribution data of [^{11}C]choline in C4-2, PC-3, CWR22rv, and LNCaP tumor cell lines implanted athymic mice are indicated in Table 1. Since it was difficult to generate C4-2 tumor model, we only had one C4-2 tumor-bearing mouse for the biodistribution study. The data presented here for PC-3 and CWR22rv tumor-bearing mice represented the average value in three mice, and the data presented here for LNCaP tumor-bearing mice represented the average value in five mice. The average values were taken not only over several mice, but also over the several tumors in each mouse. In C4-2, PC-3, CWR22rv, and LNCaP tumor-bearing athymic mice, the liver and kidneys were found to show very high accumulation of [^{11}C]choline, consistent with findings using [^{18}F]fluorocholine in CWR22rv and PC-3 xenografts.[10,41] In comparison with heart, liver, lungs, spleen, kidneys, and small intestine, biodistribution studies of [^{11}C]choline in four prostate cancer tumor models did not show higher accumulation in tumors than in other tissues; and in comparison with blood, brain, bone, and muscle, biodistribution studies of [^{11}C]choline in four prostate cancer tumor models did show higher accumulation in tumors than in other tissues. The ratios of tumor/muscle (T/M) and tumor/ blood (T/B) may serve as the important parameters to guide in vivo evaluation of [^{11}C]choline as a PET biomarker in prostate cancer tumor models. In general, the higher T/M and T/B ratios will show the higher tumor accumulation of tracer in biodistribution studies, and tumors will be more visible with the tracer in micro-PET imaging studies. In order to be able to claim that the

tumor accumulation of the tracer is high, the lower threshold for T/M and T/B ratios should be set at least more than 1.[17] The biodistribution study results of T/M and T/B ratios presented here are very similar or superior to the reported findings using [^{18}F]FDG (T/M: 1.4; T/B: 4.4) and [^{11}C]acetate (T/M: 1.5; T/B: 2.2) in CWR22rv xenograft.[42] The biodistribution data are similar in LNCaP and C4-2 mice, and different in PC-3 and CWR22rv mice, since the biological properties between LNCaP tumor and C4-2 tumor are similar, and the biological properties between LNCaP, C4-2 tumors and PC-3 tumor and CWR22rv tumor are different. These results suggest the differences in radioactivity retention in tumors might be in relation to biological differences between these various cell lines.
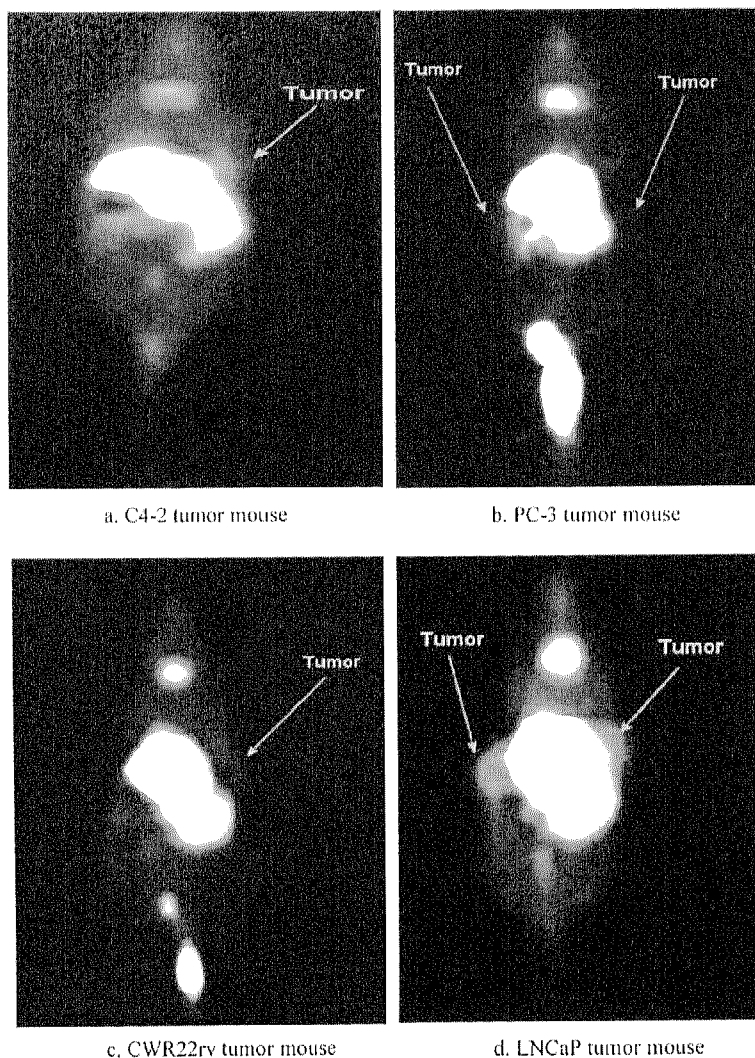
2.4. IndyPET-II scanner

The animal PET scanners, IndyPET and IndyPET-II, were designed and developed by Hutchins and co-workers.[23,24] These are high resolution (<3 mm fullwidth at half-maximum), high sensitivity, research PET scanner developed for small field-of-view (FOV) imaging applications including rodent imaging (mice and rats), intermediate size animals (dogs, pigs, and primates), and dedicated human imaging applications (brain, breast). The micro-PET scanner we used is IndyPET-II scanner.

2.5. In vivo micro-PET imaging of [^{11}C]choline in tumor models

Tumor-specific micro-PET imaging was performed using the IndyPET-II scanner for 15 min static scans after an initial 30 min accumulation period of [^{11}C]choline. In vivo micro-PET images of [^{11}C]choline in C4-2, PC-3, CWR22rv, and LNCaP tumors implanted in a nude athymic mouse are shown in Figure 1. The PET images show a lot of accumulation of the tracer in the liver. The regions of the tumor are difficult to decipher from the images, because the activity spilling over from the liver might result in overestimation of tumor accumulation. The tracer retention in C4-2 tumor mouse and

Table 1. Biodistribution data (% dose/g) of [^{11}C]choline in C4-2, PC-3, CWR22rv, and LNCaP prostate tumor-bearing athymic mice at 30 min post iv injection

| Tissue	C4-2 ($n = 1$)	PC-3 ($n = 3$)	CWR22rv ($n = 3$)	LNCaP ($n = 5$)
Blood	0.39	0.19 ± 0.12	0.49 ± 0.31	0.45 ± 0.26
Brain	0.64	0.16 ± 0.02	0.64 ± 0.31	0.45 ± 0.25
Heart	2.21	1.06 ± 0.35	4.32 ± 1.44	5.28 ± 3.06
Liver	14.16	9.07 ± 3.65	23.31 ± 6.52	14.93 ± 10.12
Lungs	3.99	1.23 ± 0.21	5.95 ± 1.96	4.60 ± 2.90
Spleen	1.84	1.28 ± 0.49	5.43 ± 1.94	2.93 ± 1.49
Kidneys	13.16	5.12 ± 1.76	14.90 ± 5.62	17.23 ± 9.11
Small intestine	2.02	1.94 ± 0.52	6.55 ± 2.02	4.67 ± 2.25
Bone	0.69	0.44 ± 0.12	1.46 ± 0.71	1.12 ± 0.68
Muscle	0.45	0.31 ± 0.12	1.46 ± 0.80	1.18 ± 0.64
Tumor	1.02	0.44 ± 0.17	3.16 ± 0.71	1.36 ± 0.68
Tumor/muscle ratio	2.27	1.42 ± 0.23	2.47 ± 0.98	1.17 ± 0.36
Tumor/blood ratio	2.62	2.55 ± 0.63	7.79 ± 3.50	3.19 ± 0.82

a. C4-2 tumor mouse   b. PC-3 tumor mouse

c. CWR22rv tumor mouse   d. LNCaP tumor mouse

Figure 1. Micro-PET images of [^{11}C]choline in a C4-2 (a), PC-3 (b), CWR22rv (c), and LNCaP (d) tumor-bearing athymic mouse.

LNCaP tumor mouse is clear, and the C4-2 tumor and LNCaP tumor in micro-PET images are visible. The tracer retention in PC-3 tumor mouse and CWR22rv tumor mouse in micro-PET images is unclear, which is not consistent with their biodistribution data.

In order to quantitate PET data, the initial dynamic micro-PET imaging studies were performed in C4-2, PC-3, CWR22rv, and LNCaP tumor-bearing mice. The time activity curves for T/M ratios versus time are shown in Figure 2 (a. C4-2 tumor; b. PC-3 tumors; c. CWR22rv tumor; d. LNCaP tumors) with the average T/M ratio at an approximate value 3.0 (C4-2), 2.1 (PC-3), 3.5 (CWR22rv), and 3.3 (LNCaP), respectively. The T/M ratio found from dynamic PET data is systematically much higher than that from biodistribution data. A region of interest (ROI) was placed on the organ or tumor of interest in the transaxial micro-PET images that include the entire organ or tumor volume. The average radioactivity concentration within a tumor or an organ was obtained from the average pixel values

within the multiple ROI volume.[42] The T/M ratio data showed the tumor retention of [^{11}C]choline in all four prostate cancer tumor models is high. T/M is more or less constant over the whole time period. This is also the case for T and M or both were increasing or decreasing at a same rate. Figure 2 demonstrated both the differences in reproducibility between tumor types and the obvious differences in kinetics between tumors. These differences are correlative with both the biodistribution data and the cell biology of the various tumor lines. In particular, the tumors with the highest overall accumulation of radioactivity (CWR22rv tumor, 3.16% dose/g) also had the more protracted uptake phase. This is also the similar case in LNCaP tumor (1.36% dose/g). It is likely the highest overall retention of radioactivity in tumors would accumulate more slowly. The dynamic IndyPET-II data are similar in LNCaP and C4-2 mice, and different in PC-3 and CWR22rv mice, because the cell biology between LNCaP tumor and C4-2 tumor are similar, and the cell biology between LNCaP, C4-2 tumors and PC-3 tumor and CWR22rv tumor are differ-
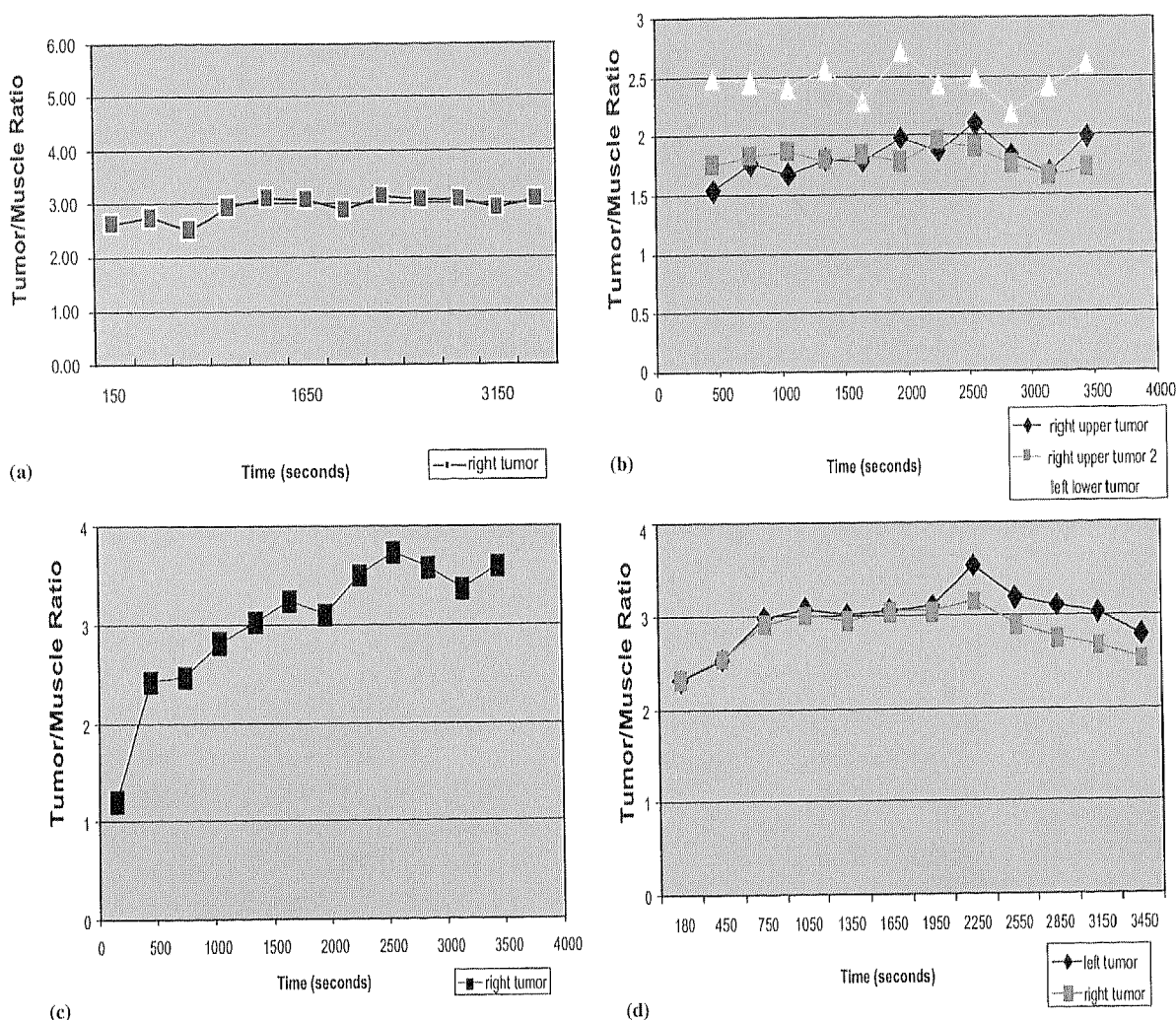
Figure 2. Tumor/muscle ratio versus time curve in C4-2 (a), PC-3 (b), CWR22rv (c), and LNCaP (d) tumors, the average tumor/muscle ratios are approximately 3.0, 2.1, 3.5, and 3.3, respectively.

ent. These results suggest the kinetic differences in radioactivity accumulation in tumors might be in relation to cell biology differences between these various cell lines.

It is interesting to note that the tumor/muscle ratios of biodistribution studies are lower than the micro-PET derived ratios in all the four models. This is unusual and the opposite finding (i.e., lower ratios by micro-PET may have been expected). This might suggest that the ROI's in PET images need to be carefully examined. With the IndyPET-II scanner, a mouse study had a quantitative accuracy of less than 10% in error, and most within the 5% range, regardless of whether the ROI is superficial or deep within the mouse body. The partial volume effect in estimating the ROI values from micro-PET images were small in these IndyPET-II scans because the resolution of the IndyPET-II scanner is around 2.5 mm and the implanted prostate tumors were in the range of 1 cm or more than 1 cm in diameter, which was well above the resolution limit of this animal PET system. Moreover, the dynamic IndyPET-II

imaging studies were co-registered with the EVS RS-9 micro-CT imaging studies,[43] which helped to select and draw ROI. Therefore, we conclude the dynamic Indy-PET-II data are more reliable and less partial volume effects were involved. However, the discrepancy between biodistribution and micro-PET data need to be further studied.

3. Conclusion

In summary, we have developed a simple technique for the radiosynthesis and routine production of [^{11}C]choline. In vivo biodistribution studies and in vivo micro-PET images of [^{11}C]choline in prostate cancer athymic mice showed that [^{11}C]choline had different accumulation with C4-2, PC-3, CWR22rv, and LNCaP tumors. These results suggest that there are significant differences in [^{11}C]choline accumulation between these different tumor types, and these differences might offer some useful measure of tumor biological process.

4. Materials and methods

4.1. General

All commercial reagents and solvents were used without further purification. The [^{11}C]methyl triflate was made according to the literature procedures[26,31] by the meta-thetical reaction of [^{11}C]methyl bromide over a hot column of silver triflate supported on porous graphite. One silver triflate column was used for 20–40 [^{11}C]methyl triflate runs before replacement.

Analytical HPLC was performed using a Prodigy (Phenomenex) 5 μm C-18 column, 4.6×250 mm; 3:1:3 $CH_3CN/MeOH/20$ mM, pH 6.7 $KHPO_4^-$ mobile phase, flow rate 1.5 mL/min, and UV (240 nm) and γ-ray (NaI) flow detectors. Semi-prep C-18 SiO_2 Sep-Pak type cartridges were obtained from Waters Corporation, Milford, MA. Sterile vented Millex-GS 0.22 μm vented filter units were obtained from Millipore Corporation, Bedford, MA.

4.2. Synthesis of [^{11}C]choline

The precursor 2-dimethylaminoethanol (10 μL) was dissolved in acetonitrile (250 μL). The mixture was transferred to a small volume, three-neck reaction tube. [^{11}C]Methyl triflate was passed into the air-cooled reaction tube at −15 to −20 °C, which was generated by a Venturi cooling device powered with 100 psi compressed air, until activity reaches a maximum (2–3 min), then the reaction tube was isolated and heated at 70–80 °C for 2–3 min. The reaction tube was connected to the SiO_2 Sep-Pak type cartridge. The product solution was passed onto the Sep-Pak cartridge for solid-phase extraction (SPE) by gas pressure. The reaction tube and Sep-Pak were washed with ethanol (2×5 mL), and the washing solution was discarded to a waste bottle. The product was eluted from the Sep-Pak with 90:8:2 $H_2O/$EtOH/HOAc (4.6 mL) and sterile-filtered through a 0.22 μm cellulose acetate membrane and collected into a sterile vial. The pH was adjusted to 5.5–7.0 with 2 M NaOH and 150 mM NaH_2PO_4 mixed solution (1:20, ∼0.4 mL). Total radioactivity was assayed and the total volume was noted. The overall synthesis time was 15–20 min. The decay-corrected yield, from $^{11}CO_2$, was 60–85%, and the radiochemical purity was 95–99% by analytical HPLC method. Retention times in the analytical HPLC system we utilized were 2.0 min for [^{11}C]choline and 2.4 min for DMAE.

4.3. Prostate cancer athymic mice

All animal experiments were performed under a protocol approved by the Indiana University institutional animal care and use committee. Six weeks old male, athymic nude mice (Harlan) were used for the generation of subcutaneous prostate tumor xenografts. For the generation of C4-2 and LNCaP models, 10 million cells (per injection site per animal) in the log phase were gently mixed with 100 μL of ice cold Matrigel (Becton-

Dickinson Biosciences) and injected in the lower flank region of the mouse using a 27 gauge 1/2 cc syringe. For generating PC-3 tumors 2 million cells/injection site per animal were used without any Matrigel. CWR22rv tumors were generated by injecting 5 million cells in the presence of Matrigel per injection site per animal. Palpable tumors became evident within 4–8 weeks post-implantation. The size of the palpable tumors was in the range of 1 cm or more than 1 cm in diameter. The tumors were firm without necrotic tissue around the tumors. The tumor sizes varied between the different models.

4.4. Biodistribution studies of [^{11}C]choline in prostate cancer athymic mice

Athymic mice 8 weeks post-xenograft implantation were injected intravenously with sub-pharmacologic doses (1–3 mCi) of [^{11}C]choline via the tail vein while under conscious restraint. At 30 min post injection, mice were sacrificed by decapitation under halothane anesthesia, their tissues quickly excised, weighed, and the decay-corrected radioactive content measured using an auto Packard Cobra Quantum gamma counter. The tissue localization at 30 min time point, expressed as % of injected dose per gram of tissue (% dose/g), weight normalized % dose/g and % of injected dose per organ were calculated from the tissue count and weight data using an Excel spreadsheet program.

4.5. Micro-PET imaging of [^{11}C]choline in prostate cancer athymic mice

The IndyPET-II scanner was used for these studies. The mouse was anesthetized with acepromazine (0.2 mg/kg, i.m.) and torbugesic (0.2 mg/kg, i.m.). One millicurie of [^{11}C]choline was administered intravenously to the mouse in tail vein. The micro-PET imaging of [^{11}C]choline in prostate cancer athymic mice was acquired by the ordered subsets expectation maximization (OSEM) using six subsets/four iterations for 5 min from a C4-2, PC-3, CWR22rv, or LNCaP tumor-bearing mouse at 30 min post iv injection of 1 mCi of the tracer. Dynamic imaging was performed for 60 min starting at the injection of 1 mCi of [^{11}C]choline to each mouse. The frame durations were defined as 300 s for entire 3600 s scan. All images were acquired in list-mode and sorted into 15×20 s frames, 10×60 s frames, and 9×300 s frames. Images were reconstructed using filtered back projection with a 70% Hanning filter (4.242 cm^{-1} cutoff frequency).

References and notes

1. Jemal, A.; Thomas, A.; Murray, T.; Thun, M. *CA Cancer J. Clin.* **2002**, *52*, 23.
2. Jadvar, H.; Pinski, J. K.; Conti, P. S. *Oncol. Rep.* **2003**, *10*, 1485.
3. Varagnolo, L.; Stokkel, M. P. M.; Mazzi, U.; Pauwels, E. K. J. *Nucl. Med. Biol.* **2000**, *27*, 103.
4. Smith, D. A. T. *Nucl. Med. Commun.* **1998**, *19*, 97.
5. Hara, T.; Kosaka, N.; Kishi, H. *J. Nucl. Med.* **1998**, *39*, 990.
6. Hara, T.; Kosaka, N.; Shinoura, N.; Kondo, T. *J. Nucl. Med.* **1997**, *38*, 842.
7. Hara, T.; Kosaka, N.; Kishi, H.; Kobori, O. *J. Nucl. Med.* **1997**, *38*, 250P.
8. Hara, T.; Yuasa, M. *Appl. Radiat. Isot.* **1999**, *50*, 531.
9. DeGrado, T. R.; Baldwin, S. W.; Wang, S.; Orr, M. D.; Liao, R. P.; Friedman, H. S.; Reiman, R.; Price, D. T.; Coleman, R. E. *J. Nucl. Med.* **2001**, *42*, 1805.
10. DeGrado, T. R.; Coleman, R. E.; Wang, S.; Baldwin, S. W.; Orr, M. D.; Robertson, C. N.; Polascik, T. J.; Price, D. T. *Cancer Res.* **2000**, *61*, 110.
11. DeGrado, T. R.; Reiman, R. E.; Price, D. T.; Wang, S.; Coleman, R. E. *J. Nucl. Med.* **2002**, *43*, 92.
12. Herschman, H. R. *Curr. Opin. Immunol.* **2003**, *15*, 378.
13. Del Guerra, A.; Belcari, N. *Q. J. Nucl. Med.* **2002**, *46*, 35.
14. Weissleder, R.; Mahmood, U. *Radiology* **2001**, *219*, 316.
15. Fei, X.; Zheng, Q.-H.; Hutchins, G. D.; Liu, X.; Stone, K. L.; Carlson, K. A.; Mock, B. H.; Winkle, W. L.; Glick-Wilson, B. E.; Miller, K. D.; Fife, R. S.; Sledge, G. W.; Sun, H. B.; Carr, R. E. *J. Label. Compd. Radiopharm.* **2002**, *45*, 449.
16. Zheng, Q.-H.; Fei, X.; Liu, X.; Wang, J.-Q.; Sun, H. B.; Mock, B. H.; Stone, K. L.; Martinez, T. D.; Miller, K. D.; Sledge, G. W.; Hutchins, G. D. *Nucl. Med. Biol.* **2002**, *29*, 761.
17. Zheng, Q.-H.; Fei, X.; DeGrado, T. R.; Wang, J.-Q.; Stone, K. L.; Martinez, T. D.; Gay, D. J.; Baity, W. L.; Mock, B. H.; Glick-Wilson, B. E.; Sullivan, M. L.; Miller, K. D.; Sledge, G. W.; Hutchins, G. D. *Nucl. Med. Biol.* **2003**, *30*, 753.
18. Liu, X.; Zheng, Q.-H.; Fei, X.; Wang, J.-Q.; Ohannesian, D. W.; Erickson, L. C.; Stone, K. L.; Hutchins, G. D. *Bioorg. Med. Chem. Lett.* **2003**, *13*, 641.
19. Zheng, Q.-H.; Liu, X.; Fei, X.; Wang, J.-Q.; Ohannesian, D. W.; Erickson, L. C.; Stone, K. L.; Hutchins, G. D. *Nucl. Med. Biol.* **2003**, *30*, 405.
20. Wang, J.-Q.; Zheng, Q.-H.; Fei, X.; Liu, X.; Gardner, T. A.; Kao, C.; Raikwar, S. P.; Glick-Wilson, B. E.; Sullivan,

M. L.; Mock, B. H.; Hutchins, G. D. *Synth. Commun.* **2004**, *34*, 917.
21. Zheng, Q.-H.; Wang, J.-Q.; Liu, X.; Fei, X.; Mock, B. H.; Glick-Wilson, B. E.; Sullivan, M. L.; Raikwar, S. P.; Gardner, T. A.; Kao, C.; Hutchins, G. D. *Synth. Commun.* **2004**, *34*, 689.
22. Zheng, Q.-H.; Wang, J.-Q.; Fei, X.; Hutchins, G. D. *Synthesis* **2003**;(18), 2785.
23. Frese, T.; Rouze, N. C.; Bouman, C. A.; Sauer, K.; Hutchins, G. D. *IEEE Trans. Med. Imaging* **2003**, *22*, 258.
24. Rouze, N. C.; Hutchins, G. D. *IEEE Trans. Nucl. Sci.* **2003**, *50*, 1491.
25. Zheng, Q.-H.; Stone, K. L.; Mock, B. H.; Miller, K. D.; Fei, X.; Liu, X.; Wang, J.-Q.; Glick-Wilson, B. E.; Sledge, G. W.; Hutchins, G. D. *Nucl. Med. Biol.* **2002**, *29*, 803.
26. Mock, B. H.; Mulholland, G. K.; Vavrek, M. T. *Nucl. Med. Biol.* **1999**, *26*, 467.
27. Zheng, Q.-H.; Mulholland, G. K. *Nucl. Med. Biol.* **1996**, *23*, 981.
28. Mulholland, G. K.; Zheng, Q.-H.; Mock, B. H.; Vavrek, M. T. *J. Label. Compd. Radiopharm.* **1999**, *42*, S459.
29. Pascali, C.; Bogni, A.; Iwata, R.; Cambie, M.; Bombardieri, E. *J. Label. Compd. Radiopharm.* **2000**, *43*, 195.
30. Mishani, E.; Ben-David, I.; Rozen, Y. *Nucl. Med. Biol.* **2002**, *29*, 359.
31. Jewett, D. M. *Appl. Radiat. Isot.* **1992**, *43*, 1383.
32. Zheng, Q.-H.; Liu, X.; Fei, X.; Wang, J.-Q.; Mock, B. H.; Glick-Wilson, B. E.; Sullivan, M. L.; Hutchins, G. D. *Bioorg. Med. Chem. Lett.* **2003**, *13*, 1787.
33. Mishani, E.; Bocher, M.; Ben-David, I.; Rozen, Y.; Laky, D.; Marciano, R.; Chisin, R. *J. Label. Compd. Radiopharm.* **2001**, *44*, S379.
34. Horoszewicz, J. S.; Leong, S. S.; Kawinski, E.; Karr, J. P.; Rosenthal, H.; Chu, T. M.; Mirand, E. A.; Murphy, G. P. *Cancer Res.* **1983**, *43*, 1809.
35. Wu, H. C.; Hsieh, J. T.; Gleave, M. E.; Brown, N. M.; Pathak, S.; Chung, L. W. *Int. J. Cancer* **1994**, *57*, 406.
36. Matsubara, S.; Wada, Y.; Gardner, T. A.; Egawa, M.; Park, M. S.; Hsieh, C. L.; Zhau, H. E.; Kao, C.; Kamidono, S.; Gillenwater, J. Y.; Chung, L. W. *Cancer Res.* **2001**, *61*, 6012.
37. Kaighn, M. E.; Narayan, K. S.; Ohnuki, Y.; Lechner, J. F.; Jones, L. W. *Invest. Urol.* **1979**, *17*, 16.
38. Pretlow, T. G.; Wolman, S. R.; Micale, M. A.; Pelley, R. J.; Kursh, E. D.; Resnick, M. I.; Bodner, D. R.; Jacobberger, J. W.; Delmoro, C. M.; Giaconia, J. M. *J. Natl. Cancer Inst.* **1993**, *85*, 394.
39. Wainstein, M. A.; He, F.; Robinson, D.; Kung, H. J.; Schwartz, S.; Giaconia, J. M.; Edgehouse, N. L.; Pretlow, T. P.; Bodner, D. R.; Kursh, E. D. *Cancer Res.* **1994**, *54*, 6049.
40. Tepper, C. G.; Boucher, D. L.; Ryan, P. E.; Ma, A. H.; Xia, L.; Lee, L. F.; Pretlow, T. G.; Kung, H. J. *Cancer Res.* **2002**, *62*, 6606.
41. Price, D. T.; Coleman, R. E.; Liao, R. P.; Robertson, C. N.; Polascik, T. J.; DeGrado, T. R. *J. Urol.* **2002**, *168*, 273.
42. Oyama, N.; Kim, J.; Jones, L. A.; Mercer, N. M.; Engelbach, J. A.; Sharp, T. L.; Welch, M. *J. Nucl. Med. Biol.* **2002**, *29*, 783.
43. Hutchins, G. D.; Rouze, N.; Stone, K. L.; Krishnamurthi, G.; Liang, Y. *J. Nucl. Med.* **2002**, *43*, 59P.

An Improved Total Synthesis of PET HSV-tk Gene Reporter Probe 9-(4-[18F]Fluoro-3-hydroxymethylbutyl)guanine ([18F]FHBG)

**Qi-Huang Zheng,[1,*] Ji-Quan Wang,[1] Xuan Liu,[1]
Xiangshu Fei,[1] Bruce H. Mock,[1] Barbara E. Glick-Wilson,[1]
Michael L. Sullivan,[1] Sudhanshu P. Raikwar,[2]
Thomas A. Gardner,[2] Chinghai Kao,[2]
and Gary D. Hutchins[1]**

Departments of [1]Radiology and [2]Urology, Indiana University School of
Medicine, Indianapolis, Indiana, USA

ABSTRACT

An improved total synthesis of [18F]FHBG starting from triethyl-1,1,2-ethanetricarboxylate and 2-amino-6-chloropurine is reported. [18F]FHBG was prepared by nucleophilic substitution of the appropriate precursor with [18F]KF/Kryptofix 2.2.2 followed by a quick deprotection reaction and purification with a simplified Silica Sep-Pak solid-phase extraction (SPE) method in 20–25% radiochemical yield.

*Correspondence: Qi-Huang Zheng, Department of Radiology, Indiana University School of Medicine, 1345 West 16th Street, L-3 Room 202, Indianapolis, IN 46202-2111, USA; E-mail: qzheng@iupui.edu.

Key Words: 9-(4-[¹⁸F]fluoro-3-hydroxymethylbutyl)guanine ([¹⁸F]FHBG);
Penciclovir (PCV); Synthesis; Positron emission tomography (PET); Herpes
simplex virus thymidine kinase (HSV-tk); Gene expression.

INTRODUCTION

In an effort to develop novel cancer biomarkers for molecular imaging,[1]
a series of positron emission tomography (PET) cancer imaging agents that
target either receptors or enzymes have been synthesized in this laboratory. In
the past, we have synthesized several carbon-11, fluorine-18 and iodine-123/
125 labeled quinazoline derivatives for epidermal growth factor receptor
(EGFr) imaging,[2,3] numerous carbon-11 labeled matrix metalloproteinase
inhibitors[4−9] that target enzymes matrix metalloproteinases, which are
overexpressed in human malignant tumor tissues of various organs including
the breast, prostate, stomach, colon, and lung, as well as a number of carbon-
11 labeled O^6-benzylguanine derivatives[10−13] that target human DNA repair
protein alkylguanine-DNA alkyltransferase overexpressed in many cancer
types. We also prepared [¹¹C]choline as PET cancer imaging agent to study
phosphatidylcholine in cancers.[14] The objective of this study was to
synthesize PET gene reporter probes such as fluorine-18 labeled ganciclovir
(GCV, 9-[(1,3-dihydroxy-2-propoxy)methyl]guanine) and penciclovir (PCV,
9-[4-hydroxy-3(hydroxymethyl)butyl]guanine) analogs 8-[¹⁸F]fluoroganci-
clovir ([¹⁸F]FGCV), 9-[(3-[¹⁸F]fluoro-1-hydroxy-2-propoxy)methyl]guanine
([¹⁸F]FHPG); 8-[¹⁸F]fluoropenciclovir ([¹⁸F]FPCV), 9-(4-[¹⁸F]fluoro-3-
hydroxymethylbutyl)guanine ([¹⁸F]FHBG) for *in vivo* imaging of herpes
simplex virus thymidine kinase (HSV-tk) expression.[15−37] In our previous
work, we have reported an improved total synthesis of [¹⁸F]FHPG.[38] Here,
we report an improved total synthesis of [¹⁸F]FHBG, which includes full
experiment procedures, yields, analytical details and new findings in synthetic
methodology for target tracer [¹⁸F]FHBG, as well as key intermediate PCV
and tosylated precursor.

RESULTS AND DISCUSSION

1. Synthesis of Penciclovir

The synthesis of penciclovir (PCV) as indicated in Sch. 1 was performed
with the modifications according to procedures reported in the literature.[25]
The commercially available starting material triethyl-1,1,2-ethanetricarboxy-
late (**2**) was converted into 2-(hydroxymethyl)butane-1,4-diol (**3**) through
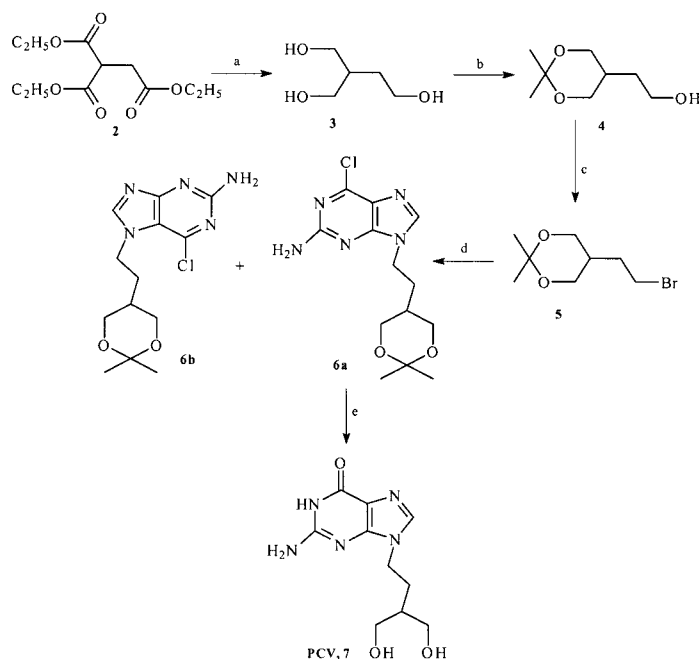
Scheme 1. Synthesis of PCV. (a) NaBH$_4$, tBuOH; (b) 2,2-dimethoxypropane, *p*-toluenesulfonic acid, THF; (c) CBr$_4$, PPh$_3$, THF, 0°C; (d) 2-amino-6-chloropurine, K$_2$CO$_3$, DMF; and (e) 2 M HCl.

reduction reaction with excessive sodium borohydride (NaBH$_4$) in *tert*-butyl alcohol in a yield of 66%. The crude product contained a polar contaminant that was suspected to be boric acid resulted from hydrolysis of NaBH$_4$. Although the contaminant did not affect the further use of **3**, it was convenient to remove it by column chromatography (10 : 1 EtOAc/MeOH). Using lithium aluminum hydride (LAH) instead of NaBH$_4$ resulted in a mixture of two unidentified components. The ^{1}H NMR spectrum of pure **3** (in D$_2$O) showed four multiplets corresponding to the CH and CH$_2$-functions in the molecule. The selective 1,3-protection of the triol **3** was achieved through the reaction with 2,2-dimethoxypropane catalyzed by *p*-toluenesulfonic acid. The reaction took 19 hours to produce 1,3-dioxane (**4**) in 57%. A small amount of 7-membered ring by-product was also formed. The separation of the desired 6-membered ring product from the undesired 7-membered ring by-product proved to be successful by column chromatography (2 : 1 EtOAc/hexane). Bromination of compound **4** with carbon tetrabromide and triphenylphosphine afforded the 2-bromoethyl-1,3-dioxane (**5**). As compound **5** decomposed

readily at room temperature, the reaction and work-up should be performed at 0°C, including removal of solvent. Purification of **5** was impracticable and unnecessary. Coupling of crude bromide **5** with 2-amino-6-chloropurine under a basic media gave a mixture of undesired 7-isomer purine (**6b**) and the desired product 9-isomer purine (**6a**) in 4% and 54%, respectively. The TLC (EtOAc) R_f values of the isomers were 0.32 and 0.31 for **6b** and **6a**, respectively, and careful column chromatography with ethyl acetate as eluant made the separation possible. 7-isomer **6b** is new and was fully characterized for the first time. ^{1}H NMR, LRMS, HRMS and elemental analysis data of **6b** confirmed its structure. Hydrolysis of 9-isomer **6a** with aqueous hydrochloric acid at reflux, followed by neutralization and filtration, afforded PCV **7** in 80% yield.

The overall chemical yield of PCV from **2** was 16%.

2. Synthesis of FHBG (1) and Radiosynthesis of [^{18}F]FHBG (1)

The synthesis of a standard sample FHBG (**1**) and target tracer [^{18}F]FHBG (**1**) as indicated in Sch. 2 was performed with the modifications reported in the literature.[15,25,33,34] The protection of the 2-amino group and one of the hydroxyl groups of PCV, **7** was achieved by reacting with monomethoxytrityl chloride in the presence of 4-dimethylaminopyridine (DMAP) and triethylamine.[30] Using 2.5 equivalent of monomethoxytrityl chloride at 50–60°C, the desired product N^2-(*p*-anisyldiphenylmethyl)-9-[(4-hydroxy)-3-*p*-anisyldiphenylmethoxymethylbutyl]guanine (**8a**) was obtained in 53% yield, and formation of the undesired fully protected by-product N^2-(*p*-anisyldiphenylmethyl)-9-[(4-*p*-anisyldiphenylmethoxy)-3-*p*-anisyldiphenylmethoxymethylbutyl]guanine (**8b**) could be limited to 16%. The compounds were separated by chromatography. Compound **8a** reacted with *p*-tosyl chloride at room temperature overnight afforded the desired precursor tosylate (**9a**) in 29%, together with undesired by-product (**9b**) in 22%. The compounds were separated by chromatography and their structures confirmed with extensive ^{1}H NMR data.[15,25,30,33,34] Fluorination of tosylate **9a** with anhydrous potassium fluoride in dry acetonitrile catalyzed by Kryptofix 2.2.2 gave intermediate 4-fluoroguanine **10** in 69%. Intermediate **10** was easily hydrolyzed by treatment with 1 N HCl aqueous solution to give the unlabeled standard sample FHBG, **1** in 97%.

The overall chemical yield of the tosylate precursor **9a** from PCV was 15%, and the overall chemical yield of the standard sample FHBG, **1** from PCV was 10%.
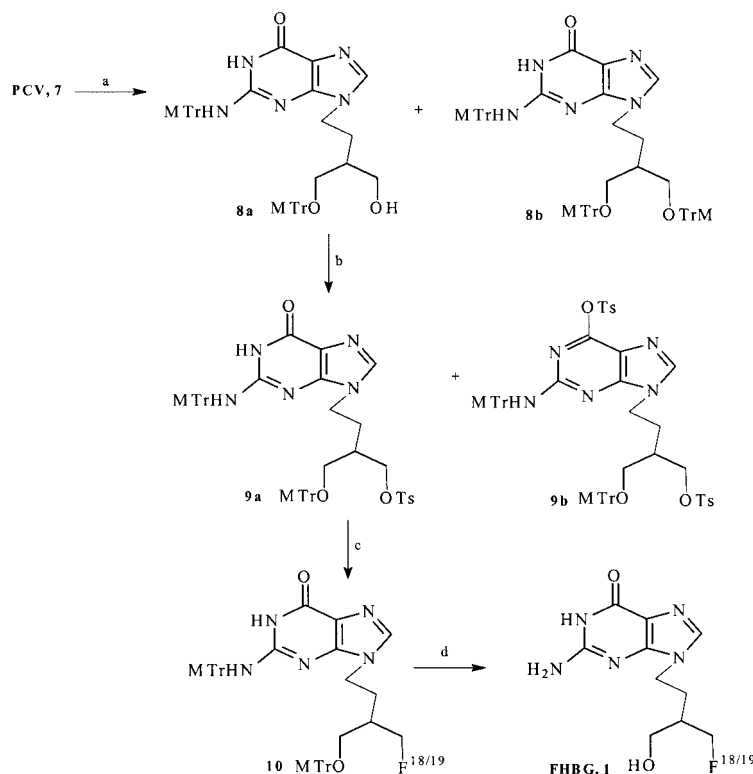
Scheme 2. Synthesis of FHPG and [¹⁸F]FHPG. (a) MTrCl, DMAP, Et₃N, DMF; (b) TsCl, pyridine; (c) K[¹⁸/¹⁹F], Kryptofix 2.2.2, CH₃CN; and (d) 1 N HCl, MeOH.

[¹⁸F]FHBG (**1**) was synthesized by a modification of the procedures reported in the literature.[15,33,34] The tosylated precursor **9a** was labeled by conventional nucleophilic substitution with K[¹⁸F]/Kryptofix 2.2.2 in CH₃CN at 120°C for 20 min to provide the radiolabeled intermediate **10**. The radio-labeling reaction was monitored by analytical radio-HPLC method by using a Prodigy (Phenomenex) 5 μm C-18 column, 4.6 × 250 mm; 3 : 1 : 1 CH₃-CN : MeOH : 20 mM, pH 6.7 KHPO₄⁻ mobile phase, 1.5 mL/min flow rate, and UV (240 nm) and γ-ray (NaI) flow detectors.[14,40] Retention times in the analytical HPLC system were: RT**10** = 17.50 min, RTK[¹⁸F] = 1.88 min. The radiolabeling mixture containing the intermediate **10** was passed through a Silica Sep-Pak column to remove Kryptofix 2.2.2 and non-reacted potassium [¹⁸F]fluoride. The large polarity difference between **10** and Kryptofix 2.2.2 and non-reacted potassium [¹⁸F]fluoride permitted the use of a simple

solid-phase extraction (SPE) technique[14,39,40] for fast isolation of **10** from the radiolabeling reaction mixture. The key part in this technique is a SiO_2 Sep-Pak type cartridge, which contains $\sim$0.5–2 g of adsorbent. The Sep-Pak was eluted with 15% $MeOH/CH_2Cl_2$ and the solvent was evaporated under high vacuum (0.1–1.0 mmHg) to give the residue **10**. As remaining catalyst Kryptofix 2.2.2 and non-reacted potassium [18F]fluoride would affect the deprotection reaction of **10**, they had to be removed prior to deprotection of **10**. Compound **10** was treated with 1 N HCl at 80°C for 10 min and the reaction mixture neutralized with 6 N NaOH to provide **1**. To simplify the synthetic procedure, the final reaction mixture was purified with the SPE method instead of HPLC which makes it amenable to automation.[33] The crude product was passed through a Silica Sep-Pak column to remove radioactive by-product with ethanol. The large polarity difference between **1** and the radioactive by-product permitted the use of SPE technique for fast purification of radiotracer **1**. The radiochemically pure compound **1** was isolated from the Sep-Pak using a 90:8:2 $H_2O/EtOH/HOAc$ eluant and the combined product containing fraction was treated with 2 M NaOH and 150 mM NaH_2PO_4 mixed solution to adjust to pH 5.5–7.0. The radiochemical yield of **1** was 20–25%, and the synthesis time was $\sim$70 min from end of bombardment (EOB). Chemical purity, radiochemical purity, and specific radioactivity were determined by analytical HPLC. Retention times in the analytical HPLC system were: RT**9a** = 19.80 min, RT**1** = 1.80 min. The chemical purity of precursor **9a** and standard sample **1** was >95%. The radiochemical purity of target radiotracer **1** was >99%, and the chemical purity $\sim$93%. The average ($n = 3$–5) specific radioactivity of radiotracer **1** was 0.8–1.2 Ci/μmol at end of synthesis (EOS).

In comparison with the results reported in the literature,[15,25,33,34] several improvements in the synthetic methodology for FHBG and [18F]FHBG have been made. They include increased radiochemical yield and specific activity, enhanced radiochemical purity, shortened synthesis time, new dual Sep-Pak techniques for fast and efficient preparative separation of [18F]FHBG from precursors, and new HPLC systems for the quality control (QC) method of target tracer [18F]FHBG.

Compounds **6b**, **8b**, and **9b** are new compounds.

In conclusion, an improved total synthesis of [18F]FHBG has been developed. Several improvements and new findings in the synthetic methodology, radiolabeling, preparative separation and analytical details for PCV, FHBG, precursor and [18F]FHBG have been made and addressed. This improved method is efficient and convenient. It is anticipated that the approaches and improvements described here can be applied with advantage to the synthesis of other radiolabeled GCV and PCV analogs for PET imaging of HSV-tk gene expression.

EXPERIMENTAL

All commercial reagents and solvents were used without further purification unless otherwise specified. Tetrahydrofuran (THF) solvent was distilled from LiAlH$_4$ immediately prior to use. Melting points were determined on a MEL-TEMP II capillary tube apparatus and were uncorrected. ^{1}H NMR spectra were recorded on a Bruker QE 300 NMR spectrometer using tetramethylsilane (TMS) as an internal standard. Chemical shift data for the proton resonances were reported in parts per million (δ) relative to internal standard TMS (δ 0.0). The low resolution mass spectra were obtained using a Bruker Biflex III MALDI-Tof mass spectrometer, and the high resolution mass measurements were obtained using a Kratos MS80 mass spectrometer, in the Department of Chemistry at Indiana University. Elemental analysis was performed by Midwest Microlab (Indianapolis, IN). Chromatographic solvent proportions are expressed on a volume: volume basis. Thin layer chromatography was run using Analtech silica gel GF uniplates (5 $\times$ 10 cm^2). Plates were visualized by UV light. Normal phase flash chromatography was carried out on EM Science silica gel 60 (230–400 mesh) with a forced flow of the indicated solvent system in the proportions described below. All moisture-sensitive reactions were performed under a positive pressure of nitrogen maintained by a direct line from a nitrogen source.

Analytical HPLC was performed using a Prodigy (Phenomenex) 5 μm C-18 column, 4.6 $\times$ 250 mm; 3 : 1 : 1 CH$_3$CN : MeOH : 20 mM, pH 6.7 KHPO$_4^-$ mobile phase, 1.5 mL/min flow rate, and UV (240 nm) and γ-ray (NaI) flow detectors. Semi-preparative C-18 SiO$_2$ Sep-Pak type cartridge was obtained from Waters Corporate Headquarters, Milford, MA. Sterile vented Millex-GS 0.22 μm vented filter unit was obtained from Millipore Corporation, Bedford, MA.

2-(Hydroxymethyl)butane-1,4-diol (3). Triethyl-1,1,2-ethanetricarboxylate, **2** (23 mL, 101.5 mmol) and NaBH$_4$ (10.0 g) were dissolved in *tert*-butyl alcohol (200 mL). The mixture was heated to reflux, and then MeOH (13 mL) was added in portions over 0.5 h. After addition the mixture was refluxed for an additional 1 h, then cooled to room temperature (r.t.). HCl (6 M, about 25 mL) was added carefully until the solution was neutral. A large amount of white solid formed. The mixture was filtered, and the residue was washed with EtOH (100 mL). After removal of solvent the residue was subject to column chromatography on silica gel eluted with 10 : 1 EtOAc/MeOH to afford a viscous colorless oil **3** (8.10 g, 66%), R$_f$ = 0.30 (10 : 1 EtOAc/MeOH). ^{1}H NMR (300 MHz, D$_2$O): δ 3.67 (t, 2H, CH$_2$*CH$_2$*OH, J = 6.61 Hz), 3.60 (d, 4H, HO*CH$_2$*CH, J = 5.15 Hz), 1.78 (h, 1H, CH, J = 5.88 Hz), 1.56 (q, 2H, *CH$_2$*CH$_2$OH, J = 6.62 Hz).

5-(2-Hydroxyethyl)-2,2-dimethyl-1,3-dioxane (4). Compound **3** (8.10 g, 67.42 mmol) and 2,2-dimethoxypropane (13 mL, 105.72 mmol) were dissolved in dry THF (20 mL). The mixture was stirred and p-toluenesulfonic acid monohydrate (0.64 g, 3.36 mmol) was added, and the clear solution was stirred at r.t. for 19 h. Triethylamine (10 mL) was added to quench the reaction, and the solution was stirred for 30 min. Then solvents were removed to leave a colorless liquid. The residue was subject to column chromatography on silica gel eluted with 2 : 1 EtOAc/hexane to give a colorless liquid **4** (6.13 g, 57%), $R_f = 0.44$ (2 : 1 EtOAc/hexane). ^{1}H NMR (300 MHz, CDCl$_3$): δ 3.95 (dd, 2H, H$_{eq.}$, $J_1 = 11.77$ Hz, $J_2 = 4.42$ Hz), 3.71 (t, 2H, CH_2OH, $J = 6.62$ Hz), 3.64 (dd, 2H, H$_{ax.}$, $J_1 = 11.77$ Hz, $J_2 = 8.09$ Hz), 1.88–2.02 (m, 2H, CH and OH), 1.52–1.59 (q, 2H, CH$_2$, $J = 6.60$ Hz), 1.43 (s, 3H, CH$_3$), 1.42 (s, 3H, CH$_3$).

5-(2-Bromoethyl)-2,2-dimethyl-1,3-dioxane (5). Compound **4** (1.11 g, 6.93 mmol) and carbon tetrabromide (3.44 g, 10.37 mmol) were dissolved in dry DMF (30 ml). The mixture was cooled under ice bath and triphenylphosphine (2.72 g, 10.37 mmol) was added, and the solution was stirred at 0°C for 2 h. To the light brown solution was added cold aqueous NaHCO$_3$ solution (30 mL), followed by cold water (30 mL). The mixture was extracted with cold hexane (50 mL × 3). The combined organic layer was washed with cold NaHCO$_3$ solution (30 mL) and cold water (30 mL), dried over Na$_2$SO$_4$. Solvent was removed under 0°C to afford a colorless liquid residue that was kept in vacuum and at 0°C for 1 h. Cold hexane (40 mL) was added to extract the bromide. After removal of solvent at 0°C the colorless liquid was kept in vacuum for 1 h to give colorless oil **5** (1.55 g, ~100%). ^{1}H NMR (300 MHz, CDCl$_3$): δ 3.96 (dd, 2H, H$_{eq.}$, $J_1 = 11.77$ Hz, $J_2 = 3.68$ Hz), 3.61 (dd, 2H, H$_{ax.}$, $J_1 = 12.13$ Hz, $J_2 = 6.62$ H), 3.44 (t, 2H, CH$_2$Br, $J = 6.62$ Hz), 1.88–2.02 (m, 3H, $CHCH_2CH_2$), 1.43 (s, 3H, CH$_3$), 1.41 (s, 3H, CH$_3$).

2-Amino-6-chloro-9-[2-(2,2-dimethyl-1,3-dioxan-5-yl)ethyl]purine (6a) and 2-amino-6-chloro-7-[2-(2,2-dimethyl-1,3-dioxan-5-yl)ethyl]purine (6b). Compound **5** (2.72 g, 12.17 mmol), 2-amino-6-chloropurine (2.26 g, 13.33 mmol) and anhydrous K$_2$CO$_3$ (3.5 g, 25.32 mmol) were dissolved in dry DMF (40 mL). The mixture was sealed by a septum and stirred at r.t. for 5 h. Then the mixture was diluted with ethyl acetate and transferred to a separation funnel, and washed with water. The water layer was extracted with another portion of ethyl acetate. The combined organic layer was washed with brine twice, dried over Na$_2$SO$_4$. Removal of solvent afforded a solid residue that was subject to column chromatography on silica gel eluted with ethyl acetate. First the by-product 7-isomer **6b** (0.13 g, 4%) eluted, mp 130°C (dec.), $R_f = 0.32$ (EtOAc). ^{1}H NMR (300 MHz, DMSO-d_6): δ 8.08 (s, 1H, 8-H), 6.91 (s, 2H, 2-NH$_2$), 3.30–4.10 (m, 6H, 1′- and 4′-H), 2.12–2.30 (m, 2H, 2′-H), 1.35–1.52 (m, 1H, 3′-H), 1.24 (s, 3H, CH$_3$), 1.19 (s, 3H, CH$_3$). The analysis

calculated for $C_{13}H_{18}ClN_5O_2$ was C, 50.08; H, 5.82. The values found were C, 50.13; H, 5.83. LRMS (EI, m/z): 154 (100%), 312 [(M + H)$^+$, 13.9%]. HRMS (FAB, m/z): calcd for $C_{13}H_{19}ClN_5O_2$ 312.1227, found 312.1234. The desired product 9-isomer **6a** eluted at $R_f = 0.31$ (EtOAc) and, after removal of the solvents, was obtained as a white solid (2.03 g, 54%). ^{1}H NMR (300 MHz, DMSO-d_6): δ 8.16 (s, 1H, 8-H), 6.91 (s, 2H, 2-NH$_2$), 4.05 (t, 2H, 1′-H, $J = 7.35$ Hz), 3.77 (dd, 2H, 4′-H$_{eq.}$, $J_1 = 11.77$ Hz, $J_2 = 4.41$ Hz), 3.53 (dd, 2H, 4′-H$_{ax.}$, $J_1 = 11.77$ Hz, $J_2 = 8.83$ Hz), 1.72 (q, 2H, 2′-H, $J = 7.35$ Hz), 1.50–1.60 (m, 1H, 3′-H), 1.31 (s, 3H, CH$_3$), 1.25 (s, 3H, CH$_3$).

9-[4-Hydroxy-3-(hydroxymethyl)butyl]guanine (penciclovir, PCV, 7). Compound **6a** (1.92 g, 6.16 mmol) was dissolved in aqueous hydrochloric acid (2 M, 6 mL). The mixture was refluxed for 2 h. When it was still hot 10% aqueous NaOH solution was added to neutralize the solution. Then the solution was allowed to cool to r.t. A large amount of off-white solid formed. The solid was filtered, washed with water and then acetone, dried under vacuum to give a off-white solid **7** (1.24 g, 80%). ^{1}H NMR (300 MHz, DMSO-d_6): δ 10.52 (s, 1H, 1-NH), 7.67 (s, 1H, 8-CH), 6.41 (s, 2H, 2-NH$_2$), 4.42 (t, 2H, OH, $J = 5.15$ Hz,), 3.98 (t, 2H, 1′-H, $J = 7.35$ Hz,), 3.25–3.48 (m, 4H, 4′-H), 1.69 (q, 2H, 2′-H, $J = 7.36$ Hz,), 1.43 (h, 1H, 3′-H, $J = 5.88$ Hz).

N^2-(p-Anisyldiphenylmethyl)-9-[(4-hydroxy)-3-p-anisyldiphenylmethoxymethylbutyl]guanine (8a) and N^2-(p-anisyldiphenylmethyl)-9-[(4-p-anisyldiphenylmethoxy)-3-p-anisyldiphenylmethoxymethylbutyl]guanine (8b). PCV **7** (1.00 g, 3.95 mmol), monomethoxytrityl chloride (3.00 g, 9.72 mmol), dimethylaminopyridine (0.050 g, 0.41 mmol) and triethylamine (3.5 mL) were dissolved in dry DMF (50 mL). The mixture was heated at 50–60°C for 6 h. After cooling to r.t. ethyl acetate was added, and the mixture was washed with water. The water layer was extracted with another portion of EtOAc. The combined organic layer was washed with water, dried over MgSO$_4$, evaporated to dryness. The residue was subject to column chromatography on silica gel eluted with 2.5% and 4.5% MeOH/ CH$_2$Cl$_2$. Undesired by-product **8b** was obtained at $R_f = 0.26$ (4% MeOH/ CH$_2$Cl$_2$) and gave a white solid (0.68 g, 16%), m.p. 145°C (dec.). ^{1}H NMR (300 MHz, DMSO-d_6): δ 10.48 (s, 1H, 1-NH), 7.55 (s, 1H, 2-NH), 6.66–7.32 (m, 43H, Ph and 8-CH), 3.72 (s, 6H, 9-OCH$_3$), 3.59 (s, 3H, 2-OCH$_3$), 3.24 (t, 2H, 1′-H, $J = 6.62$ Hz), 2.78–2.92 (m, 4H, 4′-H), 1.52–1.65 (m, 1H, 3′-H), 1.08–1.20 (m, 2H, 2′-H). The analysis calculated for $C_{70}H_{63}N_5O_6$ was C, 78.55; H, 5.93. The values found were C, 77.56; H, 5.92. LRMS (EI, m/z): 273 (100%), 1092 [(M + Na)$^+$, 3.9%]. HRMS (FAB, m/z): calcd for $C_{70}H_{63}N_5NaO_6$ 1092.4676, found 1092.4684. The second compound obtained from fractions at $R_f = 0.13$ (4% MeOH/CH$_2$Cl$_2$) gave product **8a** as a white solid (1.66 g, 53%). ^{1}H NMR (300 MHz, DMSO-d_6): δ 10.49 (s, 1H, 1-NH), 7.57 (s, 1H, 2-NH), 7.44 (s, 1H, 8-CH), 7.05–7.37 (m, 24H, Ph), 6.89 (d, 2H,

Ph, $J = 8.82\,Hz$), 6.75 (d, 2H, Ph, $J = 8.82\,Hz$), 4.38 (t, 1H, OH, $J = 5.14\,Hz$), 3.73 (s, 3H, 9-OCH_3), 3.65 (s, 3H, 2-OCH_3), 3.08–3.45 (m, 4H, 1′-and 4′-H), 2.67–2.85 (m, 2H, 5′-H), 1.35–1.45 (m, 1H, 3′-H), 1.15–1.25 (m, 2H, 2′-H).

N^2-(*p*-Anisyldiphenylmethyl)-9-[(4-tosyl)-3-*p*-anisyldiphenylmethoxymethylbutyl]guanine (9a) and 1-tosyl-N^2-(*p*-anisyldiphenylmethyl)-9-[(4-tosyl)-3-*p*-anisyldiphenylmethoxymethylbutyl]guanine (9b). Compound **8a** (1.12 g, 1.40 mmol) and *p*-tosyl chloride (1.56 g, 8.18 mmol) were dissolved in dry pyridine (20 mL). The mixture was stirred at r.t. for 21 h. To this solution was added water (10 mL) to quench the reaction, and then stirred for 15 min. The mixture was evaporated to dryness. The residue was dissolved in ethyl acetate, washed with water. The aqueous phase was extracted with another portion of ethyl acetate. The combined organic phase was washed with brine twice, dried over $MgSO_4$ and evaporated to dryness. The residue was purified by column chromatography on silica gel eluted with 2.5% MeOH/CH_2Cl_2 to give two components. By-product **9b** was obtained as a brown solid (0.34 g, 22%), m.p. 95–98°C, $R_f = 0.35$ (4% MeOH/CH_2Cl_2). ^{1}H NMR (300 MHz, $CDCl_3$): δ 7.96 (d, 2H, Ph, $J = 7.35\,Hz$), 7.74 (d, 2H, Ph, $J = 8.09\,Hz$), 6.95–7.45 (m, 29H, Ph and 2-NH), 6.80 (d, 2H, Ph, $J = 8.09\,Hz$), 6.70 (d, 2H, Ph, $J = 8.82\,Hz$), 6.37 (s, 1H, 8-CH), 3.78–4.03 (m, 2H, 4′-CH_2OTs), 3.77 (s, 3H, 9-OCH_3), 3.72 (s, 3H, 2-OCH_3), 3.28–3.47 (m, 2H, 1′-CH_2), 2.80–3.04 (m, 2H, 5′-CH_2OTrM), 2.42 (s, 6H, CH_3), 1.45 (brs, 1H, 3′-CH), 1.20–1.38 (m, 2H, 2′-CH_2). The analysis calculated for $C_{64}H_{59}N_5O_9S_2$: C, 69.48; H, 5.38. The values found were C, 68.88; H, 5.40. LRMS (EI, m/z): 273 (100%), 1106 [$(M + H)^+$, 2.6%]. HRMS (FAB, m/z): calcd for $C_{64}H_{60}N_5O_9S_2$ 1106.3833, found 1106.3861. Product **9a** eluted at $R_f = 0.29$ (4% MeOH/CH_2Cl_2) and was isolated as a light purple solid (0.38 g, 29%). ^{1}H NMR (300 MHz, $CDCl_3$): δ 11.63 (brs, 1H, 1-NH, D_2O exchangeable), 7.87 (brs, 1H, 2-NH, D_2O exchangeable), 7.75 (d, 2H, Ph, $J = 7.36\,Hz$), 6.87–7.45 (m, 27H, Ph and 8-H), 6.81 (d, 2H, Ph, $J = 8.09\,Hz$), 6.61 (d, 2H, Ph, $J = 8.09\,Hz$), 3.75–4.05 (m, 2H, 4′-CH_2OTs), 3.76 (s, 3H, 9-OCH_3), 3.62 (s, 3H, 2-OCH_3), 3.15–3.35 (m, 2H, 1′-H), 2.76–3.04 (m, 2H, 5′-CH_2OTrM), 2.41 (s, 3H, CH_3), 1.51 (brs, 1H, 3′-H), 1.26 (br.s, 2H, 2′-H).

N^2-(*p*-Anisyldiphenylmethyl)-9-[(4-fluoro)-3-*p*-anisyldiphenylmethoxymethylbutyl]guanine (10). Tosylate **9a** (0.050 g, 0.053 mmol), Kryptofix 2.2.2 (0.12 g, 0.32 mmol) and anhydrous potassium fluoride (0.070 g, 1.21 mmol) were dissolved in anhydrous acetonitrile (5 mL) in a 10 mL V-vial. The vial was sealed and heated to 115–120°C for 40 min while stirring. TLC showed no starting material remained. Solvent was removed by evaporation, and the residue was transferred to the top of a column (silica gel) with the aid of CH_2Cl_2. The column was eluted with 2.0–2.5% MeOH/CH_2Cl_2. A yellowish solid **10** (0.029 g, 69%) was obtained, $R_f = 0.29$ (4% MeOH/

CH$_2$Cl$_2$). ^{1}H NMR (300 MHz, CDCl$_3$): δ 6.62–7.42 (m, 28H, Ph), 4.57 (s, 2H, 4′-CH$_2$), 4.21 (t, 2H, 1′-CH$_2$, $J = 4.41$ Hz), 3.75 (s, 3H, 9-OCH$_3$), 3.70 (s, 3H, 2-OCH$_3$), 3.31 (d, 2H, 5′-CH$_2$, $J = 70.59$ Hz), 1.51–1.98 (m, 2H, 2′-CH$_2$), 0.78–0.93 (m, 1H, 3′-CH). LRMS (EI, m/z): 154 (100%), 780 [(M-F)$^+$, 1.0%]. HRMS (FAB, m/z): calcd for C$_{50}$H$_{46}$N$_5$O$_4$ 780.3550, found 780.3547.

9-(4-Fluoro-3-hydroxymethylbutyl)guanine (FHBG, 1). The solution of compound **10** (0.029 g, 0.036 mmol) in methanol (2.5 mL) was acidified with 1 N HCl (0.5 mL), and then heated at 115°C for 10 min. The solution was neutralized with 1 N aqueous NaOH. A small amount of silica gel was added to absorb the solution, and the mixture was dried under vacuum, and transferred to the top of a silica gel column. The column was eluted with 4:1 MeCN/H$_2$O to afford **1** as a white solid (9.0 mg, 97%), R$_f = 0.19$ (4:1 MeCN/H$_2$O). ^{1}H NMR (300 MHz, DMSO-d_6): δ 7.53 (s, 1H, 8-CH), 6.74 (s, 2H, 2-NH$_2$, D$_2$O exchangeable), 5.06 (brs, 1H, OH, D$_2$O exchangeable), 4.30 (brs, 2H, 1′-CH$_2$), 4.13 (dd, 2H, 4′-CH$_2$, $J = 47.06$ Hz), 3.35 (d, 2H, 5′-CH$_2$, $J = 52.94$ Hz), 2.05–2.32 (m, 2H, 2′-CH$_2$), 1.59–1.74 (m, 1H, 3′-CH).

9-(4-[^{18}F]fluoro-3-hydroxymethylbutyl)guanine ([^{18}F]FHBG, 1). No-carrier-added (NCA) aqueous H^{18}F (0.5 mL) prepared by ^{18}O(p,n)^{18}F nuclear reaction in a RDS-112 cyclotron on an enriched H$_2^{18}$O water (95 + %) target was added to a Pyrex vessel which contains K$_2$CO$_3$ (4 mg, in 0.2 mL H$_2$O) and Kryptofix 2.2.2 (10 mg, in 0.5 mL CH$_3$CN). Azeotropic distillation at 115°C with HPLC grade CH$_3$CN (3 × 1 mL) under a nitrogen steam efficiently removed water. The tosylated precursor **9a** (2–3 mg, dissolved in 0.5 mL CH$_3$CN) was introduced to the anhydrous potassium [^{18}F]fluoride-Kryptofix 2.2.2 complex. The reaction mixture was sealed and heated at 120°C for 20 min and was subsequently allowed to cool down, at which time the crude product was passed through a Silica Sep-Pak cartridge to remove Kryptofix 2.2.2 and un-reacted potassium [^{18}F]fluoride. The Sep-Pak column was eluted with 15% MeOH/CH$_2$Cl$_2$ (3.5 mL), and the fractions were passed onto a rotatory evaporator. The solvent was removed by evaporation under high vacuum (0.1–1.0 mmHg). The residue was acidified with 1 N HCl (0.6 mL) and heated for 10 min at 80°C. The contents were neutralized with 6 N NaOH (0.1 mL), diluted with ethanol (3 mL), and evaporated under vacuum. The crude product was passed through a Silica Sep-Pak cartridge with the aid of ethanol. The Sep-Pak was eluted with EtOH to remove the radioactive by-product. The radiochemically pure product [^{18}F]FHBG, **1** was eluted from the Sep-Pak with 90:8:2 H$_2$O/EtOH/HOAc and adjusted pH to 5.5–7.0 by addition of a 2 M NaOH and 150 mM NaH$_2$PO$_4$ mixed solution, whose volume was dependent upon the use of the labeled product in tissue biodistribution studies (~3 mL, 3 × 1 mL) or in micro-PET imaging studies (1.5 mL, 3 × 0.5 mL) of HSV-tk prostate cancer tumors in athymic mice. The mixture

was sterile-filtered through a 0.22 µm cellulose acetate membrane and collected into a sterile vial. The radiochemical yield of [^{18}F]FHBG was 20–25%, and the synthesis time was ∼70 min from EOB. Retention times in the analytical HPLC system were: RT**9a** = 19.80 min, RT**1** = 1.80 min. The chemical purities of precursor **9a** and standard sample **1** were >95%, the radiochemical purity of target radiotracer **1** was >99%, and the chemical purity of radiotracer **1** was ∼93%. The average ($n = 3–5$) specific radioactivity of radiotracer **1** was 0.8–1.2 Ci/µmol at EOS.

ACKNOWLEDGMENTS

REFERENCES

1. Weissleder, R.; Mahmood, U. Molecular imaging. Radiology **2001**, *219*, 316–333.
2. Mulholland, K.M.; Winkle, W.; Mock, B.H.; Sledge, G. Radioiodinated epidermal growth factor receptor ligands as tumor probes, dramatic potentiation of binding to MDA-468 cancer cells in presence of EGF. J. Nucl. Med. **1995**, *36* (Suppl), 71P.
3. Mulholland, K.M.; Zheng, Q.-H.; Winkle, W.; Carlson, K.A. Synthesis and biodistribution of new C-11 and F-18 labeled epidermal growth factor receptor ligands. J. Nucl. Med. **1999**, *38* (Suppl), 141P.
4. Fei, X.; Zheng, Q.-H.; Hutchins, G.D.; Liu, X.; Stone, K.L.; Carlson, K.A.; Mock, B.H.; Winkle, W.L.; Glick-Wilson, B.E.; Miller, K.D.; Fife, R.S.; Sledge, G.W.; Sun, H.B.; Carr, R.E. Synthesis of MMP inhibitor radiotracers [^{11}C]methyl-CGS 27023A and its analogs, new potential PET breast cancer imaging agents. J. Labelled Cpd. Radiopharm. **2002**, *45*, 449–470.

5. Fei, X.; Zheng, Q.-H.; Liu, X.; Wang, J.-Q.; Stone, K.L.; Miller, K.D.; Sledge, G.W.; Hutchins, G.D. Synthesis of MMP inhibitor radiotracer [^{11}C]CGS 25966, a new potential PET tumor imaging agent. J. Labelled Cpd. Radiopharm. **2003**, *46*, 343–351.

6. Fei, X.; Zheng, Q.-H.; Liu, X.; Wang, J.-Q.; Sun, H.B.; Mock, B.H.; Stone, K.L.; Miller, K.D.; Sledge, G.W.; Hutchins, G.D. Synthesis of radiolabeled biphenylsulfonamide matrix metalloproteinase inhibitors as new potential PET cancer imaging agents. Bioorg. Med. Chem. Lett. **2003**, *13*, 2217–2222.

7. Zheng, Q.-H.; Fei, X.; Wang, J.-Q.; Stone, K.L.; Martinez, T.D.; Gay, D.J.; Baity, W.L.; Mock, B.H.; Glick-Wilson, B.E.; Sullivan, M.L.; Miller, K.D.; Sledge, G.W.; Hutchins, G.D. Synthesis and biological evaluation of potential cancer biomarkers radiolabelled MMP inhibitors [^{11}C]FMAME and [^{18}F]FMAME. J. Labelled Cpd. Radiopharm. **2003**, *46* (Suppl. 1), S110.

8. Zheng, Q.-H.; Fei, X.; Liu, X.; Wang, J.-Q.; Stone, K.L.; Martinez, T.D.; Gay, D.J.; Baity, W.L.; Miller, K.D.; Sledge, G.W.; Hutchins, G.D. Comparative studies of potential cancer biomarkers carbon-11 labelled MMP inhibitors [^{11}C] MSMA and [^{11}C]CGS 25966. J. Labelled Cpd. Radiopharm. **2003**, *46* (Suppl. 1), S111.

9. Zheng, Q.-H.; Fei, X.; Liu, X.; Wang, J.-Q.; Sun, H.B.; Mock, B.H.; Stone, K.L.; Martinez, T.D.; Miller, K.D.; Sledge, G.W.; Hutchins, G.D. Synthesis and preliminary biological evaluation of MMP inhibitor radiotracers [^{11}C]methyl-halo-CGS 27023A analogs, new potential PET breast cancer imaging agents. Nucl. Med. Biol. **2002**, *29*, 761–770.

10. Liu, X.; Zheng, Q.-H.; Fei, X.; Wang, J.-Q.; Ohannesian, D.W.; Erickson, L.C.; Stone, K.L.; Hutchins, G.D. Synthesis and preliminary biological evaluation of 6-O-[^{11}C]-[(methoxymethyl)benzyl]guanines, new potential PET breast cancer imaging agents for the DNA repair protein AGT. Bioorg. Med. Chem. Lett. **2003**, *13*, 641–644.

11. Liu, X.; Zheng, Q.-H.; Hutchins, G.D.; Fei, X.; Erickson, L.C.; Miller, K.D.; Mock, B.H.; Glick-Wilson, B.E.; Winkle, W.L.; Stone, K.L.; Carlson, K.A. A convenient procedure for the synthesis of O^6-benzylguanine derivatives by phase transfer catalysis. Syn. Commun. **2003**, *33*, 941–952.

12. Zheng, Q.-H.; Liu, X.; Fei, X.; Wang, J.-Q.; Ohannesian, D.W.; Erickson, L.C.; Stone, K.L.; Hutchins, G.D. Synthesis and preliminary biological evaluation of radiolabeled O^6-benzylguanine derivatives, new potential PET imaging agents for the DNA repair protein O^6-alkylguanine-DNA alkyltransferase in breast cancer. Nucl. Med. Biol. **2003**, *30*, 405–415.

13. Zheng, Q.-H.; Liu, X.; Fei, X.; Wang, J.-Q.; Ohannesian, D.W.; Erickson, L.C.; Stone, K.L.; Martinez, T.D.; Miller, K.D.; Hutchins, G.D. Synthesis of radiolabeled O^6-benzylguanine derivatives as new potential PET tumor imaging agent for the DNA repair protein O^6-alkylguanine-DNA alkyltransferase. J. Labelled Cpd. Radiopharm. **2002**, *45*, 1239–1252.

14. Zheng, Q.-H.; Stone, K.L.; Mock, B.H.; Miller, K.D.; Fei, X.; Liu, X.; Wang, J.-Q.; Glick-Wilson, B.E.; Sledge, G.W.; Hutchins, G.D. [^{11}C]Choline as a potential PET marker for imaging of breast cancer athymic mice. Nucl. Med. Biol. **2002**, *29*, 803–807.

15. Alauddin, M.M.; Conti, P.S. Synthesis and preliminary evaluation of 9-(4-[^{18}F]-fluoro-3-hydroxymethylbutyl)guanine ([^{18}F] FHBG): a new potential imaging agent for viral infection and gene therapy using PET. Nucl. Med. Biol. **1998**, *25*, 175–180.

16. Alauddin, M.M.; Conti, P.S.; Mazza, S.M.; Hamzeh, F.M.; Lever, J.R. 9-[(3-[^{18}F]-Fluoro-1-hydroxy-2-propoxy)methyl]guanine ([^{18}F]-FHPG): a potential imaging agent of viral infection and gene therapy using PET. Nucl. Med. Biol. **1996**, *23*, 787–792.

17. Alauddin, M.M.; Shahinian, A.; Gordon, E.M.; Bading, J.R.; Conti, P.S. Preclinical evaluation of the penciclovir analog 9-(4-[^{18}F]fluoro-3-hydroxymethylbutyl)guanine for in vivo measurement of suicide gene expression with PET. J. Nucl. Med. **2001**, *42*, 1682–1690.

18. Alauddin, M.M.; Shahinian, A.; Kundu, R.K.; Gordon, E.M.; Conti, P.S. Evaluation of 9-[(3-^{18}F-fluoro-1-hydroxy-2-propoxy)methyl]guanine ([^{18}F]-FHPG) in vitro and in vivo as a probe for PET imaging of gene incorporation and expression in tumors. Nucl. Med. Biol. **1999**, *26*, 371–376.

19. Brust, P.; Haubner, R.; Friedrich, A.; Scheunemann, M.; Anton, M.; Koufaki, O.N.; Hauses, M.; Noll, S.; Noll, B.; Haberkorn, U.; Schackert, G.; Schackert, H.K.; Avril, N.; Johannsen, B. Comparison of [^{18}F]FHPG and [$^{124/125}$I]FIAU for imaging herpes simplex virus type 1 thymidine kinase gene expression. Eur. J. Nucl. Med. **2001**, *28*, 721–729.

20. de Vries, E.F.; van Waarde, A.; Harmsen, M.C.; Mulder, N.H.; Vaalburg, W.; Hospers, G.A. [^{11}C]FMAU and [^{18}F]FHPG as PET tracers for herpes simplex virus thymidine kinase enzyme activity and human cytomegalovirus infections. Nucl. Med. Biol. **2000**, *27*, 113–119.

21. Gambhir, S.S.; Barrio, J.R.; Herschman, H.R.; Phelps, M.E. Assays for noninvasive imaging of reporter gene expression. Nucl. Med. Biol. **1999**, *26*, 481–490.

22. Gambhir, S.S.; Barrio, J.R.; Phelps, M.E.; Iyer, M.; Namavari, M.; Satyamurthy, N.; Wu, L.; Green, L.A.; Bauer, E.; MacLaren, D.C.; Nguyen, K.; Berk, A.J.; Cherry, S.R.; Herschman, H.R. Imaging

adenoviral-directed reporter gene expression in living animals with positron emission tomography. Proc. Natl. Acad. Sci. U.S.A. **1999**, *96*, 2333–2338.

23. Gambhir, S.S.; Bauer, E.; Black, M.E.; Liang, Q.; Kokoris, M.S.; Barrio, J.R.; Iyer, M.; Namavari, M.; Phelps, M.E.; Herschman, H.R. A mutant herpes simplex virus type 1 thymidine kinase reporter gene shows improved sensitivity for imaging reporter gene expression with positron emission tomography. Proc. Natl. Acad. Sci. U.S.A. **2000**, *97*, 2785–2790.

24. Hakimelahi, G.H.; Khalafi-Nezhad, A. Catalytic effect of tetrabutylammonium fluoride in the preparation of securibo-nucleosides. Helv. Chim. Acta **1989**, *72*, 1495–1500.

25. Harnden, M.R.; Jarvest, R.L.; Bacon, T.H.; Boyd, M.R. Synthesis and antiviral activity of 9-[4-hydroxy-3-(hydroxymethyl)but-1-yl]purines. J. Med. Chem. **1987**, *30*, 1636–1642.

26. Hospers, G.A.; Calogero, A.; van Waarde, A.; Doze, P.; Vaalburg, W.; Mulder, N.H.; de Vries, E.F. Monitoring of herpes simplex virus thymidine kinase enzyme activity using positron emission tomography. Cancer Res. **2000**, *60*, 1488–1491.

27. Hustinx, R.; Shiue, C.Y.; Alavi, A.; McDonald, D.; Shiue, G.G.; Zhuang, H.; Lanuti, M.; Lambright, E.; Karp, J.S.; Eck, S.L. Imaging in vivo herpes simplex virus thymidine kinase gene transfer to tumour-bearing rodents using positron emission tomography and [¹⁸F]FHPG. Eur. J. Nucl. Med. **2001**, *28*, 5–12.

28. Inubushi, M.; Wu, J.C.; Gambhir, S.S.; Sundaresan, G.; Satyamurthy, N.; Namavari, M.; Yee, S.; Barrio, J.R.; Stout, D.; Chatziioannou, A.F.; Wu, L.; Schelbert, H.R. Positron-emission tomography reporter gene expression imaging in rat myocardium. Circulation **2003**, *107*, 326–332.

29. Iyer, M.; Barrio, J.R.; Namavari, M.; Bauer, E.; Satyamurthy, N.; Nguyen, K.; Toyokuni, T.; Phelps, M.E.; Herschman, H.R.; Gambhir, S.S. 8-[¹⁸F]Fluoropenciclovir: an improved reporter probe for imaging HSV1-tk reporter gene expression in vivo using PET. J. Nucl. Med. **2001**, *42*, 96–105.

30. Martin, J.C.; McGee, D.P.C.; Jeffrey, G.A.; Hobbs, D.W.; Smee, D.F.; Mattews, T.R.; Verheyden, J.P.H. Synthesis and anti-herpes-virus activity of acyclic 2′-deoxyguanosine analogues related to 9-[(1,3-dihydro-2-propoxy)methyl]guanine. J. Med. Chem. **1986**, *29*, 1384–1389.

31. Ogilvie, K.K.; Cheriyan, U.O.; Radatus, B.K. Biologically active acyclonucleoside analogues. II. The synthesis of 9-[[2-hydroxy-1-(hydroxymethyl)ethoxy]methyl]guanine (BIOLF-62). Can. J. Chem. **1982**, *60*, 3005–3010.

32. Pantuck, A.J.; Berger, F.; Zisman, A.; Nguyen, D.; Tso, C.L.; Matherly, J.; Gambhir, S.S.; Belldegrun, A.S. CL1-SR39: A noninvasive molecular imaging model of prostate cancer suicide gene therapy using positron emission tomography. J. Urol. **2002**, *168*, 1193–1198.

33. Shiue, G.G.; Shiue, C.Y.; Lee, R.L.; MacDonald, D.; Hustinx, R.; Eck, S.L.; Alavi, A.A. A simplified one-post synthesis of 9-[(3-[^{18}F]fluoro-1-hydroxy-2-propoxy)methyl]guanine([^{18}F]FHPG) and 9-(4-[^{18}F]fluoro-3-hydroxymethylbutyl)guanine ([^{18}F]FHBG) for gene therapy. Nucl. Med. Biol. **2001**, *28*, 875–883.

34. Tjuvajev, J.G.; Doubrovin, M.; Akhurst, T.; Cai, S.; Balatoni, J.; Alauddin, M.M.; Finn, R.; Bornmann, W.; Thaler, H.; Conti, P.S.; Blasberg, R.G. Comparison of radiolabeled nucleoside probes (FIAU, FHBG, and FHPG) for PET imaging of HSV1-tk gene expression. J. Nucl. Med. **2002**, *43*, 1072–1083.

35. Wu, J.C.; Inubushi, M.; Sundaresan, G.; Schelbert, H.R.; Gambhir, S.S. Positron emission tomography imaging of cardiac reporter gene expression in living rats. Circulation **2002**, *106*, 180–183.

36. Yaghoubi, S.; Barrio, J.R.; Dahlbom, M.; Iyer, M.; Namavari, M.; Satyamurthy, N.; Goldman, R.; Herschman, H.R.; Phelps, M.E.; Gambhir, S.S. Human pharmacokinetic and dosimetry studies of [^{18}F]FHBG: a reporter probe for imaging herpes simplex virus type-1 thymidine kinase reporter gene expression. J. Nucl. Med. **2001**, *42*, 1225–1234.

37. Yaghoubi, S.S.; Wu, L.; Liang, Q.; Toyokuni, T.; Barrio, J.R.; Namavari, M.; Satyamurthy, N.; Phelps, M.E.; Herschman, H.R.; Gambhir, S.S. Direct correlation between positron emission tomographic images of two reporter genes delivered by two distinct adenoviral vectors. Gene Ther. **2001**, *8*, 1072–1080.

38. Zheng, Q.-H.; Wang, J.-Q.; Fei, X.; Liu, X.; Gardner, T.A.; Kao, C.; Raikwar, S.P.; Glick-Wilson, B.E.; Sullivan, M.L.; Mock, B.H.; Hutchins, G.D. An improved total synthesis of PET HSV-tk reporter probe [^{18}F]FHPG. J. Labelled Cpd. Radiopharm. **2003**, *46* (Suppl. 1), S221.

39. Mulholland, K.M.; Zheng, Q.-H.; Mock, B.H.; Vavrek, M.T. Convenient labeling and isolation of [^{11}C-methyl]quaternary amines. J. Labelled Cpd. Radiopharm. **1999**, *42* (Suppl. 1), S459–S461.

40. Zheng, Q.-H.; Liu, X.; Fei, X.; Wang, J.-Q.; Mock, B.H.; Glick-Wilson, B.E.; Sullivan, M.L.; Hutchins, G.D. Facile synthesis of [^{11}C]edrophonium and its analogs as new potential PET imaging agents for heart acetylchlolinesterase. Bioorg. Med. Chem. Lett. **2003**, *13*, 1787–1790.

An Improved Total Synthesis of PET HSV-tk Gene Expression Imaging Agent 9-[(3-[18F]Fluoro-1-hydroxy-2-propoxy)methyl]guanine ([18F]FHPG)

Ji-Quan Wang,[1] Qi-Huang Zheng,[1,*] Xiangshu Fei,[1] Xuan Liu,[1] Thomas A. Gardner,[2] Chinghai Kao,[2] Sudhanshu P. Raikwar,[2] Barbara E. Glick-Wilson,[1] Michael L. Sullivan,[1] Bruce H. Mock,[1] and Gary D. Hutchins[1]

Departments of [1]Radiology and [2]Urology, Indiana University School of Medicine, Indianapolis, Indiana, USA

ABSTRACT

An improved total synthesis of [18F]FHPG starting from 1,3-dibenzyloxy-2-propanol and guanine has been developed. [18F]FHPG was prepared by nucleophilic substitution of the appropriate precursor with [18F]KF/Kryptofix 2.2.2 followed by a quick deprotection reaction and purification with a simplified Silica Sep-Pak solid-phase extraction (SPE) method in 10–15% radiochemical yield, and 70 min synthesis time from end of bombardment (EOB).

*Correspondence: Qi-Huang Zheng, Ph.D., Department of Radiology, Indiana University School of Medicine, 1345 West 16th Street, L-3 Room 202, Indianapolis, IN 46202-2111, USA; Fax: (317) 278-9711; E-mail: qzheng@iupui.edu.

917

INTRODUCTION

Radiolabeled ganciclovir (GCV, 9-[(1,3-dihydroxy-2-propoxy)methyl]-guanine) and penciclovir (PCV, 9-[4-hydroxy-3(hydroxymethyl)butyl]gua-nine) analogs such as 8-[^{18}F]fluoroganciclovir ([^{18}F]FGCV), 9-[(3-[^{18}F]fluoro-1-hydroxy-2-propoxy)methyl]guanine ([^{18}F]FHPG); 8-[^{18}F]fluor-openciclovir ([^{18}F]FPCV), 9-(4-[^{18}F]fluoro-3-hydroxymethylbutyl)guanine ([^{18}F]FHBG) (Fig. 1) have shown great potential as positron emission tomography (PET) imaging agents to detect herpes simplex virus thymidine kinase (HSV-tk) gene expression.[1–16] Considerable efforts have been devoted to the synthesis of these gene reporter probes and numerous improved synthesis were reported in the literature,[11,13,17–19] in which [^{18}F]FGCV and [^{18}F]FPCV were labeled with fluorine-18 at 8-position of guanine ring of GCV and PCV; [^{18}F]FHPG and [^{18}F]FHBG were labeled with fluorine-18 at the side chain of GCV and PCV. The potential importance of these compounds as gene therapy imaging tools is great, and broader research investigation to fully explore and validate their utility is important. However, the limited commercial availability, complicated synthetic procedure and high costs of starting materials GCV and PCV can present an obstacle to more widespread evaluation of these intriguing agents.

X=O, GCV
X=CH$_2$, PCV

X=O, [^{18}F]FGCV
X=CH$_2$, [^{18}F]FPCV

X=O, [^{18}F]FHPG
X=CH$_2$, [^{18}F]FHBG
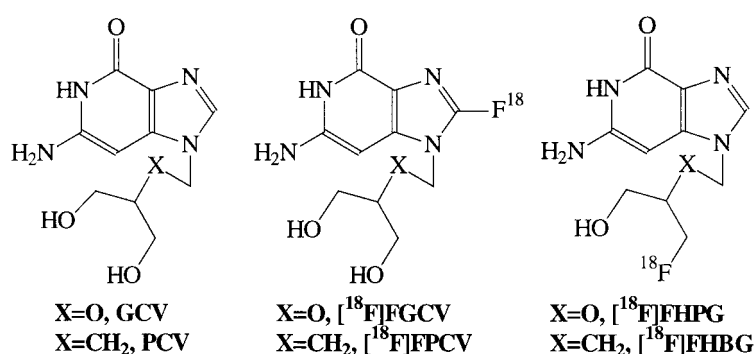
Figure 1. Chemical structures of GCV, PCV, [^{18}F]FGCV, [^{18}F]FPCV, [^{18}F]FHPG, [^{18}F]FHBG.

Wishing to study these compounds in this laboratory, we decided to make our own material by following the literature methods. Although several papers dealing with the synthesis of [18F]FHPG from GCV have appeared, there are gaps in synthetic detail among them, and certain key steps gave poor yields or were difficult to repeat in our hands. Consequently, we investigated alternate approaches and modifications that eventually resulted in an improved total synthesis of [18F]FHPG starting from very beginning materials 1,3-dibenzyloxy-2-propanol and guanine that was superior to previous works or addressed more synthetic details to reveal and explain technical tricks. In this paper we provide full experiment procedures, yields, analytical details and new findings for this improved [18F]FHPG total synthesis, as well as key intermediate GCV and tosylated precursor.

RESULTS AND DISCUSSION

Synthesis of Ganciclovir

The synthesis of ganciclovir (GCV) as indicated in Sch. 1 was performed with the modifications according to procedures reported in the literature.[20,21]

The commercially available starting material 1,3-dibenzyloxy-2-propanol (**2**) was converted into its chloromethyl ether 1,3-dibenzyloxy-2-chloro-
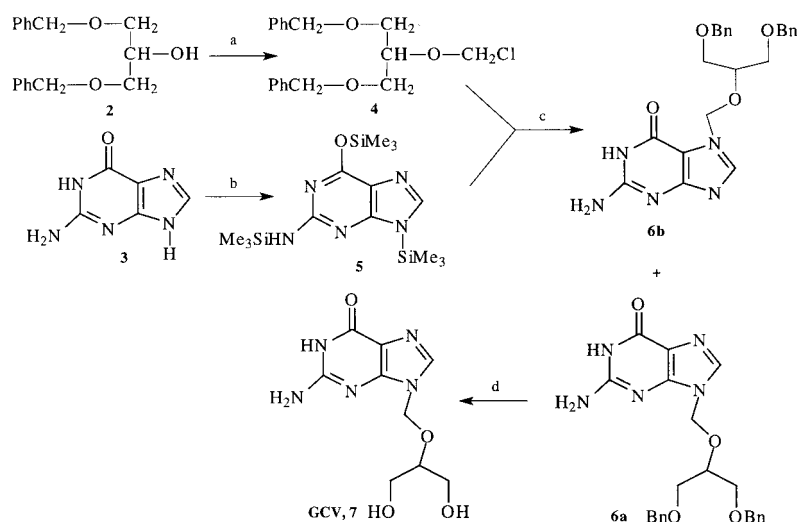
Scheme 1. Synthesis of GCV. a (CH$_2$O)n, HCl (gas), ClCH$_2$CH$_2$Cl, 0°C; b. NH(SiMe$_3$)$_2$, (NH$_4$)$_2$SO$_4$; c. Bu$_4$NF, THF; d. Pd black, cyclohexene, EtOH.

methoxypropane (**4**) through a chloromethylation reaction. Compound **4** was easy to decompose on silica gel column. Therefore, the purification of crude product **4** is impossible and unnecessary. The staring material guanine (**3**) was reacted with 1,1,1,3,3,3-hexamethyldisilazane (HMDS) to provide guanine derivative 2,6,9-tris(trimethylsilyl)guanine (**5**). The reaction went very slow, which took 4 days. The indication of reaction completion was that the initial suspension turned to be a clear solution. Compound **5** was sensitive to moisture, and it should be used for next step reaction immediately after removal of volatiles. The coupling reaction between **4** and **5** gave desired product 9-isomer 9-[(1,3-dibenzyloxy-2-propoxy)methyl]guanine (**6a**) and undesired by-product 7-isomer 7-[(1,3-dibenzyloxy-2-propoxy)methyl]guanine (**6b**). The reaction needed to be catalyzed by either tetrabutylammonium fluoride (TBAF)[20] or tetrabutylammonium iodide (TBAI).[21] However, there was not much difference observed in the reaction, and the ratio of products **6a/6b** was around 2 : 1 for both catalysts. The claimed high yield of 9-isomer with TBAF[20] was not achievable in our hands. The separation of the two isomers was challenging, since they gave the same R_f value on TLC. Thus, the preparative TLC and the flash column chromatography did not work for the purification of 9-isomer from its mixture with 7-isomer. Fortunately, repeated recrystallization of the mixture of the two isomers in ethanol could provide pure 9-isomer **6a** and 7-isomer **6b**. **6b** came out from their solution first, and then **6a**. The purities of **6a** and **6b** could be monitored by ^{1}H NMR spectrum, which was used to guide the recrystallization. The transfer hydrogenolysis reaction of compound **6a** to remove the protecting benzyl groups gave the key intermediate GCV, **7**. The reaction was catalyzed by either palladium chloride (PdCl$_2$)[20] or palladium black.[21] However, we found with PdCl$_2$[20] the chain of the reaction product GCV was cleaved; with 1 : 1 palladium black/**6a**[21] the deprotection reaction would not complete no matter how long the reaction was heated. The ratio of palladium black/**6a** we used was 3 : 1, which gave deprotective GCV, **7** in a yield of 87.7%.

The overall chemical yield of GCV from **2** and **3** was 15.6%.

Synthesis of FHPG (1) and Radiosynthesis of [18F]FHPG (1)

The syntheses of standard sample 9-[(3-fluoro-1-hydroxy-2-propoxy)-methyl]guanine (FHPG, **1**) and target tracer [18F]FHPG (**1**) as indicated in Sch. 2 were performed with the modifications according to procedures reported in the literature.[13,18,19,22]

The protection of the 2-amino group and one of the two hydroxyl groups of GCV, **7** was furnished by reacting with monomethoxytrityl chloride in the presence of 4-dimethylaminopyridine (DMAP) and triethylamine.[22] The
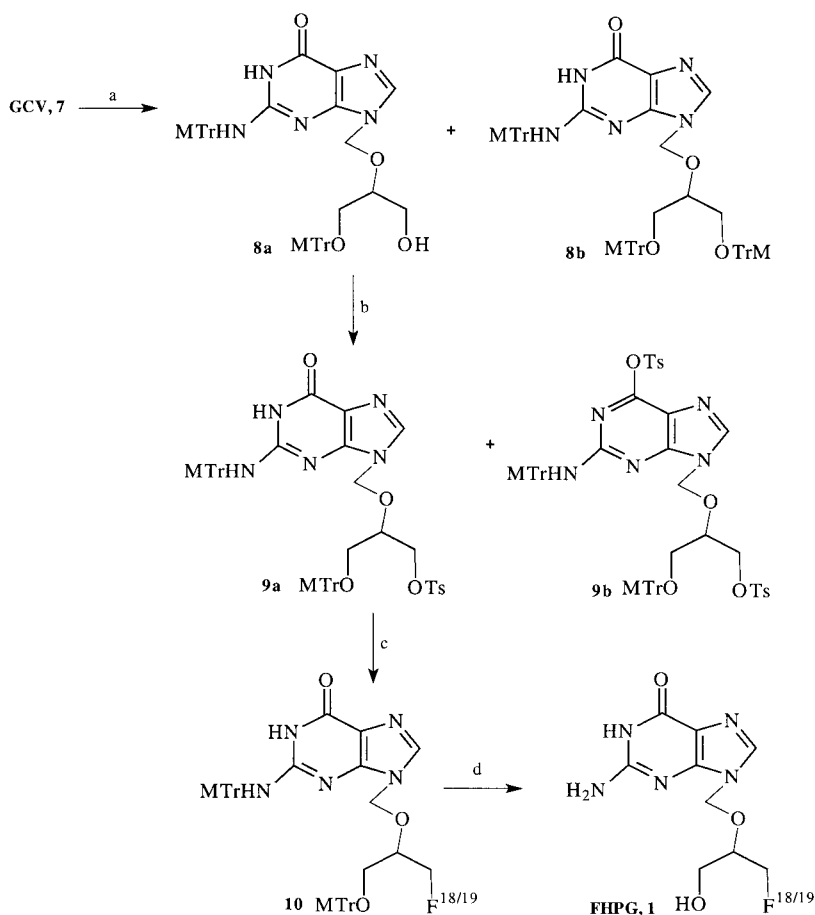
Scheme 2. Synthesis of FHPG and [^{18}F]FHPG. a. MTrCl, DMAP, Et$_3$N, DMF; b. TsCl, pyridine; c. K[$^{18/19}$F], Kryptofix 2.2.2, CH$_3$CN; d. 1 N HCl, MeOH.

bulky methoxytrityl group favored the desired product N^2-(P-anisyldiphenyl-methyl)-9-[[1-(P-anisyldiphenylmethoxy)-3-hydroxy-2-propoxy]methyl]gua-nine (**8a**) in 36.2% chemical yield, if the ratio of starting materials and reaction temperature are appropriate, although the formation of the undesired fully protected by-product N^2-(p-anisyldiphenylmethyl)-9-[[1,3-bis(p-anisyl-diphenylmethoxy)-2-propoxy]methyl]guanine (**8b**) is not avoidable, in 20.7% chemical yield. Compound **8a** reacted with p-tosyl chloride at room temp-erature afforded the desired precursor tosylate N^1-(p-anisyldiphenylmethyl)-9-[((1-anisyldiphenylmethoxy)-3-tosyl-2-propoxy)methyl]guanine (**9a**) in a

yield of 50.8%, together with the undesired by-product 1-tosyl-N^2-(*p*-anisyldiphenylmethyl)-9-[((1-anisyldiphenylmethoxy)-3-tosyl-2-propoxy)-methyl]guanine (**9b**) in a yield of 17.5%. The tosylate **9a** was purified by recrystallization from ethanol in the literature.[22] We found it was convenient to perform flash column chromatography to produce pure and reliable precursor **9a**. The fluorination of the tosylate **9a** with anhydrous potassium fluoride in dry acetonitrile catalyzed by Kryptofix 2.2.2 gave the intermediate N^2-(*p*-anisyldiphenylmethyl)-9-[[1-(*p*-anisyldiphenylmethyl)-3-fluoro-2-propoxy]methyl]guanine (**10**) in a yield of 29.7%. This intermediate **10** was easily hydrolyzed by 1 N HCl aqueous solution to give the unlabeled standard sample FHPG, **1** in a yield of 87.3%.

The overall chemical yield of the tosylate precursor **9a** from GCV was 18.4%, and the overall chemical yield of the standard sample FHPG, **1** from GCV was 4.8%.

[^{18}F]FHPG (**1**) was synthesized by a modification of the procedures as reported in the literature.[13,18,19] The tosylated precursor **9a** was labeled by a conventional nucleophilic substitution with K[^{18}F]/Kryptofix 2.2.2 in CH_3CN at 120°C for 20 min to provide a radiolabeling intermediate **10**. The radiolabeling reaction was monitored by analytical radio-HPLC method, in which we employed a new HPLC system[23,24] by using a Prodigy (Phenomenex) 5 μm C-18 column, 4.6 × 250 mm; 3 : 1 : 1 CH_3CH: MeOH: 20 mM, pH 6.7 $KHPO_4^-$ mobile phase, 1.5 mL/min flow rate, and UV (240 nm) and γ-ray (NaI) flow detectors. Retention times in the analytical HPLC system were: RT**10** = 15.00 min, RTK[^{18}F] = 1.88 min. The radiolabeling mixture containing the intermediate **10** was passed through a Silica Sep-Pak to remove Kryptofix 2.2.2 and non-reacted K[^{18}F]. The large polarity difference between **10** and Kryptofix 2.2.2 and non-reacted K[^{18}F] permitted the use of a simple solid-phase extraction (SPE) technique[23–25] for fast isolation of **10** from the radiolabeling reaction mixture. The key part in this technique is a SiO_2 Sep-Pak type cartridge, which contains ∼0.5–2 g of adsorbent. The Sep-Pak was eluted with 15% MeOH/CH_2Cl_2 and the solvent was evaporated under high vacuum to give the residue **10**. The existence of the catalyst Kryptofix 2.2.2 and non-reacted K[^{18}F] would affect the deprotection reaction of **10**; therefore, they needed to be removed before **10** was deprotected to give the target labeled product **1**. The residue **10** was followed a quick deprotection with 1 N HCl for 10 min and neutralized with 6 N NaOH to provide **1**. To simplify the synthetic procedure, the final reaction mixture was purified with SPE method instead of HPLC method so that it will be amenable for automation.[19] The crude product was once again passed through the second Silica Sep-Pak to remove radioactive by-product by simple SPE with ethanol. The large polarity difference between **1** and radioactive by-product permitted the use of SPE technique for fast purification of radiotracer **1** from radiolabeling mixture.

The radiochemically pure compound **1** was isolated with $90:8:2$ $H_2O/$ EtOH/HOAc from the Sep-Pak and adjusted pH to 5.5–7.0 with 2 M NaOH and 150 mM NaH_2PO_4 mixed solution. The radiochemical yield of **1** was 10–15%, and the synthesis time was $\sim$70 min from EOB. Chemical purity, radiochemical purity, and specific radioactivity were determined by analytical HPLC method. Retention times in the analytical HPLC system were: RT**9a** = 14.03 min, RT**1** = 2.02 min. The chemical purities of precursor **9a** and standard sample **1** were >95%, the radiochemical purity of target radiotracer **1** was >99%, and the chemical purity of radiotracer **1** was $\sim$93%. The average ($n = 3$–5) specific radioactivity of radiotracer **1** was 0.8–1.2 Ci/ μmol at EOS.

In comparison with the results reported in the literature,[13,18,19,22] several improvements in the synthetic methodology for FHPG and [^{18}F]FHPG have been made. They include increased radiochemical yield and specific activity, enhanced radiochemical purity, shortened synthesis time, new Sep-Pak techniques for fast and efficient preparative separation of [^{18}F]FHPG from precursors, and new HPLC systems for the quality control (QC) method of target tracer [^{18}F]FHPG.

Compounds **6b**, **8b**, and **9b** are new compounds.

In conclusion, an improved total synthesis of [^{18}F]FHPG has been developed. Several improvements and new findings in the synthetic methodology, radiolabeling, preparative separation and analytical details for GCV, FHPG, precursor and [^{18}F]FHPG have been made and addressed. This improved method is efficient and convenient. It is anticipated that the approaches and improvements described here can be applied with advantage to the synthesis of other radiolabeled GCV and PCV analogs for PET imaging of HSV-tk gene expression.

EXPERIMENTAL SECTION

All commercial reagents and solvents were used without further purification unless otherwise specified. Tetrahydrofuran (THF) solvent was distilled from $LiAlH_4$ immediately prior to use. Melting points were determined on a MEL-TEMP II capillary tube apparatus and were uncorrected. ^{1}H NMR spectra were recorded on a Bruker QE 300 NMR spectrometer using tetramethylsilane (TMS)as an internal standard. Chemical shift data for the proton resonances were reported in parts per million (δ) relative to internal standard TMS (δ 0.0). The low resolution mass spectra were obtained using a Bruker Biflex III MALDI-Tof mass spectrometer, and the high resolution mass measurements were obtained using a Kratos MS80 mass spectrometer, in the Department of Chemistry at Indiana University. Chromatographic solvent

proportions are expressed on a volume : volume basis. Thin layer chromatography was run using Analtech silica gel GF uniplates ($5 \times 10 \, cm^2$). Plates were visualized by UV light. Normal phase flash chromatography was carried out on EM Science silica gel 60 (230–400 mesh) with a forced flow of the indicated solvent system in the proportions described below. All moisture-sensitive reactions were performed under a positive pressure of nitrogen maintained by a direct line from a nitrogen source.

Analytical HPLC was performed using a Prodigy (Phenomenex) 5 µm C-18 column, 4.6×250 mm; $3 : 1 : 1$ CH_3CN: MeOH: 20 mM, pH 6.7 $KHPO_4^-$ mobile phase, 1.5 mL/min flow rate, and UV (240 nm) and γ-ray (NaI) flow detectors. Semi-preparative C-18 SiO_2 Sep-Pak type cartridge was obtained from Waters Corporate Headquarters, Milford, MA. Sterile vented Millex-GS 0.22 µm vented filter unit was obtained from Millipore Corporation, Bedford, MA.

1,3-Dibenzyloxy-2-chloromethoxypropane (4)

The mixture of 1,3-dibenzyloxy-2-propanol **2** (9.1 mL, 36.7 mmol) and paraformaldehyde (2.39 g, 79.6 mmol) in anhydrous 1,2-dichloroethane (100 mL) was cooled to 0°C. Dry HCl gas was bubbled through the suspension at 0°C for 6 h. Anhydrous Na_2SO_4 was added to the mixture. After stirring the solvent was removed under vacuum to give a viscous liquid residue **4** (∼100%). The crude product was used for the next step reaction without further purification.

2,6,9-Tris(trimethylsilyl)guanine (5)

The mixture of guanine **3** (5.50 g, 36.4 mmol), ammonium sulfate (0.70 g, 132.1 mmol) and 1,1,1,3,3,3-hexamethyldisilazane (250 mL) was refluxed under nitrogen for 4 days until it became clear. Volatiles were removed under reduced pressure to give viscous syrup **5** (∼100%). The crude product was used for the next step reaction without further purification.

9-[(1,3-Dibenzyloxy-2-propoxy)methyl]guanine (6a) and 7-[(1,3-Dibenzyloxy-2-propoxy)methyl]guanine (6b)

Compounds **2** and **4** as obtained above were combined through the aid of dry THF (200 mL). The mixture was stirred at room temperature (r.t.). Tetrabutylammonium fluoride (TBAF, 0.40 g) dried by azeotroping

distillation in anhydrous benzene (40 mL) was added to the mixture. The resulting solution was then refluxed for 22 h. After removal of solvent, the yellowish residue was transferred to a separation funnel with the aid of ethyl acetate, and then more ethyl acetate and water were added. Large amount of yellowish precipitate formed when shaking. The solid was filtered, washed with water and ethyl acetate, and dried under vacuum. The organic layer of the filtrate was washed twice with water. After removal of solvent the yellow viscous residue was subject to column chromatography on silica gel eluted with 9 : 1 EtOAc/MeOH to give a yellow solid. Both of solids were a mixture (9.33 g, 58.9%) of undesired by-product 7-isomer **6b** and desired 9-isomer **6a**, which could not be separated by TLC and gave the same R_f value ($R_f = 0.29$, 9 : 1 EtOAc/MeOH) on TLC. The NMR spectrum showed the ratio of **6a/6b** was about 2 : 1. They were separated and purified by recrystallization in ethanol. Crude product ($\sim$7.0 g) was stirred with ethyl acetate (200 mL) at r.t., and then filtered. The solid was transferred to a 1000 mL flask containing ethanol (500 mL). The suspension was heated to reflux, and filtered through a frit (fine). The clear yellowish solution was left at 4°C overnight to give the first precipitate that was mostly 7-isomer **6b**. ^{1}H NMR (300 MHz, DMSO-d_6): δ 10.92 (s, 1H, 1-NH), 8.11 (s, 1H, 8-CH), 7.10–7.40 (m, 10H, Ph), 6.24 (s, 2H, 2-NH$_2$), 5.68 (s, 2H, 1′-CH$_2$), 4.40 (s, 4H, PhCH_2), 4.10 (q, 1H, 3′-CH, $J = 4.78$ Hz), 3.30–3.60 (m, 4H, 4′-CH$_2$). LRMS (EI, m/z): 91 (100%), 436 [(M + H)$^+$, 0.4%]. HRMS (FAB, m/z): calcd for C$_{23}$H$_{26}$N$_5$O$_4$ 436.4838, found 436.1993. The filtrate was then left at -16°C overnight to give the second precipitate that was pure 9-isomer **6a**. The solution was concentrated, and left at -16°C to give third, forth and more portions of pure 9-isomer **6a**. The purity was monitored by NMR spectrum. The pure product **6a** (2.81 g, 17.8%) was obtained. **6a**, ^{1}H NMR (300 MHz, DMSO-d_6): δ 10.63 (s, 1H, 1-NH), 7.81 (s, 1H, 8-CH), 7.15–7.35 (m, 10H, Ph), 6.49 (s, 2H, 2-NH$_2$), 5.45 (s, 2H, 1′-CH$_2$), 4.40 (s, 4H, PhCH_2), 4.02 (q, 1H, 3′-CH, $J = 4.78$ Hz), 3.30–3.50 (m, 4H, 4′-CH$_2$).

9-[(1,3-Dihydroxy-2-propoxy)methyl]guanine (Ganciclovir, GCV, 7)

Compound **6a** (0.50 g, 1.15 mmol) was dissolved in hot ethanol (30 mL), and then palladium black (1.50 g) and cyclohexene (20 mL) were added. The mixture was refluxed under nitrogen for 24 h until TLC showed starting material was gone. The catalyst was filtered through celite while the mixture was hot, washed with ethanol and hot DMF until the filtrate on TLC plate

showed no spot under UV. The ethanol and DMF filtrates were evaporated to dryness separately. The solid residues were combined with 1:1 EtOH/H_2O, heated to dissolve, and filtered through celite topped with activate charcoal. After removal of solvents the colorless solid was recrystallized with 4:1 EtOH/H_2O to afford a white crystal solid **7** (0.26 g, 87.7%). ^1H NMR (300 MHz, DMSO-d_6): δ 10.63 (s, 1H, 1-NH, D_2O exchangeable), 7.79 (s, 1H, 8-CH), 6.48 (s, 2H, 2-NH_2, D_2O exchangeable), 5.42 (s, 2H, 1′-CH_2), 4.60 (t, 2H, OH, $J = 5.15$ Hz, D_2O exchangeable), 3.20–3.65 (m, 5H, 3′-CH and 4′-CH_2).

N^2-(*p*-Anisyldiphenylmethyl)-9-[[1-(*p*-anisyldiphenylmethoxy)-3-hydroxy-2-propoxy]methyl]guanine (8a) and N^2-(*p*-Anisyldiphenylmethyl)-9-[[1,3-*bis*(*p*-anisyldiphenylmethoxy)-2-propoxy]methyl]guanine (8b)

GCV **7** (1.00 g, 3.98 mmol), monomethoxytrityl chloride (2.65 g, 8.58 mmol), 4-dimethylaminopyridine (DMAP, 0.030 g, 0.25 mmol), and triethylamine (2.5 mL) were dissolved in dry DMF (50 mL). The mixture was stirred at 55°C for 6 h. Methanol (10 mL) was added to quench the reaction, and solvents were evaporated. The residue was transferred to a separation funnel through the aid of ethyl acetate, washed with aqueous NaHCO$_3$ solution and water, dried over MgSO$_4$. After evaporation the resulting solid was dissolved in 4% MeOH/CH_2Cl_2, absorbed by a small amount of silica gel, and dried under vacuum. This silica gel was then transferred to the top of a column, and eluted with 2.5–3.0% MeOH/CH_2Cl_2. Two components were collected. The first component was undesired by-product **8b** as a white solid (0.87 g, 20.7%), mp 115°C (dec.), $R_f = 0.34$ (5% MeOH/CH_2Cl_2). ^1H NMR (300 MHz, DMSO-d_6): δ 10.68 (s, 1H, 1-NH), 7.84 (s, 1H, 8-CH), 7.67 (s, 1H, 2-NH), 6.53–7.36 (m, 42H, Ph), 4.91 (s, 2H, 1′-CH_2), 3.75 (s, 6H, OCH$_3$), 3.57–3.67 (m, 1H, 3′-CH), 3.48 (s, 3H, OCH$_3$), 2.63 (brs, 4H, 4′-CH_2). LRMS (EI, m/z): 273 (100%), 1094 [(M + Na)$^+$, 1.6%]. HRMS (FAB, m/z): calcd for $C_{69}H_{61}NaN_5O_7$ 1094.4469, found 1094.4452. The second component was the desired product **8a** as a white solid (1.13 g, 36.2%), $R_f = 0.15$ (5% MeOH/CH_2Cl_2). ^1H NMR (300 MHz, DMSO-d_6): δ 10.67 (s, 1H, 1-NH, D_2O exchangeable), 7.78 (s, 1H, 8-CH), 7.68 (s, 1H, 2-NH, D_2O exchangeable), 6.66–7.33 (m, 28H, Ph), 4.97 (dd, 2H, 1′-CH_2, $J_1 = 36.03$ Hz, $J_2 = 11.03$ Hz), 4.44 (t, 1H, OH, $J = 5.14$ Hz, D_2O exchangeable), 3.74 (s, 3H, OCH$_3$), 3.56 (s, 3H, OCH$_3$), 3.40–3.50 (m, 1H, 3′-CH), 2.80–3.07 (m, 2H, 5′-CH_2), 2.51–2.80 (m, 2H, 4′-CH_2).

N^2-(*p*-Anisyldiphenylmethyl)-9-[((1-anisyldiphenylmethoxy)-3-tosyl-2-propoxy)methyl]guanine (9a) and 1-Tosyl-N^2-(*p*-anisyldiphenylmethyl)-9-[((1-anisyldiphenylmethoxy)-3-tosyl-2-propoxy)methyl]guanine (9b)

Compound **8a** (0.28 g, 0.35 mmol) and *p*-tosyl chloride (0.26 g, 1.35 mmol) were dissolved in dry pyridine (5 mL). The mixture was stirred at r.t. for 2 days. To this brown solution was added water (1 mL) to quench the reaction, and then solvents were evaporated. The residue was dissolved in ethyl acetate, washed with water, dried over Na_2SO_4. After removal of solvent the solid was dissolved in a small volume of CH_2Cl_2, and transferred to a silica gel column, then eluted with 1% $MeOH/CH_2Cl_2$ to afford undesired by-product **9b** as a light brown solid (0.067 g, 17.5%), mp. 95°C (dec.), $R_f = 0.36$ (1% $MeOH/CH_2Cl_2$). ^{1}H NMR (300 MHz, DMSO-d_6): δ 6.56–8.27 (m, 38H, Ph and 8-CH), 5.11 (dd, 2H, 1′-CH$_2$, $J_1 = 44.85$ Hz, $J_2 = 11.03$ Hz), 3.73 (s, 3H, OCH$_3$), 3.53 (s, 3H, OCH$_3$), 3.38–3.57 (m, 3H, 3′-CH and 4′-CH$_2$), 2.30–2.71 (m, 2H, 5′-CH$_2$), 2.41 (s, 6H, CH$_3$). LRMS (EI, m/z): 273 (100%), 1108 [(M + H)$^+$, 1.4%]. HRMS (FAB, m/z): calcd for $C_{63}H_{58}N_5O_{10}S_2$ 1108.3625, found 1108.3667. Then the column was eluted with 3% $MeOH/CH_2Cl_2$ to give the desired product **9a** as a light brown solid (0.17 g, 50.8%), $R_f = 0.15$ (3% $MeOH/CH_2Cl_2$). ^{1}H NMR (300 MHZ, DMSO-d_6): δ 10.67 (s, 1H, 1-NH), 7.77 (s, 1H, 8-CH), 7.73 (s, 1H, 2-NH), 6.62–7.67 (m, 32H, Ph), 4.93 (dd, 2H, 1′-CH$_2$, $J_1 = 59.56$ Hz, $J_2 = 11.76$ Hz), 3.75 (s, 3H, OCH$_3$), 3.37–3.64 (m, 3H, 3′-CH and 4′-CH$_2$), 3.54 (s, 3H, OCH$_3$), 2.37–2.67 (m, 2H, 5′-CH$_2$), 2.43 (s, 3H, CH$_3$).

N^2-(*p*-Anisyldiphenylmethyl)-9-[[1-(*p*-anisyldiphenylmethyl)-3-fluoro-2-propoxy]methyl]guanine (10)

Tosylate **9a** (0.10 g, 0.11 mmol), potassium fluoride (0.14 g, 2.41 mmol) and Kryptofix 2.2.2. (0.24 g, 0.64 mmol) were dissolved in dry acetonitrile (8 mL). The mixture was heated to 115–120°C for 40 min. The solvent was removed, and the residue was transferred to the top of a silica gel column with the aid of CH_2Cl_2. The column was eluted with 2% $MeOH/CH_2Cl_2$ to give the desired compound **10** as a light brown solid (0.025 g, 29.7%), $R_f = 0.25$ (5% $MeOH/CH_2Cl_2$). ^{1}H NMR (300 MHz, CDCl$_3$): δ 11.64 (brs, 1H, 1-NH), 7.80 (brs, 1H, 2-NH), 6.52–7.40 (m, 28H, Ph), 4.97 (s, 2H, 1′-CH$_2$), 3.89–4.29 (m, 2H, 5′-CH$_2$), 3.74 (s, 3H, OCH$_3$), 3.58 (s, 3H, OCH$_3$), 3.42–3.66 (m, 1H, 3′-CH), 2.73–2.93 (m, 2H, 4′-CH$_2$).

9-[(3-Fluoro-1-hydroxy-2-propoxy)methyl]guanine (FHPG, 1)

The solution of compound **10** (0.025 g, 0.031 mmol) in methanol (2.5 mL) and 1 N aqueous HCl (0.5 mL) was refluxed for 15 min while TLC showed no starting material left. The solution was neutralized with 1 N aqueous NaOH to pH ~7–8. Silica gel was added to absorb the solution, and then the mixture was made to dry under vacuum and transferred to the top of a column. The column was eluted with 20 : 1 MeCN/H$_2$O to give the target compound FHPG **1** as a light brown solid (7.0 mg, 87.3%), R$_f$ = 0.34 (12 : 1 MeCN/H$_2$O). ^{1}H NMR (300 MHz, DMSO-d_6): δ 10.89 (s, 1H, 1-NH, D$_2$O exchangeable), 7.81 (s, 1H, 8-CH), 6.78 (s, 2H, 2-NH$_2$, D$_2$O exchangeable), 5.42 (s, 2H, 1′-CH$_2$), 4.93 (t, 1H, OH, J = 5.88 Hz, D$_2$O exchangeable), 4.24–4.58 (m, 2H, 4′-CH$_2$F), 3.73–3.88 (m, 1H, 3′-CH), 3.28–3.43 (m, 2H, 5′-CH$_2$).

9-[(3-[^{18}F]Fluoro-1-hydroxy-2-propoxy)methyl]guanine ([^{18}F]FHPG, 1)

No-carrier-added (NCA) aqueous H[^{18}F] (0.5 mL) prepared by ^{18}O(p,n)^{18}F nuclear reaction in a RDS-112 cyclotron on an enriched H$_2^{18}$O water (95 + %) target was added to a Pyrex vessel which contains K$_2$CO$_3$ (4 mg, in 0.2 mL H$_2$O) and Kryptofix 2.2.2 (10 mg, in 0.5 mL CH$_3$CN). Azeotropic distillation at 115°C with HPLC grade CH$_3$CN (3 × 1 mL) under a nitrogen steam efficiently removed the target H$_2$O. The tosylated precursor **9a** (2–3 mg, dissolved in 0.5 mL CH$_3$CN) was introduced to the anhydrous potassium [^{18}F]fluoride-Kryptofix 2.2.2 complex. The reaction mixture was sealed and heated at 120°C for 20 min and was subsequently allowed to cool down, at which time the crude product was passed through a Silica Sep-Pak cartridge to remove Kryptofix 2.2.2 and non-reacted K[^{18}F]. The Sep-Pak was eluted with 15% MeOH/CH$_2$Cl$_2$ (3.5 mL), and then passed onto a rotatory evaporator. The solvent was removed by evaporation under high vacuum. The residue was acidified with 1 N HCl (0.6 mL) and heated for 10 min at 80°C. The contents were neutralized with 6 N NaOH (0.1 mL), diluted with ethanol (3 mL), and evaporated in vacuo. The crude product was passed through they second Silica Sep-Pak cartridge through the aid of ethanol. The Sep-Pak was eluted with EtOH to remove radioactive by-product. The radiochemically pure product [^{18}F]FHPG, **1** was eluted from the Sep-Pak with 90 : 8 : 2 H$_2$O/EtOH/ HOAc and adjusted pH to 5.5–7.0 with 2 M NaOH and 150 mM NaH$_2$PO$_4$ mixed solution, whose volume was dependent upon the use of the labeled product in tissue biodistribution studies (~3 mL, 3 × 1 mL) or in micro-PET imaging studies (1.5 mL, 3 × 0.5 mL) of HSV-tk prostate cancer tumors in athymic mice, and sterile-filtered through a 0.22 μm cellulose acetate

membrane and collected into a sterile vial. The radiochemical yield of [^{18}F]FHPG was 10–15%, and the synthesis time was $\sim$70 min from end of bombardment (EOB). Retention times in the analytical HPLC system were: RT**9a** = 14.03 min, RT**1** = 2.02 min. The chemical purities of precursor **9a** and standard sample **1** were >95%, the radiochemical purity of target radiotracer **1** was >99%, and the chemical purity of radiotracer **1** was $\sim$93%. The average (n = 3–5) specific radioactivity of radiotracer **1** was 0.8–1.2 Ci/ μmol at end-of-synthesis (EOS).

REFERENCES

1. Alauddin, M.M.; Shahinian, A.; Gordon, E.M.; Bading, J.R.; Conti, P.S. Preclinical evaluation of the penciclovir analog 9-(4-[^{18}F]fluoro-3-hydroxymethylbutyl)guanine for in vivo measurement of suicide gene expression with PET. J. Nucl. Med. **2001**, *42*, 1682–1690.
2. Alauddin, M.M.; Shahinian, A.; Kundu, R.K.; Gordon, E.M.; Conti, P.S. Evaluation of 9-[(3-^{18}F-fluoro-1-hydroxy-2-propoxy)methyl]guanine ([^{18}F]-FHPG)in vitro and in vivo as a probe for PET imaging of gene incorporation and expression in tumors. Nucl. Med. Biol. **1999**, *26*, 371–376.
3. Brust, P.; Haubner, R.; Friedrich, A.; Scheunemann, M.; Anton, M.; Koufaki, O.N.; Hauses, M.; Noll, S.; Noll, B.; Haberkorn, U.; Schackert, G.; Schackert, H.K.; Avril, N.; Johannsen, B. Comparison of [^{18}F]FHPG and [$^{124/125}$I]FIAU for imaging herpes simplex virus type 1 thymidine kinase gene expression. Eur. J. Nucl. Med. **2001**, *28*, 721–729.
4. de Vries, E.F.; van Waarde, A.; Harmsen, M.C.; Mulder, N.H.; Vaalburg, W.; Hospers, G.A. [^{11}C]FMAU and [^{18}F]FHPG as PET tracers

for herpes simplex virus thymidine kinase enzyme activity and human cytomegalovirus infrections. Nucl. Med. Biol. **2000**, *27*, 113–119.

5. Gambhir, S.S.; Barrio, J.R.; Herschman, H.R.; Phelps, M.E. Assays for noninvasive imaging of reporter gene expression. Nucl. Med. Biol. **1999**, *26*, 481–490.

6. Gambhir, S.S.; Barrio, J.R.; Phelps, M.E.; Iyer, M.; Namavari, M.; Satyamurthy, N.; Wu, L.; Green, L.A.; Bauer, E.; MacLaren, D.C.; Nguyen, K.; Berk, A.J.; Cherry, S.R.; Herschman, H.R. Imaging adenoviral-directed reporter gene expression in living animals with positron emission tomography. Proc. Natl. Acad. Sci. USA **1999**, *96*, 2333–2338.

7. Gambhir, S.S.; Bauer, E.; Black, M.E.; Liang, Q.; Kokoris, M.S.; Barrio, J.R.; Iyer, M.; Namavari, M.; Phelps, M.E.; Herschman, H.R. A mutant herpes simplex virus type 1 thymidine kinase reporter gene shows improved sensitivity for imaging reporter gene expression with positron emission tomography. Proc. Natl. Acad. Sci. USA **2000**, *97*, 2785–2790.

8. Hospers, G.A.; Calogero, A.; van Waarde, A.; Doze, P.; Vaalburg, W.; Mulder, N.H.; de Vries, E.F. Monitoring of herpes simplex virus thymidine kinase enzyme activity using positron emission tomography. Cancer Res. **2000**, *60*, 1488–1491.

9. Hustinx, R.; Shiue, C.Y.; Alavi, A.; McDonald, D.; Shiue, G.G.; Zhuang, H.; Lanuti, M.; Lambright, E.; Karp, J.S.; Eck, S.L. Imaging in vivo herpes simplex virus thymidine kinase gene transfer to tumour-bearing rodents using positron emission tomography and [^{18}F]FHPG. Eur. J. Nucl. Med. **2001**, *28*, 5–12.

10. Inubushi, M.; Wu, J.C.; Gambhir, S.S.; Sundaresan, G.; Satyamurthy, N.; Namavari, M.; Yee, S.; Barrio, J.R.; Stout, D.; Chatziioannou, A.F.; Wu, L.; Schelbert, H.R. Positron-emission tomography reporter gene expression imaging in rat myocardium. Circulation **2003**, *107*, 326–332.

11. Iyer, M.; Barrio, J.R.; Namavari, M.; Bauer, E.; Satyamurthy, N.; Nguyen, K.; Toyokuni, T.; Phelps, M.E.; Herschman, H.R.; Gambhir, S.S. 8-[^{18}F]Fluoropenciclovir: an improved reporter probe for imaging HSV1-tk reporter gene expression in vivo using PET. J. Nucl. Med. **2001**, *42*, 96–105.

12. Pantuck, A.J.; Berger, F.; Zisman, A.; Nguyen, D.; Tso, C.L.; Matherly, J.; Gambhir, S.S.; Belldegrun, A.S. CL1-SR39: a noninvasive molecular imaging model of prostate cancer suicide gene therapy using positron emission tomography. J. Urol. **2002**, *168*, 1193–1198.

13. Tjuvajev, J.G.; Doubrovin, M.; Akhurst, T.; Cai, S.; Balatoni, J.; Alauddin, M.M.; Finn, R.; Bornmann, W.; Thaler, H.; Conti, P.S.; Blasberg, R.G. Comparison of radiolabeled nucleoside probes (FIAU,

FHBG, and FHPG) for PET imaging of HSV1 tk gene expression. J. Nucl. Med. **2002**, *43*, 1072–1083.

14. Wu, J.C.; Inubushi, M.; Sundaresan, G.; Schelbert, H.R.; Gambhir, S.S. Position emission tomography imaging of cardiac reporter gene expression in living rats. Circulation **2002**, *106*, 180–183.

15. Yaghoubi, S.; Barrio, J.R.; Dahlbom, M.; Iyer, M.; Namavari, M.; Satyamurthy, N.; Goldman, R.; Herschman, H.R.; Phelps, M.E.; Gambhir, S.S. Human pharmacokinetic and dosimetry studies of [^{18}F]FHBG: a reporter probe for imaging herpes simplex virus type-1 thymidine kinase reporter gene expression. J. Nucl. Med. **2001**, *42*, 1225–1234.

16. Yaghoubi, S.S.; Wu, L.; Liang, Q.; Toyokuni, T.; Barrio, J.R.; Namavari, M.; Satyamurthy, N.; Phelps, M.E.; Herschman, H.R.; Gambhir, S.S. Direct correlation between positron emission tomographic images of two reporter genes delivered by two distinct adenoviral vectors. Gene Ther. **2001**, *8*, 1072–1080.

17. Alauddin, M.M.; Conti, P.S. Synthesis and preliminary evaluation of 9-(4-[^{18}F]-fluoro-3-hydroxymethylbutyl)guanine ([^{18}F]FHBG): a new potential imaging agent for viral infection and gene therapy using PET. Nucl. Med. Biol. **1998**, *25*, 175–180.

18. Alauddin, M.M.; Conti, P.S.; Mazza, S.M.; Hamzeh, F.M.; Lever, J.R. 9-[(3-[^{18}F]-Fluoro-1-hydroxy-2-propoxy)methyl]guanine ([^{18}F]-FHPG): a potential imaging agent of viral infection and gene therapy using PET. Nucl. Med. Biol. **1996**, *23*, 787–792.

19. Shiue, G.G.; Shiue, C.Y.; Lee, R.L.; MacDonald, D.; Hustinx, R.; Eck, S.L.; Alavi, A.A. A simplified one-pot synthesis of 9-[(3-[^{18}F]fluoro-1-hydroxy-2-propoxy)methyl]guanine([^{18}F]FHPG) and 9-(4-[^{18}F]fluoro-3-hydroxymethylbutyl)guanine ([^{18}F]FHBG) for gene therapy. Nucl. Med. Biol. **2001**, *28*, 875–883.

20. Hakimelahi, G.H.; Khalafi-Nezhad, A. Catalytic effect of tetrabutylammonium fluoride in the preparation of secoribo-nucleosides. Helv. Chim. Acta **1989**, *72*, 1495–1500.

21. Ogilvie, K.K.; Cheriyan, U.O.; Radatus, B.K. Biologically active acyclonucleoside analogues. II. The synthesis of 9-[[2-hydroxy-1-(hydroxymethyl ethoxy]methyl]guanine (BIOLF-62). Can. J. Chem. **1982**, *60*, 3005–3010.

22. Martin, J.C.; McGee, D.P.C.; Jeffrey, G.A.; Hobbs, D.W.; Smee, D.F.; Mattews, T.R.; Verheyden, J.P.H. Synthesis and anti-herpes-virus activity of acyclic 2′-deoxyguanosine analogues related to 9-[(1,3-dihydro-2-propoxy)methyl]guanine. J. Med. Chem. **1986**, *29*, 1384–1389.

23. Zheng, Q.-H.; Liu, X.; Fei, X.; Wang, J.-Q.; Mock, B.H.; Glick-Wilson, B.E.; Sullivan, M.L.; Hutchins, G.D. Facile synthesis of [^{11}C]

edrophonium and its analogs as new potential PET imaging agents for heart acetylcholinesterase. Bioorg. Med. Chem. Lett. **2003**, *13*, 1787–1790.

24. Zheng, Q.-H.; Stone, K.L.; Mock, B.H.; Miller, K.D.; Fei, X.; Liu, X.; Wang, J.-Q.; GlickWilson, B.E.; Sledge, G.W.; Hutchins, G.D. [^{11}C]Choline as a potential PET marker for imaging of breast cancer athymic mice. Nucl. Med. Biol. **2002**, *29*, 803–807.
25. Mulholland, K.M.; Zheng, Q.-H.; Mock, B.H.; Vavrek, M.T. Convenient labeling and isolation of [^{11}C-methyl]quaternary amines. J. Labelled Cpd. Radiopharm. **1999**, *42* (Suppl. 1), S459–S461.

Tumor-specific suicide gene therapy for prostate cancer using PSES promoter-driven herpes simplex virus thymidine kinase and ganciclovir

Miwon Ahn,[1,3] Xiong Li,[1,3] Sang-Jin Lee,[1,3] Juan Antonio Jiménez,[1,2,3] Yan-Ping Zhang,[1,3] Kyung-Hee Bae,[1,3] Chinghai Kao,[1,2,3] and Thomas A. Gardner[1,2,3]

Departments of [1]Urology, [2]Microbiology and Immunology, and [3]Walther Oncology Center, Indiana University School of Medicine, Indianapolis, Indiana.

Corresponding Author:

Thomas A. Gardner, MD
Indiana University School of Medicine
Department of Urology
535 Barnhill Drive
Suite 420
Indianapolis, IN   46202
Phone: 317-278-3434; Fax: 317-274-0174; E-mail: thagardn@iupui.edu

Running Title: Please include running title

Key words: Suicide gene therapy, PSA, PSMA, prostate-specific promoter, PSES, HSV-TK, GCV

Abstract

Enzyme prodrug suicide gene therapy has been hindered by gene delivery and transduction efficiency. In order to further explore the potential of this approach, we developed a prostate-restricted replicative adenovirus (PRRA) armed with herpes simplex virus thymidine kinase (HSV-TK). This suicide gene (*HSV-TK*) and prodrug (ganciclovir (GCV)) combination has been extensively explored in both preclinical and clinical studies. In our previous Ad-OC-TK/ACV phase I clinical trial, we demonstrated both safety and proof of principle using a prostate-specific promoter in men with prostate cancer. In this study, we aimed to inhibit the growth of androgen-independent (AI), PSA/PSMA-positive prostate cancer cells by AdIU1, an HSV-TK-armed prostate-restricted replicative adenovirus (PRRA). *In vitro*, the growth of an androgen-independent PSA/PSMA-expressing prostate cancer cell line, CWR22rv, was significantly inhibited by treatment with AdIU1 plus GCV (10 µg/ml), as compared to AdIU1 treatment alone. AdIU1 alone or AdE4PSESE1a (a PRRA lacking HSV-TK) with and without GCV (10 µg/ml) treatment demonstrated no *in vitro* cytotoxicity. *In vitro* cytotoxicity was observed following treatment with AdIU1 plus GCV only in PSA/PSMA-positive CWR22rv and C4-2 cells, but not the PSA/PSMA-negative cell line, DU-145. *In vivo* assessment of AdIU1 plus GCV treatment revealed a therapeutic effect against CWR22rv tumors in nude mice, which was not seen following treatment with AdIU1 alone, AdE4PSESE1a or AdE4PSESE1a plus GCV. In summary, we developed a novel therapeutic strategy for the treatment of AI prostate cancer.

Introduction

Prostate cancer remains the leading cancer diagnosis in men. The incidence of prostate cancer is age-dependent and has steadily increased over the last several decades (ref). Localized prostate cancer can be managed effectively with numerous improving modalities, while advanced and metastatic disease eventually progresses to an androgen-independent (AI) state with limited treatment options. The aging population of men with an increasing prostate cancer incidence combined with an absence of successful therapies for advanced disease, require the development of novel therapies.

Tumor-specific suicide gene therapy using a tissue-specific promoter is a rational treatment strategy for prostate cancer (ref: cmv-tk, OC-TK). Herpes simplex virus *thymidine kinase* (*HSV-TK*)-based suicide gene therapy has been used to target prostate cancer for over a decade (ref: Baylor, uva). The prodrug ganciclovir (GCV) is phosphorylated by HSV-TK to its monophosphate form, which is rapidly converted to di- and triphosphate forms by cellular kinases, the latter of which is toxic to cells. The GCV-triphosphate is incorporated into DNA during cell division, causing single-strand DNA breaks and inhibition of DNA polymerase (ref). Prior preclinical studies have demonstrated that HSV-TK/prodrug-based suicide gene therapy inhibited the growth of mouse and human prostate cancer cells *in vivo* (ref). Clinical studies using the HSV-TK/GCV system for the treatment of prostate cancer have also shown the effectiveness of this suicide gene therapy strategy (ref). However, previous HSV-TK/GCV studies suffered from inefficient gene transduction rates *in vivo*.

Tumor-specific oncolytic adenoviruses have been effective and safe treatment options for patients with metastatic disease. We have demonstrated that Ad-OC-E1a, a PRRA could specifically and effectively inhibit the growth of human prostate cancer *in vitro* and *in vivo* (ref). Others have demonstrated similar *in vitro* and *in vivo* efficacy as well as safe administration to men with locally advanced and metastatic prostate cancer (ref: CN706,

CN787).   More recently, Freytag *et. al.* have demonstrated the safety and efficacy of a conditionally replicating, non-tissue-specific adenovirus containing the suicide genes *TK* and *CD* when combined with external beam radio therapy (ref).

We recently develop a prostate-specific chimeric enhancer, *PSES*, by combining enhancers from *PSA* and *PSMA* genes.   *PSES* showed high activity specifically in PSA/PSMA-positive prostate cancer cells, regardless of androgen status (ref).   This *PSES* promoter has been used to control the replication of a PRRA, which demonstrated prostate-specific replication and therapeutic efficacy both *in vitro* and *in vivo* (ref: E4).   In this study, we developed a novel *HSV-TK*-armed replicative adenovirus, AdIU1, using the *PSES* promoter to drive the expression of adenoviral *E1a*, *E1b* and *E4* genes in addition to *HSV-TK*. AdIU1 demonstrated its selective cytotoxicity toward androgen-independent (AI) PSA/PSMA-expressing prostate cancer both *in vitro* and *in vivo*.

Materials and Methods

Cells and Cell Culture

HER 911E4 cells are derived from adenoviral *E1b* (bp 79 to 5,789)-immortalized HER 911 (human embryonic retinoblastoma) cells that stably express adenoviral E4 proteins under control of the *tetR* promoter. HER911E4 cells were cultured in DMEM, supplemented with 10% FBS, 1% penicillin/streptomycin, 0.1 mg/mL hygromycin B (Calbiochem, San Diego, CA) and 2 μg/mL doxycycline (Sigma, St. Louis, MO). AI, androgen receptor (AR)- and PSA/PSMA-positive prostate cancer cell lines C4-2 and CWR22rv, and AI, AR- and PSA-negative cell lines DU-145 and PC3 were cultured in RPMI 1645 supplemented with 10% FBS and 1% penicillin/streptomycin. The cells were maintained at 37°C in a 5% CO_2 incubator.

Construction of the prostate-restricted replicative andenovirus (PRRA), AdIU1.

The construction of the backbone for AdIU1, AdE4PSESE4, was described previously (ref). To construct AdIU1, the *CMV-EGFP* expression cassette in AdE4PSESE1a was replaced by a *PSES-HSV-TK* expression cassette. *HSV-TK* and *E1b* in the left arm and *E4* and *E1a* in the right arm were placed under the transcriptional control of *PSES*. Figure 1 illustrates the structure of the each virus used in this study. The adenoviral genome was released from the cloning vector by digestion with Pac I restriction enzyme and transfected into HER911E4 cells using Lipofectamine 2000 transfection reagent (Invitrogen, CA, USA). The plate was incubated at 37°C under 5% CO_2 for 7 to 10 days after transfection, until a cytopathic effect was observed. AdIU1 was further amplified in HER911E4 cells. The recombinant adenovirus was purified by CsCl gradient centrifugation. All gradient-purified viral stocks were dialyzed in dialysis buffer (1mM $MgCl_2$, 10mM Triz HCl (pH 7.5) and 10% glycerol) for 24 hours at 4°C, changing the buffer three times. Aliquots of purified virus were stored at -70°C.

Viral replication assay

CWR22rv, C4-2, PC-3 and DU-145 cells were seeded in 6-well plates (1×10^6 cells per well) 1 day prior to viral infection and subsequently infected with AdIU1 or AdE4PSESE1a (1000 virus particles (v.p.)/cell). The media were changed 24 hours after infection, and the viral supernatants were harvested 3 days after infection. The cells were examined under light microscopy daily for up to 5 days. Then, the titers of the harvested viral supernatants were determined by titer assay. HER911E4 cells were seeded in 96-well plates (5×10^3 cells per well) 1 day prior to infection. The cells were infected with serial volume dilutions of the harvested supernatants, ranging from 1 to 10^{-11} µL per well, with each row of 8-wells receiving the same dose of virus. The media were changed on day 4, and the cells were examined under the microscope on day 7. The dose of the produced viruses was represented as an LD_{50} value, the dilution factor that caused a cytopathic effect in at least 4 wells of cells in a single row on a 96-well plate by day 7.

Dose-dependent *in vitro* cell killing assay

CWR22rv and DU145 cells were seeded on to 24-well plates at a density of 1.5×10^5 cells/well. After 24 hours, the cells were infected with 0.1-1000 v.p. per cell of AdIU1 or AdE4PSESE1a. 24 hours after infection, the media were removed and replaced by fresh media with or without GCV (10µg/ml). Media with or without GCV were changed every 2 days. Viable cells were analyzed by crystal violet assay 7 days post-infection.

Time-dependent *in vitro* killing assay

CWR22rv and DU-145 cells were plated in 24-well plates at densities of 1×10^5 cells/well. Cells were divided into 4 treatment groups, no treatment, AdIU1 (100 v.p./cell), GCV, and AdIU1 (100 v.p./cell) plus GCV. The media were changed 24 hours after infection, and

GCV (10μg/ml) was added 24 hours after the media change. Cell viability was analyzed at day 1, 3, 5 and 7 by crystal violet assay.

In vivo evaluation of AdIU1 therapy

All animal methods and procedures were approved by the Indiana University School of Medicine Institutional Animal Care and Use Committee (IACUC). CWR22rv xenografts were established by injecting 2×10^6 cells s.c. in the flanks of 6 week-old male, athymic nude mice. The injected mice were castrated 3 days after cells injection. Mice with similar tumor sizes (3 – 5 mm) were divided into four groups receving, AdE4PSESE1a (negative control PRRA), AdE4PSESE1a plus GCV, AdIU1, or AdIU1 plus GCV treatment. 2×10^9 v.p. of either AdE4PSESE1a or AdIU1 in 100μL 1xPBS were injected intratumorally. 5 days after virus injection, GCV (40 mg/kg) was administered i.p. twice-daily for 10 days. Tumor sizes were measured every 5 days, and the following formula was applied to calculate tumor volume, length x $width^2$ x 0.5236. Mice were sacrificed and tumors harvested for histological examination 30 days after injection.

Histology and Immunohistochemistry

Tumors were harvested, immediately fixed in formalin and embedded in paraffin. The tissue sections were stained with hematoxylin and eosin (H&E), according to the standard protocol. For immunohistochemistry, tumor sections were deparaffinized, rehydrated and heated in a microwave oven for 20 min in activity antigen-retrieval solution (10mM citric buffer, pH 6.0). Endogenous peroxidase was blocked with 3% hydrogen peroxide solution. The slides were rinsed with distilled water, washed twice with PBS for 3 min and blocked with Superblock (Scytek Laboratories, Burlingame, CA, USA) in a humidified chamber for 60 min at room temperature. After rinsing with PBS, the slides were incubated with avidin (Vector Laboratories, Inc., Burlingame, CA, USA) for 15 min, washed with PBS and blocked

with biotin in a humidified chamber for 15 min at room temperature.   A monoclonal mouse antibody to adenovirus type 5 (Abcam, Cambridge, MA, USA) and a mouse monoclonal antibody Ki67 antigen (Novovastra Laboratories Ltd., UK) were applied.   These slides were incubated with primary antibodies overnight in humidified chambers at 4°C.   After 1 PBS rinse, a biotinylated secondary antibody was applied to the slides and incubated for 1h. After washing with PBS, slides were incubated with avidin-peroxidase complex (ABC) reagent (Vector Laboratories, Inc., Burlingame, CA, USA) for 30min, washed once with PBS, stained with freshly prepared diaminobenzidin (DAB) solution for 15 min and counterstained with hematoxylin.

In situ Terminal Deoxynucleotide Transferase-Mediated Nick End Labeling Assay.

The _in situ_ apoptosis detection kit was purchased from Roche Diagnostics (Indianapolis, IN). Tumor tissue sections were deparafinized using a sequential xylene protocol and rehydrated through gradients of ethanol and distilled water.   Slides were treated with 10nmol/L Tris solution containing 1 µg/ml proteinase K for 15 min.   All slides were rinsed with PBS and incubated with 100µL terminal deoxynucleotidyl transfererase-mediated nick end labeling (TUNEL) reaction mixture (or 100µL control labeling solution for negative control) in a humid chamber at 37°C for 30 min. The slides were washed 3X with PBS and incubated with 100µL TUNEL POD solution in a humid chamber at 37°C for 30min.   After washing with PBS, the slides were stained with freshly prepared DAB solution for 10min, rinsed with PBS, and counterstained with hematoxylin.

Results

Construction of a TK-armed PRRA.

AdIU1 was constructed by replacing the *CMV-GFP* expression cassette in AdE4PSESE1a with a *PSES-HSV-TK* expression cassette to extend the therapeutic potential of the PSES-based PRRA (Fig. 1). HER911E4 cells were transfected with recombinant adenoviral *HSV-TK* plasmid linearized by Pac I restriction enzyme digestion, and AdIU1 was purified from the harvest viral supernatant. To assess the prostate-specificity and viral replication efficiency of AdIU1, we performed an *in vitro* viral replication assay. PSA/PSMA-positive and –negative cells were infected with AdIU1. Viral plaques were observed only in the PSA/PSMA-positive cells (Table 1), demonstrating the fact that AdIU1 replication is tightly controlled by PSES and restricted to PSA/PSMA-positive cells.

Selective cell killing activity of AdIU1 plus GCV against AI, PSA/PSMA-positive human prostate cancer cells *in vitro*.

We performed a prodrug sensitivity assay *in vitro*. Each cell line, AI, PSA/PSMA-positive CWR22rv and C4-2, as well as AI, PSA/PSMA-negative DU-145 were seeded in triplicate in 24-well plates at a density of 2×10^4 cells/well and were incubated with increasing concentrations of GCV (0 to 100 μg/ml). Cell viability was determined after 5 days using crystal violet assay, and a corresponding IC_{50} dose was determined for each cell line (data not shown). We determined the optimal GCV treatment dose to be 10ug/ml.

To evaluate the selective cytotoxicity of AdIU1 and AdE4PSESE1a viruses, we infected each cell line with wide dose ranges (0.1-1000 v.p./cell) of virus, and then treated infected cells with or without GCV (10 μg/ml) (Fig. 2). The AI, PSA/PSMA-positive human prostate cancer cell, CWR22rv was significantly inhibited by 0.1 v.p. of AdIU1 in the presence of GCV. AdIU1 without GCV had similar killing activity as AdE4PSESE1a (negative control) either in the presence or absence of GCV. The AI, AR- and PSA/PSMA-

negative cell line, DU 145 was unaffected by either virus.

AdIU1/GCV showed cytotoxicity in AI, PSA/PSMA-positive cancer cells

CWR22rv (PSA/PSMA-positive) and DU-145 (PSA/PSMA-negative) cells were seeded in-24 well plates. The 24 wells were divided into 4 groups, no treatment, AdIU1, GCV alone, and AdIU1 plus GCV treatment. The GCV alone group demonstrated limited cytotoxicity. This confirmed that 10ug/mL GCV treatment was not toxic to either prostate cancer cell lines. The CWR22rv cell line demonstrated cell growth inhibition at day 7 after AdIU1 exposure, which was significantly enhanced when GCV was administered following AdIU1 infection. The DU-145 cell line demonstrated limited cytotoxicity in all four groups investigated (Fig. 3).

In vivo growth inhibition of CWR22rv xenograft by AdIU1/GCV

Human prostate CWR22rv xenograft tumors were induced by subcutaneous injection of CWR22rv cells into athymic nude mice. The mice were castrated 3 days after CWR22rv inoculation to test whether AdIU1 or AdE4PSESE1a was able to eliminate AI tumors in a castrated host. After tumor formation, the mice were randomized into 4 groups (AdIU1, AdE4PSESE1a, AdIU1 plus GCV and AdE4PSESE1a plus GCV). The mice were injected intratumorally with AdIU1 or AdE4PSESE1a as a control. Day 0 was the time of virus injection. On day 5, groups receiving GCV treatments were injected with GCV (40 mg/kg) 2 times a day for 10 days. Tumor volumes were measured at the times indicated in Figure 4. AdIU1/GCV effectively caused growth delay of CWR22rv xenografts. Light microscopic observation of H&E-stained tumors in mice injected with AdIU1/GCV showed substantial treatment effect. (Fig. 5). We also observed a large number of fibroblasts following combined treatment. To compare proliferation between the GCV treatment group and non-treated group, we performed immunohistochemistry using the proliferation antigen, Ki67.

We observed no significant difference in proliferation antigen expression between both groups.   Also, we observed that all necrotic tumors stained positive for apoptosis by TUNEL assay.   Anti-adenovirus type 5 E1a immunohistochemical staining revealed that extensive viral infection existed throughout the AdIU1, AdE4PSESE1a, and AdE4PSESE1a plus GCV treatment group tumors; however, adenovirus staining was absent in the AdIU1 plus GCV treatment group.

Discussion

       Replication-defective recombinant adenoviruses have been widely studied *in vitro* and *in vivo* as a vector to deliver cancer therapeutic genes. Adenoviral based cancer gene therapy still maintains unrealized potential. The ability to infect and transduce a variety of mammalian cells, including prostate cells (ref: PhaseI OC-TK) in a cell cycle replication-independent manner without genotoxicity. However, there are several limitations in the use of these vectors for cancer gene therapy. Prior adenoviral investigations have demonstrated decreased Coxsackie-Adenoviral receptors on some cancer types. Additionally, the absence of integration into the genome allows for only a transient duration of exogenous gene expression expression.

       The current investigations build on the ability of the adenovirus to infect prostate cancer cells and provide both expanded infection and longer exogenous gene expression with a prostate restricted replication-competent oncolytic virus, AdIU1. AdIU1 can replicate and kill infected cells by viral lysis, leading to *in vivo* amplification of input viral dose, spreading to adjacent cancer cells after lysis of initially infected cells. Additionally, AdIU1-infected cells produce HSV-TK to enhance killing with prodrug administration and allow for imaging of the viral process (ref: PET-TK). Several studies have demonstrated the importance of tissue-specific vectors, revealing systemic toxicity with the administration of high dose of nonspecific vectors. Through the use of prostate-specific promoters and enhancers, the expression of a therapeutic gene or adenoviral replication can be limited to cells that contain the appropriate activators and transcription factors. Currently, *kallikrein 2*, *PSA*, *rat probasin*, and *osteocalcin (OC)* are each under extensive investigation as regulators of prostate restricted replication adenovirus (ref). In our previous investigations, prostate-specific enhance sequence (PSES), was developed by locating the minimal sequence, AREc3 and PSME(del2) in AREc and PSME, respectively and placing AREc3 upstream from PSME (del2) (ref). PSES showed high activity specifically in PSA/PSMA-positive and AI prostate

cancer cells (ref AdE4).

Gene therapy with *HSV-TK* as a suicide gene has been performed in a variety of tumor models *in vitro* as well as in *vivo*. We already showed that both *PSA* and *OC* promoters can trascriptionally regulate *HSV-TK* gene-based therapy to inhibit the growth of AI PSA-producing cells. In this study, we investigated the gene-directed enzyme/prodrug therapeutic effect of AdIU1 (a novel PRRA expressing *PSES* promoter-driven *HSV-TK* suicide gene).

The *in vitro* tissue-specific cytotoxicity of AdIU1/GCV (10 ug/ml) in CWR22rv, C4-2 and DU-145 cells were assessed. Whereas the growth of CWR22rv and C4-2 cell lines were significantly inhibited by a small number of AdIU1 virus particles and GCV, the growth of the DU 145 could only be inhibited by a much greater exposure to AdIU1/GCV, this was expected, as DU-145 cells are PSA/PSMA-negative prostate cancer cells.

Collectively these results demonstrate that AdIU1/GCV has selective cytotoxicity in AI, PSA/PSMA-expressing cells with a good therapeutic window. As expected, intratumoral injection of AdIU1 and treatment with GCV effectively induced growth delay of CWR22rv tumors in nude mice. H&E staining revealed a large fibroblast infiltrate within the virus plus prodrug treatment groups. Furthermore, AdIU1/GCV-treated tumors were significantly inhibited in growth. To compare proliferation between GCV-treated tumors and non-treateed tumors, we performed immunohistochemistry using the proliferation antigen, Ki67. We observed no different expression proliferation each groups. We observed heavy necrosis and apoptosis induction in combined treated groups.

In conclusion, we have established a prostate-restricted replication-competent adenovirus using *PSES* promoter to drive both oncolysis and *HSV-TK* expression only in AI PSA/PSMA-positive prostate cancer cells.

Acknowledgements

Figure Legend

Figure 1.   Schematic illustration of AdIU1. AdIU1 was constructed by placing adenoviral E1a and E4 genes under the control of PSES to direct adenovirus replication, and HSV-TK gene, a pro-drug enzyme gene, under the control of another copy of PSES enhancer to restrict specific expression to maximize cell-killing activity through a bystander effect under the catalysis of gancivlovir (GCV).

Figure 2. In Vitro Killing assay. 1.5×10^5 CWR22rv and DU145 cells were seeded in 24-well plates and infected by serial dilutions of AdIU1 from 0.1v.p/cell to 1000 v.p/cell, with replicative-deficient adenovirus AdE1aPSESE4 as controls. Crystal violet staining was performed to detect attached cells. Then 1% SDS was added to lyses the cells and for OD_{590} reading. Cell survival rate curves were drawn to evaluate the killing activity of AdIU-1.

Figure 3. In vitro cytotoxicity assay. Growth of cells, infected with 100 virus particle/cell of AdIU1 virus, was significantly inhibited by addition of Ganciclovir (GCV) (10ug/mL), especially in CWR22rv(a). The other hand DU 145 (b) cells had no effect.

Figure 4. Effect of antitumor of AdIU1 in vivo.CWR22rv prostate tumor xenografts was established S.C. in athymic nude mice. Tumors were treated with AdE4PSESE1a (n=7), AdE4PSESE1a+GCV (n=8), AdIU1 (n=8) or AdIU1+GCV (n=8) by intratumoral injection at day 0 and after 5 days, injected GCV (100 mg/kg of body weight/day) 2times a day for 10days. And tumor volumes were measured every 5 days.

Figure 5. Tumors were removed for histological examination after the mice were killed at 30 days. (a) AdIU1 plus GCV, (b) AdIU1, (C) AdE4PSESE1a plus GCV and (d) AdE4PSESE1a treatment group (H&E, X 2). These slide showed a lot of fibroblast GCV treatment groups, also AdIU1 with GCV group showed small number of necrosis spot and tumor volume is very small. All necrosis spot show the apoptotic signal by the TUNEL Assay. AdIU1 with GCV group, E1a expression is rare.

Proliferation antigen, Ki67 immunohistochemistry, we observed no different expression proliferation each groups.

Table Legend.

Table 1. Tissue/tumor-specific replication ability of AdIU1

Table 1 *Tissue/tumor-specific replication ability of Ad-IU-1 [a]*

Cell lines	Input Doses[b] (IFU)	Output Viral Doses [c] (LD50[d])	
		AdIU-1	AdE4
C4-2	6.6×10^4	10^6	10^6
CWR22rv	2×10^4	10^6	10^6
PC-3	2.3×10^5	10^2	10^2
DU145	1.6×10^5	5×10^2	5×10^2

[a] Cells were seeded and infected with AdE4PSESE1a or AdIU-1, and the supernatants were harvested for titer assay as described in "Materials and Methods".

[b] Input viral doses mean the virus doses used to infect cells.

[c] Output viral doses mean the titered virus doses in titer assay.

[d] The virus production was expressed as a LD50 value (the dilution factor that caused a CPE in at least 4 wells of cells in a row on a 96-well plate on day 7).

Figure 1.
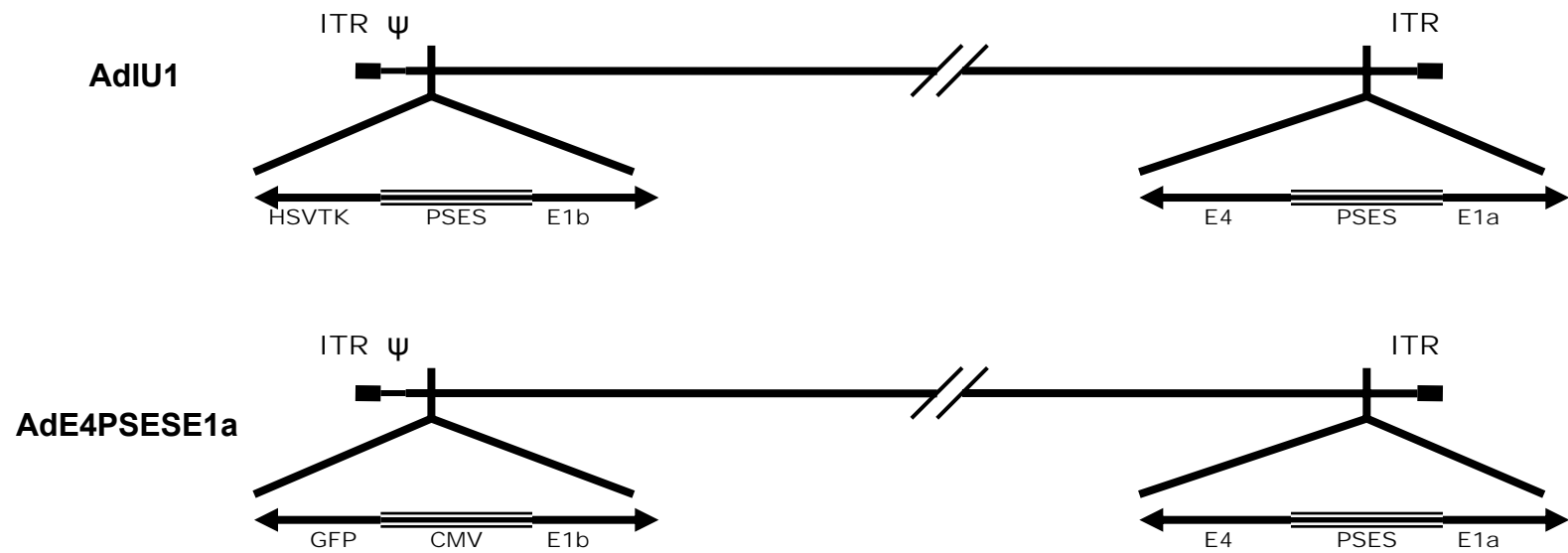
Figure 2.
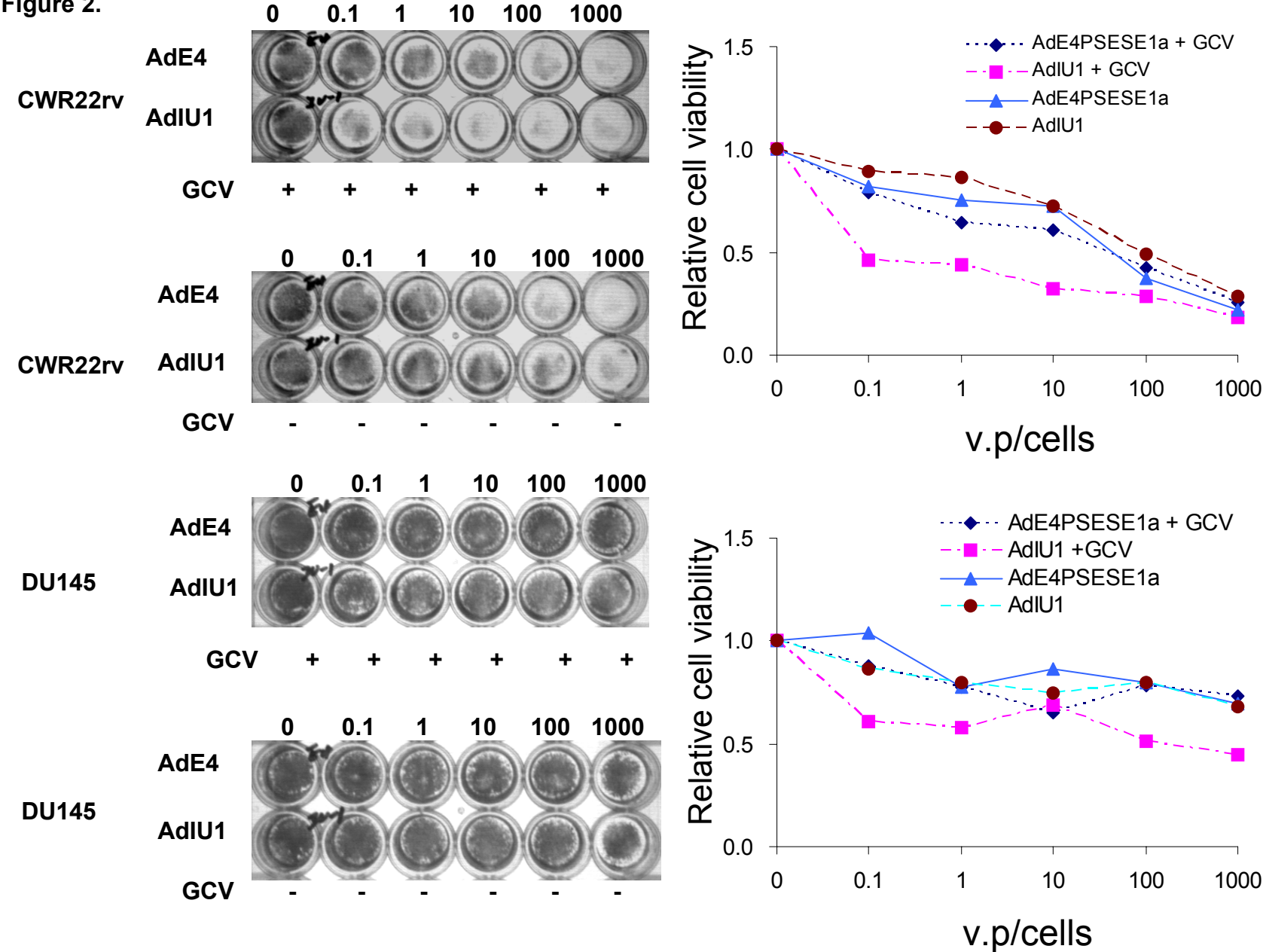
a) CWR22rv
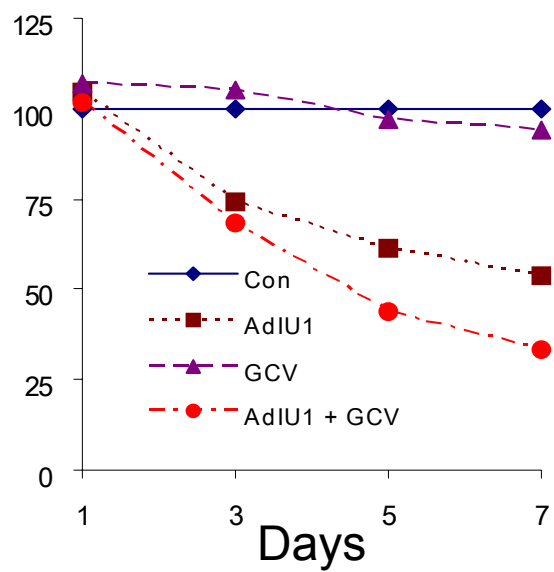
b) DU 145
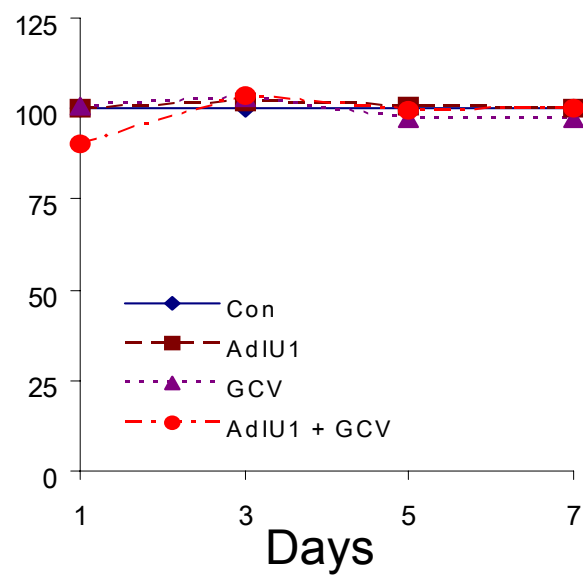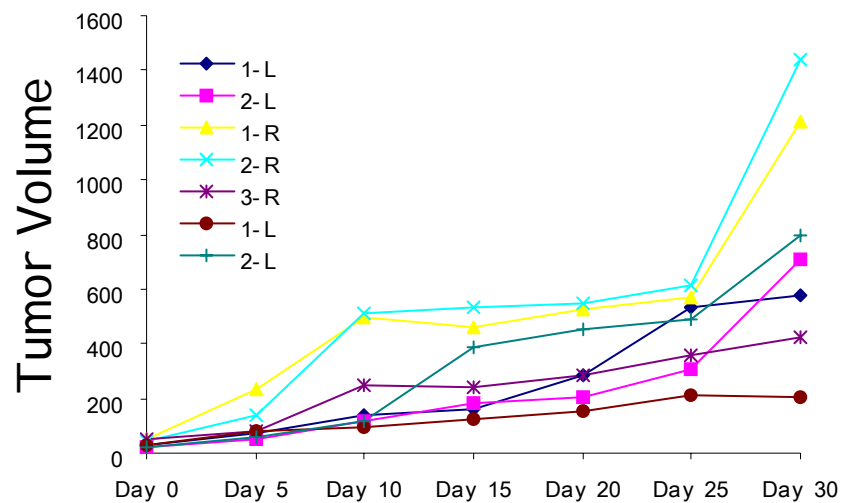
AdE4PSESE1a
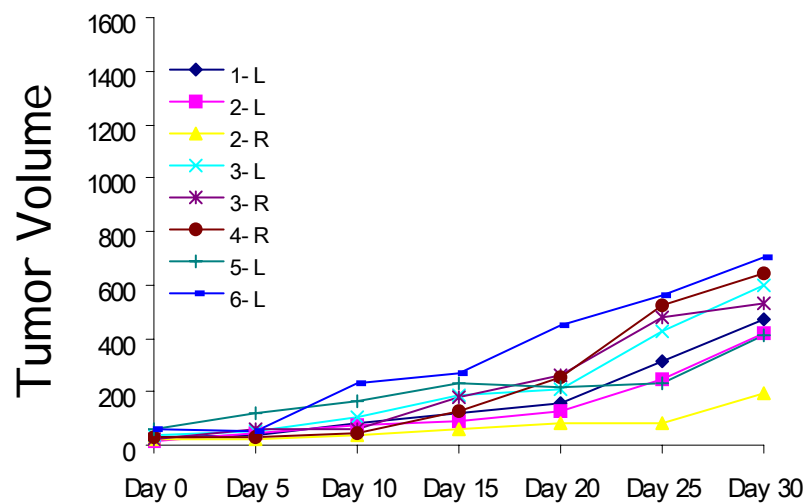
AdE4PSESE1a+GCV
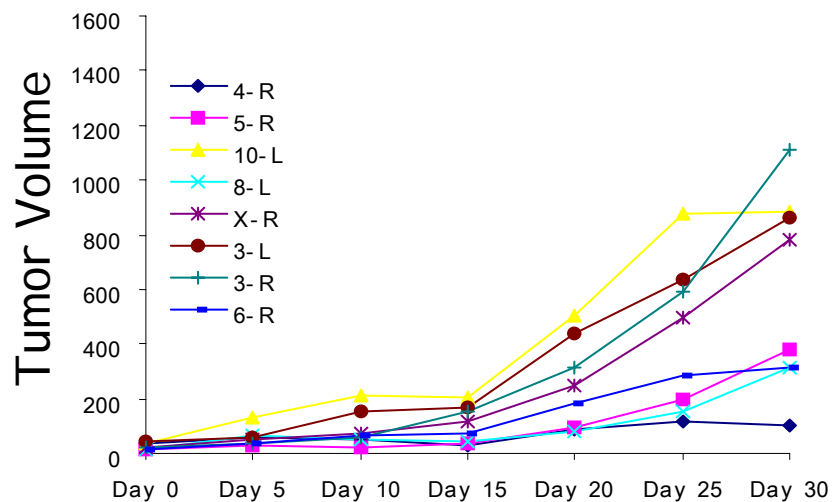
AdI U1
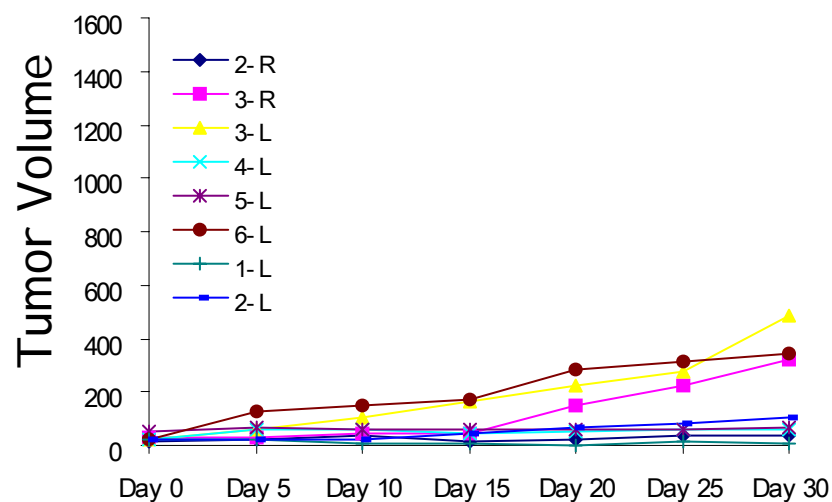
AdI U1+GCV
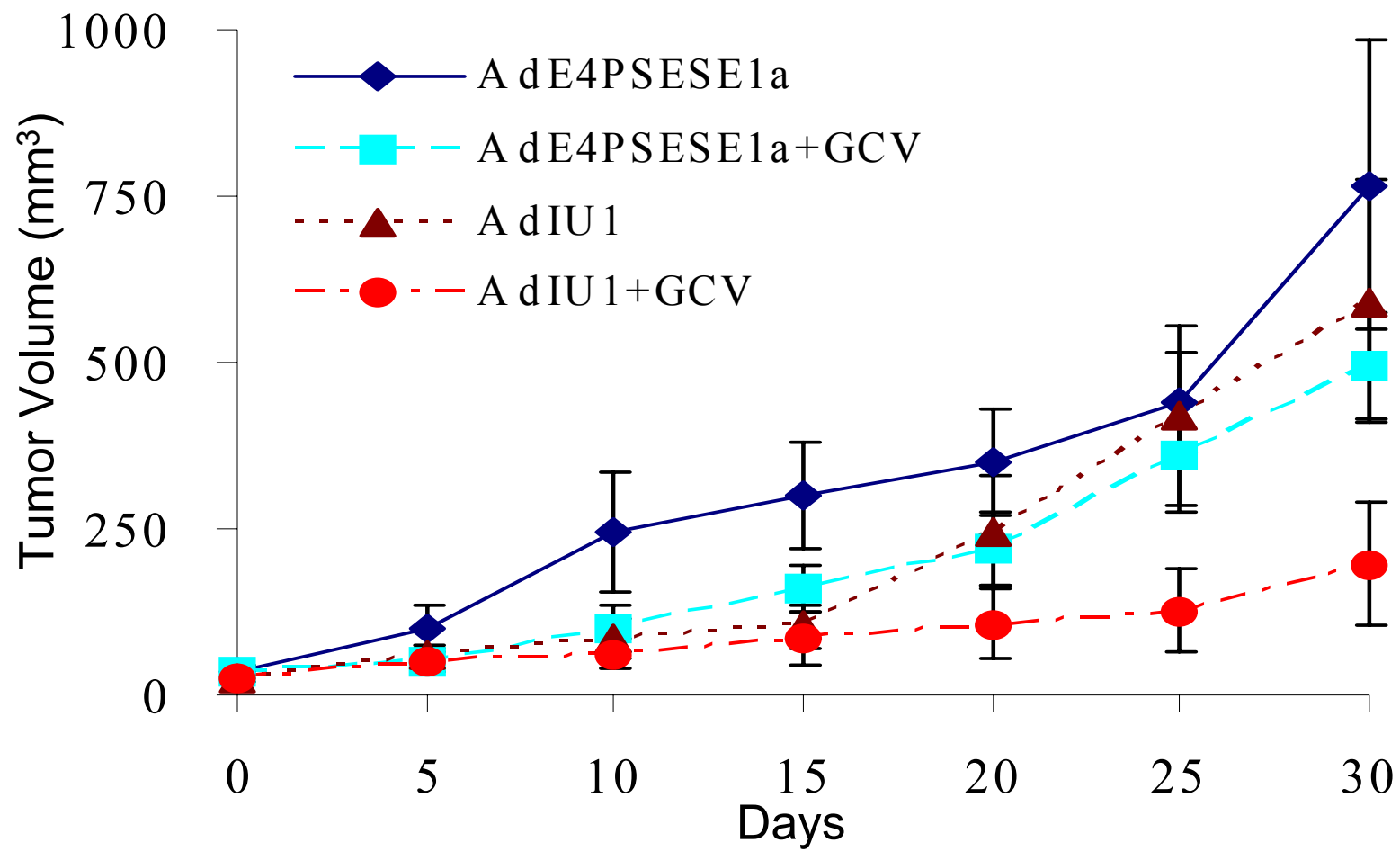
	H & E	TUNEL	Ad5E1a	Ki 67
a				
b				
c				
d				

a

b